

Doctorate Program in Molecular
Oncology and Endocrinology
Doctorate School in Molecular
Medicine

XXVII cycle - 2011–2014

Coordinator: Prof. Massimo Santoro

**“Cancer-associated fibroblasts (CAFs)
release exosomal microRNAs that
dictate an aggressive phenotype in
breast cancer cells”**

Elvira Donnarumma

University of Naples Federico II

Dipartimento di Medicina Molecolare e Biotecnologie Mediche

Administrative Location

Dipartimento di Medicina Molecolare e Biotecnologie Mediche
Università degli Studi di Napoli Federico II

Partner Institutions

Italian Institutions

Università degli Studi di Napoli “Federico II”, Naples, Italy
Istituto di Endocrinologia ed Oncologia Sperimentale “G. Salvatore”, CNR, Naples, Italy
Seconda Università di Napoli, Naples, Italy
Università degli Studi di Napoli “Parthenope”, Naples, Italy

Foreign Institutions

Université Libre de Bruxelles, Bruxelles, Belgium
Universidade Federal de Sao Paulo, Brazil
University of Turku, Turku, Finland
University of Madras, Chennai, India
University Pavol Jozef Šafárik, Kosice, Slovakia

Supporting Institutions

Dipartimento di Medicina Molecolare e Biotecnologie Mediche, Università degli Studi di Napoli
“Federico II”, Naples
Istituto di Endocrinologia ed Oncologia Sperimentale “G. Salvatore”, CNR, Naples
Istituto Superiore di Oncologia
Regione Campania

Italian Faculty

Francesco Beguinot
Roberto Bianco
Bernadette Biondi
Francesca Carlomagno
Maria Domenica Castellone
Gabriella Castoria
Angela Celetti
Annamaria Cirafici
Annamaria Colao
Gerolama Condorelli
Valentina De Falco
Vittorio De Franciscis
Sabino De Placido
Gabriella De Vita
Monica Fedele
Pietro Formisano
Alfredo Fusco
Fabrizio Gentile
Domenico Grieco
Michele Grieco

Maddalena Illario
Paolo Laccetti
Antonio Leonardi
Paolo Emidio Macchia
Rosa Marina Melillo
Claudia Miele
Nunzia Montuori
Roberto Pacelli
Giuseppe Palumbo
Giovanna Maria Pierantoni
Rosario Pivonello
Giuseppe Portella
Maria Fiammetta Romano
Giuliana Salvatore
Massimo Santoro
Donatella Tramontano
Giancarlo Troncone
Giancarlo Vecchio
Mario Vitale

**“Cancer-associated
fibroblasts (CAFs)
release exosomal
microRNAs that dictate
an aggressive phenotype
in breast cancer cells”**

TABLE OF CONTENTS

	Page
LIST OF PUBLICATIONS	4
LIST OF ABBREVIATIONS	5
ABSTRACT	8
1. BACKGROUND	9
1.1 Breast cancer	9
1.1.1 Breast cancer: risk factors and incidence	9
1.1.2 Breast cancer classifications and treatment	9
1.1.3 Breast cancer stem cells	12
1.2 Tumor microenvironment	14
1.2.1 The distinctive microenvironments of tumors	14
1.2.2 Multifactorial contributions of tumor-associated stromal cells to the hallmarks of cancer	15
1.2.3 Cancer-associated fibroblasts (CAFs)	20
1.3 Exosomes	26
1.3.1 Biogenesis and secretion of exosomes	26
1.3.2 Exosome composition	28
1.3.3 The sorting mechanisms and the function of exosomal miRs	29
1.3.4 Exosomes in cancer development and metastasis	30
2. AIM OF THE STUDY	32
3. MATERIALS AND METHODS	33
3.1 Primary and continuous cells and mammosphere cultures	33
3.2 Isolation of primary cell cultures from human breast biopsies	33
3.3 Immunocytochemistry	33
3.4 Exosome isolation	34
3.5 Cell transfection	34
3.6 RNA extraction and Real Time PCR	34
3.7 NCounter miRNA assay	35
3.8 Protein isolation and Western blotting	35
3.9 Immunofluorescence analysis	36

3.10 TGF- β treatment	36
3.11 Mammosphere formation assay	37
3.12 Statistical analysis	37
4. RESULTS	38
4.1 Isolation and characterization of primary fibroblasts from human breast biopsies	38
4.2 Identification of exosomal proteins in breast fibroblast exosomes	40
4.3 Identification of oncogenic miRs in CAF exosomes	40
4.4 TGF- β increases miR-21, miR-143, and miR-378e levels in normal fibroblast exosomes	42
4.5 Breast fibroblast-derived exosomes are transferred to T47D cells	43
4.6 miRs released by CAFs are shuttled into breast cancer cells via exosomes	46
4.7 CAF exosomes increase stem cell and EMT markers in breast cancer cells	49
4.8 CAF exosomes increase mammosphere formation ability	51
4.9 miR-21, miR-143 and miR378e increase stem cell and EMT markers in breast cancer cells	53
4.10 miR-21, miR-143 and miR378e increase mammosphere formation ability	54
4.11 Anti-miRs -21, -143 and -378e decrease stemness phenotype	56
5. DISCUSSION	58
6. CONCLUSIONS	63
7. REFERENCES	64

LIST OF PUBLICATIONS

This dissertation is based upon the following publications:

Quintavalle C, Mangani D, Roscigno G, Romano G, Diaz-Lagares A, Iaboni M, **Donnarumma E**, Fiore D, De Marinis P, Soini Y, Esteller M, Condorelli G. MiR-221/222 target the DNA methyltransferase MGMT in glioma cells. PLoS One 2013; 8(9):e74466.

Quintavalle C*, **Donnarumma E***, Iaboni M, Roscigno G, Garofalo M, Romano G, Fiore D, De Marinis P, Croce CM, Condorelli G. Effect of miR-21 and miR-30b/c on TRAIL-induced apoptosis in glioma cells. Oncogene 2013; 32(34):4001-8.

*co-first authors

LIST OF ABBREVIATIONS

AVCs: Angiogenic Vascular Cells

BC: Breast Cancer

BLBCs: Basal-Like Breast Cancers

BMP: Bone Morphogenetic Protein

CAF: Cancer-Associated Fibroblast

CCL2: Chemokine (C-C motif) Ligand 2

CCs: Cancer Cells

CDK4/6: Cyclin Dependent Kinase 4/6

CIS: Carcinoma In Situ

CSC: Cancer Stem Cell

CXCR4: Chemokine (C-X-C motif) Receptor 4

DCIS: Ductal Carcinoma In Situ

ECM: Extracellular Matrix

ECs: Endothelial Cells

EGF: Epidermal Growth Factor

EMT: Epithelial–Mesenchymal Transition

EndMT: Endothelial–Mesenchymal Transition

EPCs: Endothelial Progenitor Cells

ER: Estrogen Receptor

ESCRT: Endosomal-Sorting Complex Required for Transport

EV: Extracellular Vesicle

FABP4: Fatty Acid Binding Protein-4

FGF: Fibroblast Growth Factor

FSP1: Fibroblast-Specific Protein 1

HER2: Human Epidermal growth factor Receptor 2

HGF: Hepatocyte Growth Factor

HIF: Hypoxia Inducible transcription Factor

hnRNPs: heterogeneous nuclear RiboNucleoProteins

Hsp: Heat Shock Protein

ICs: Immune inflammatory Cells

IGF-1: Insulin-like Growth Factor-1

IICs: Infiltrating Immune Cells

IL: Interleukin

ILV: Intra-luminal Vesicle

iPSCs: induced Pluripotent Stem Cells

MCP1: Monocyte Chemotactic Protein 1

MDSCs: Myeloid-Derived Suppressor Cells

MHC: Major Histocompatibility Complex

miRNA, miR: microRNA

MMPs: Metalloproteinases

MSCs: Mesenchymal Stem Cells

mTOR: mammalian Target Of Rapamycin

MVB: Multi-Vesicular Body

NF: Normal Fibroblast

nSMase2: neural SphingoMyelinase 2

oncomiRs: oncogenic miRs

PCs: Pericytes

PDGF: Platelet-Derived Growth Factor

PR: Progesterone Receptor

PTEN: Phosphatase and Tensin homolog

RISC: RNA-Induced Silencing Complex

SDF-1: Stromal cell-Derived Factor-1

SNARE: Soluble NSF-Attachment protein Receptor

TAMs: Tumor-Associated Macrophages

TGF- β : Transforming Growth Factor- β

TIMP: Tissue Inhibitor of MetalloProteinases

TLRs: Toll-Like Receptors

TM: Tumor Microenvironment

TNBC: Triple Negative Breast Cancer

TNF- α : Tumor Necrosis Factor- α

Tsg101: Tumor Susceptibility Gene 101

VAMP7: Vesicle-Associated Membrane Protein 7

VCAM-1: Vascular Cell Adhesion Molecule-1

VEGF: Vascular Endothelial Growth Factor

α -SMA: alpha Smooth Muscle Actin

ABSTRACT

Despite many novel therapeutic approaches, breast cancer remains one of the leading cause of cancer mortality among women. Recent findings indicate that cancer-associated fibroblasts (CAFs), the major components of the tumor microenvironment, play a crucial role in breast cancer progression, but how they promote tumorigenesis is poorly understood. Increasing evidence indicates that exosomes, membrane vesicles sized 30-100 nm in diameter, play an important role in cell-cell communication. Exosomes and their cargo, including microRNAs (miRs), may vehiculate between cells and affect the biological behavior of recipient cells. Therefore, one alternative mechanism of the promotion of breast cancer progression by CAFs may be through cancer-associated fibroblast-secreted exosomes, which would deliver oncogenic miRs to breast cancer cells. Firstly, to investigate the potential role of miRs in stroma-tumor communication, we compared miR expression profile in exosomes from 2 cancer-associated fibroblasts and 2 normal fibroblasts. We found that in CAF exosomes the levels of miR-21, miR-378e, and miR-143 were increased as compared to normal fibroblast exosomes, and we validated the array data by real-time PCR. By immunofluorescence experiments, we demonstrated that PKH26-labeled-exosomes could be transferred from fibroblasts to a breast cancer epithelial cell line, T47D. Furthermore, to elucidate whether the identified miRs were shuttled into T47D cells via exosomes, we transfected CAFs with cy3-labeled-miRs (cy3-miR-21, cy3-miR-143, cy3-miR-378e), and, then, we isolated the released exosomes. Interestingly, when these exosomes were added to T47D cells, the cy3-miRs were detected in the cytoplasm of T47D cells, and they co-localized with the signals of an exosomal marker, CD63. Then, we demonstrated that TGF- β , apart from its direct role in the activation of normal fibroblasts to CAFs, increased the levels of these miRs in normal fibroblast exosomes. Finally, for the first time, we provided evidence of the role of CAF exosomes and their miR contents in the induction of stemness phenotype in T47D cells. In fact, T47D cells exposed to CAF exosomes or transfected with the identified miRs exhibited a significantly increased capacity to form mammospheres, and increased stem cell and epithelial-mesenchymal transition markers, SOX2, Nanog, Oct3/4, Snail and Zeb. We conclude that CAFs regulate the stemness phenotype of breast cancer cells through exosome-mediated delivery of oncogenic miRs. Our data provide insight into the mechanisms underlying the stemness maintenance in breast cancer.

1. BACKGROUND

1.1 Breast cancer

1.1.1 Breast cancer: risk factors and incidence

Breast cancer (BC) is the most common cancer in women. Aside from age, sex, and family history (for instance BRCA1 and BRCA2 mutation carriers), risk of developing breast cancer is largely linked to reproductive factors, which characterize exposure to sex hormones. Specifically, risk of developing breast cancer is increased by early menarche, late menopause, and nulliparity, whereas risk is reduced by higher parity and lactation (Anderson et al. 2014). Variation in incidence rates worldwide is thought to be due to differences in reproductive patterns and other hormonal factors as well as early detection. In the United States, BC mortality rates have been decreasing over the last 2-3 decades, largely as result of early detection as well as improved targeted therapy. Thanks to early detection via mammogram, most of breast cancers in developed parts of world are diagnosed in the early stage of the disease. Early stage breast cancers can be completely cut by surgery. Over time however, the disease may come back even after complete resection, which has prompted the development of an adjuvant therapy. Surgery followed by adjuvant treatment has been the gold standard for breast cancer treatment for a long time (Miller et al. 2014).

1.1.2 Breast cancer classifications and treatment

Breast cancer is a heterogeneous disease with a number of morphological subtypes. Invasive ductal carcinoma is the most common morphological subtype, representing 80% of the invasive breast cancers. Invasive lobular carcinoma is the next most common subtype, representing approximately 10% of invasive breast cancers. The less common subtypes of the invasive breast cancers include: mucinous, cribriform, micropapillary, papillary, tubular, medullary, metaplastic, and inflammatory carcinomas (Malhotra et al. 2010) (Figure 1).

Further important breast cancer classifications are the immunohistochemical and molecular classifications. In fact, the molecular subtype of breast cancer carries important predictive and prognostic values, and, thus, has been incorporated in the basic initial process of breast cancer diagnosis.

Breast cancers can be divided into 5 molecular subtypes:

- luminal type A and B,
- human epidermal growth factor receptor 2 (HER2) type,

- normal breast-like,
- basal-like types.

Routine sub-classification of invasive ductal carcinomas is accomplished by the immunostaining of tumor tissues for HER2, estrogen (ER) and progesterone (PR). Approximately 70%–75% of invasive breast cancers express ER (ER+). Collectively, the ER+ BCs are classified as luminal cancers. These cancers are further sub-classified into luminal A (HER2-) and luminal B (HER2+) subtypes based on their HER2 status and proliferation rate. Most of ER+ tumors also express PR. The ER- breast cancers are sub-classified as HER2+ (ER-, PR-, HER2+) and basal-like (ER-, PR-, HER2-) (Figure 2). While the luminal-type cancers are consistently estrogen receptor positive and have favorable prognosis, the basal-like breast cancers (BLBCs) are negative for 3 markers (ER-, PR-, HER2-), and, thus, belong to the group of triple negative breast cancers (TNBCs) with a bad prognosis (Sandhu et al. 2010, Rivenbark et al. 2013).

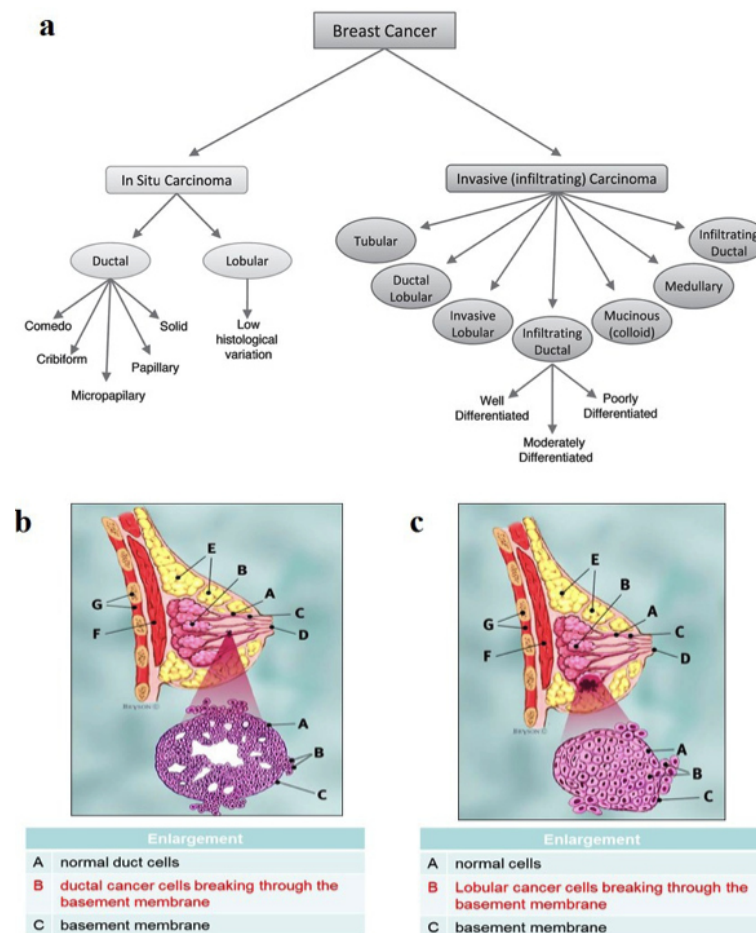


Figure 1. Morphological subtypes of breast cancer (a), schematic representation of invasive ductal carcinoma (b) and invasive lobular carcinoma (c)

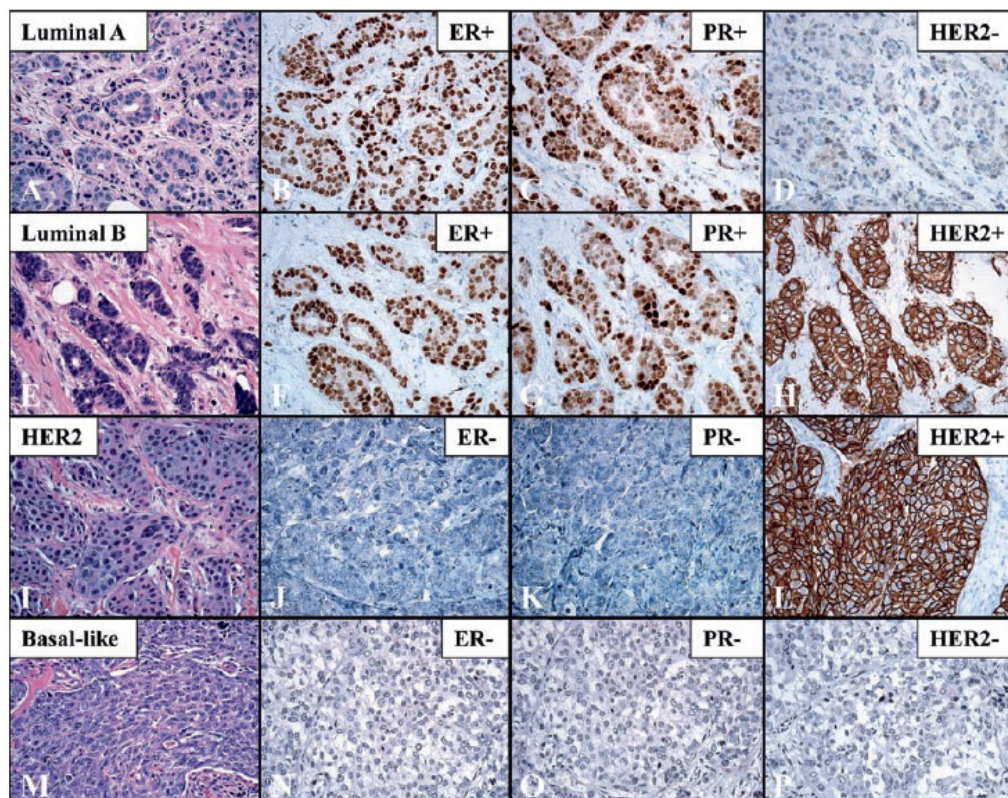


Figure 2. Immunohistochemical and molecular classifications of breast cancer

Luminal breast cancer (luminal A and luminal B subtypes) responds to estrogen (hormonal) manipulation. Standard hormonal therapies include aromatase inhibitors (anastrozole, exemestane and letrozole) and ER targeted therapy (tamoxifen and fulvestrant). 50% of patients with previously hormonal positive breast cancer fail to respond to hormonal manipulation at relapse. It is therefore clear that it is important to develop newer treatment strategies to overcome this resistance. In terms of hormonal sensitive HER2-positive breast cancers this can be achieved with simultaneous targeting of both receptors. However, for hormonal sensitive HER2-negative breast cancers, alternative approaches are required, such as mammalian target of rapamycin (mTOR) or cyclin dependent kinase 4/6 (CDK4/6) inhibitors.

HER2-positive breast cancers represent approximately 20% of breast cancers and confer a poorer prognosis. HER2 targeted therapy with the anti-HER2 antibody trastuzumab has improved disease free survival and overall survival in the adjuvant and metastatic setting. Unfortunately, there is evidence that HER2-positive BC becomes resistant to anti-HER2 therapies. Current strategies to overcome resistance include blockade with multiple anti-HER2 antibodies, dual tyrosine kinase inhibitors, and antibody-drug conjugates, alone or in combination.

12 to 17% of BCs are TNBCs. Eighty-five percent of basal like breast cancers and a high proportion of BRCA mutant breast cancers are triple negative. The standard palliative treatment of TNBC remains systemic chemotherapy. TNBC patients initially respond well to treatment, but these responses lack durability resulting in a poorer prognosis. There is, thus, a need to identify new targets for this subgroup (Sharp and Harper-Wynne 2014) (Figure 3).

	Luminal A	Luminal B	Her2 positive	Triple negative (85% basal-like)
Percentage at diagnosis	40%	20%	10-15%	15-20%
Receptor expression	Estrogens and progesterone	Estrogens and progesterone	Her2	
Treatment strategies	Chemotherapy	Chemotherapy	Chemotherapy	Chemotherapy
		Her2 targeted therapies		
	Hormonal manipulation			
	Novel targeted therapies	Novel targeted therapies	Novel targeted therapies	Novel targeted therapies

Figure 3. Breast cancer subtypes and treatment strategies

1.1.3 Breast cancer stem cells

Cancer stem cells (CSCs) are rare, tumor-initiating cells that exhibit stem cell properties: capacity of self-renewal, pluripotency, highly tumorigenic potential, and resistance to therapy (Czerwinska and Kaminska 2015). Cancer stem cells have been characterized and isolated from many cancers, including breast cancer. The best characterized signaling pathways controlling self-renewal and differentiation in normal stem cells, such as Wnt/ β -catenin, Notch, Hedgehog, and transforming growth factor- β /bone morphogenetic protein (TGF- β /BMP) pathways, are frequently deregulated in breast cancer cells, which leads to the acquisition of the stem-cell phenotype. Moreover, deregulation of these signaling pathways is frequently linked to an epithelial-mesenchymal transition (EMT), and breast CSCs often possess properties of cells that have undergone the EMT process (Mani et al. 2008, Morel et al. 2008, Pinto et al. 2013). EMT is a process by which epithelial cells attain a mesenchymal phenotype, allowing them to break free from the primary tumor site and metastasize at distant sites. Thus, EMT signaling is involved in development and maintenance of breast CSCs. Furthermore, while overexpression of Oct3/4, Sox2, Klf4, and c-myc genes in somatic cells leads to dedifferentiation into induced pluripotent stem cells (iPSCs), the activation of the molecular targets of these pluripotency-associated genes is frequently

observed in poorly differentiated breast tumors and other cancers (Takahashi et al. 2006). Notably, accumulating evidence indicates that the expression of Oct3/4, Nanog, and Sox2 transcription factors has a strong correlation with CSCs: knockdown of these genes decreased tumor sphere formation and inhibited tumor formation in xenograft tumor models (Leis et al 2012, Wang et al. 2014). In addition, recent studies have elucidated that the expression of these factors in CSCs is regulated by epigenetic mechanisms (Munoz et al. 2012).

The CSCs have important implications in cancer treatment. Current anti-cancer therapy is effective for removing the tumor mass, but often treatment effects are transient, thus tumor relapses and metastatic disease occurs. A possible explanation is that anti-cancer therapies fail to kill CSCs (Figure 4). Different mechanisms could explain breast CSC chemo-resistance: aberrant ABC transporter expression/activity, increased aldehyde dehydrogenase activity, enhanced DNA damage response, activation of self-renewal signaling pathways, and epigenetic deregulations (Kaminska et al. 2013). Moreover, CSCs have a slow rate of cell turnover, and, thus, can escape from chemotherapeutic agents that target rapidly proliferating cells. However, targeting differentiated as well as tumor stem cells is a prerequisite for therapy to be efficient. In fact, whereas CSCs can differentiate into non-CSCs giving rise to the tumor heterogeneity, non-CSCs could be reprogrammed into CSCs. This phenotypic plasticity has implications for cancer treatment: if non-CSCs can give rise to CSCs, therapeutic elimination of CSCs may be followed by their regeneration from residual non-CSCs, allowing tumor re-growth and clinical relapse (Pinto et al. 2013).

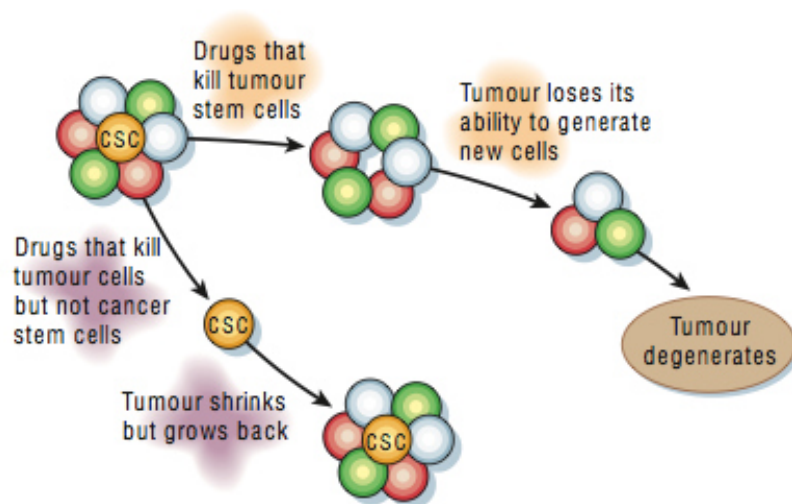


Figure 4. Comparison between conventional therapies and CSC targeted therapies

1.2 Tumor microenvironment

1.2.1 The distinctive microenvironments of tumors

The neoplastic epithelial cells constitute a compartment, referred to as the parenchyma, that is strictly associated to the mesenchymal cells forming the tumor-associated stroma. As interactions between cells and their microenvironment are crucial for normal tissue homeostasis in physiological conditions, also communication between epithelial cells and stroma is necessary for tumor initiation and progression. The multiple stromal cell types create a succession of tumor microenvironments that change as tumors invade normal tissue, and then, seed and colonize distant tissues (Figure 5). This histopathological progression must reflect underlying changes in heterotypic signaling between tumor parenchyma and stroma. Thus, incipient neoplasias begin the interplay by recruiting and activating stromal cell types that assemble into an initial pre-neoplastic stroma, which in turn responds reciprocally by enhancing the neoplastic phenotypes of the nearby cancer cells. The cancer cells, which may further evolve genetically, again feed signals back to the stroma, continuing the reprogramming of normal stromal cells; ultimately, signals originating in the tumor stroma enable cancer cells to invade normal adjacent tissues and disseminate. This model of reciprocal heterotypic signaling must be extended to encompass the final stage of multistep tumor progression-metastasis. In fact, once reached distant organs, the circulating cancer cells that are released from primary tumors encounter a naive, fully normal, tissue microenvironment, that they must educate in order to proceed to colonize the new site. However, in some cases, certain tissue microenvironments, referred as “metastatic niches”, for various reasons, may already be supportive of the seeded cancer cells. This permissiveness may be intrinsic to the tissue site (Talmadge et al. 2010) or pre-induced by circulating factors released by the primary tumor (Peinado et al. 2011). The most well-documented components of induced pre-metastatic niches are tumor-promoting inflammatory cells, although other cell types and the extracellular matrix (ECM) may play important roles in different metastatic contexts (Hanahan and Weinberg 2011).

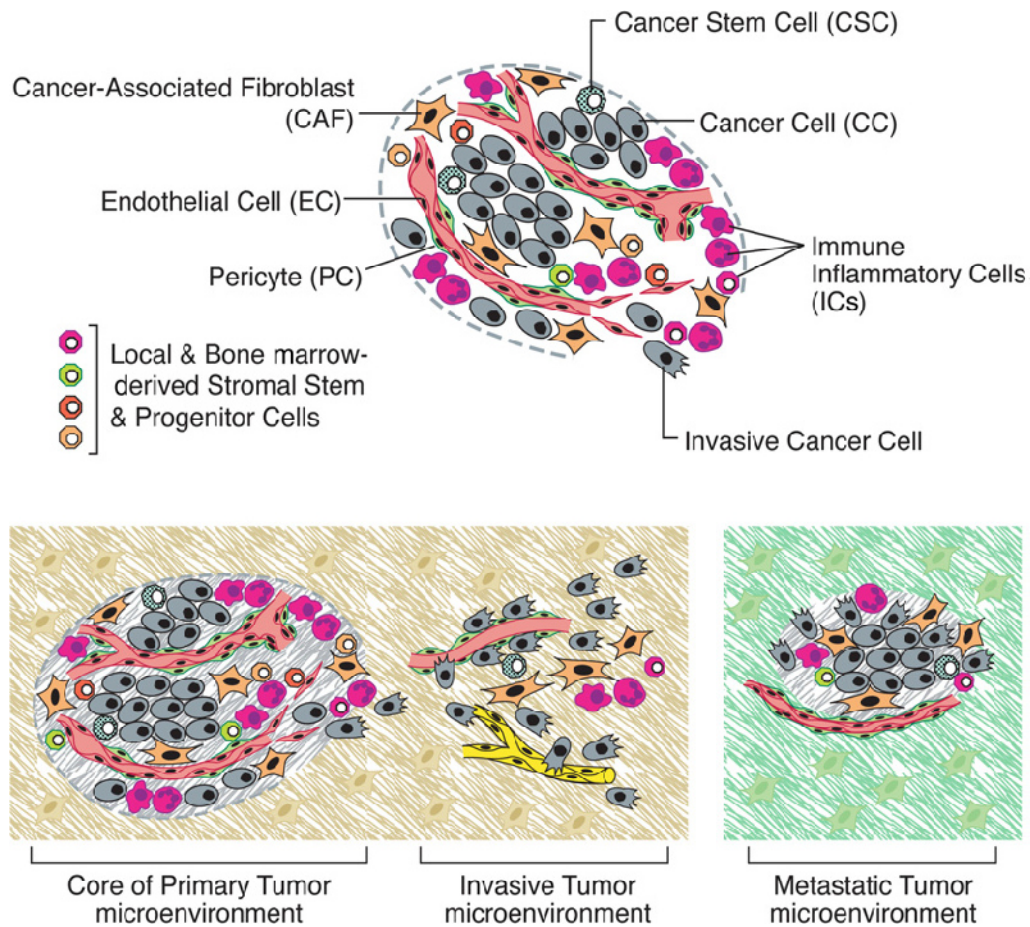


Figure 5. The distinctive microenvironments of tumors

1.2.2 Multifactorial contributions of tumor-associated stromal cells to the hallmarks of cancer

Most of the hallmarks of cancer are enabled and sustained through contributions from different stromal cell types and distinctive subcell types. The stromal cells can be divided into three general classes: angiogenic vascular cells (AVCs), infiltrating immune cells (IICs), and cancer-associated fibroblastic cells (Hanahan et al. 2012) (Figure 6).

Angiogenic vascular cells

AVCs consist of endothelial cells and pericytes, that can sustain five of the main hallmarks of cancer: the promotion of proliferative signaling, the resistance to cell death, the activation of invasion and metastasis, the reprogramming of energy metabolism, and the capability of evading immune destruction. The neovascularization, involving AVCs, is the best modulator of tumor growth, in fact, the “angiogenic switch” increases cancer cell proliferation in tumors (Folkman J et al. 1989) as well the inhibition of

angiogenesis can impair hyperproliferation, reflecting reduced bioavailability of blood-borne mitogenic growth factors.

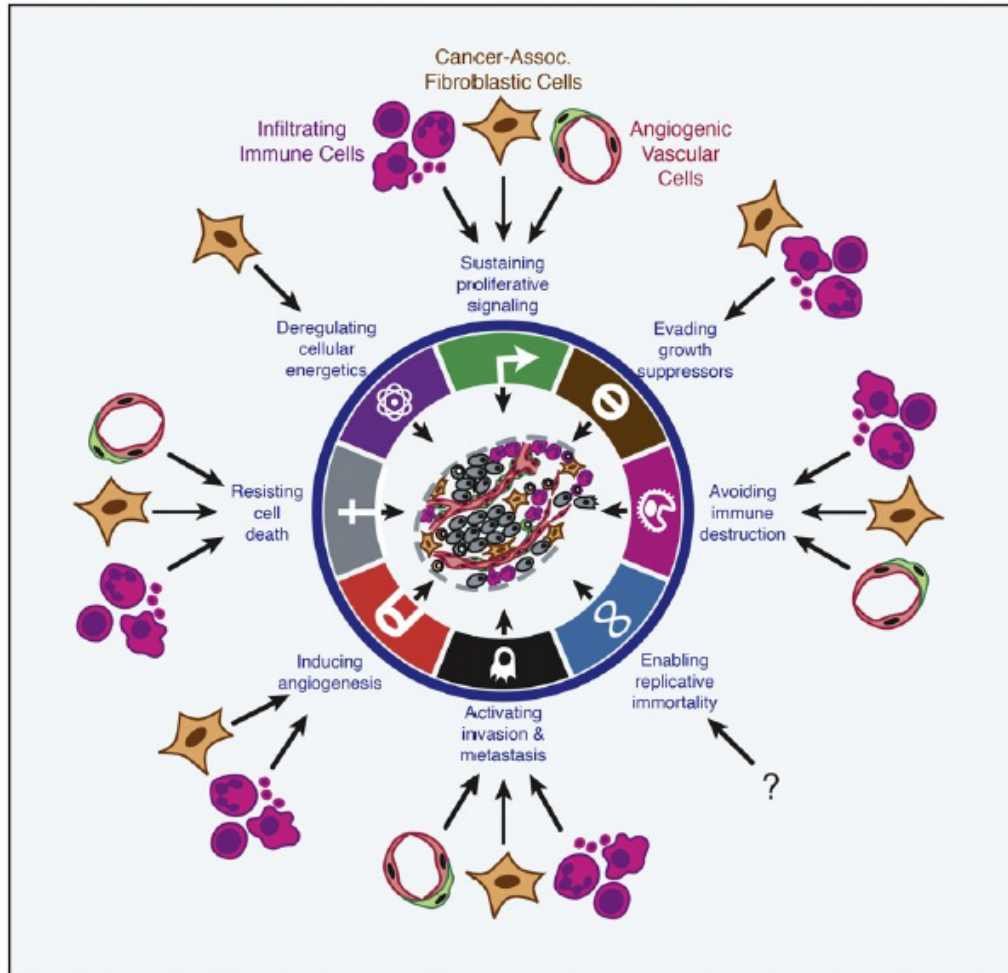


Figure 6. Stromal cells sustain the hallmarks of cancer

Furthermore, the vascularization allows avoiding cell death that would result from hypoxia and lack of serum-derived nutrients and survival factors. The proangiogenic factor, vascular endothelial growth factor (VEGF), is overexpressed in many tumors and leads to the reduction of pericyte coverage and the decrease of association between pericytes and endothelium. Thus, impairing vascular integrity, it facilitates dissemination of cancer cells from primary human tumors. In the same manner, VEGF can facilitate both loosening of vessel walls for extravasation, and subsequent induction of angiogenesis to support metastatic tumor growth, at distant sites. Inadequate vascular function can result in hypoxia, activating the hypoxia inducible transcription factor (HIF) response system, that enables cancer cells to survive

and proliferate more effectively in conditions of vascular insufficiency (Branco-Price C et al. 2012).

Infiltrating immune cells

IICs consist of Th2-CD4 T cells, B cells, CD8 T cells, Natural Killer cells, tumor-associated macrophages (TAMs), inflammatory monocytes, myeloid-derived suppressor cells (MDSCs), neutrophils, mast cells, and platelets. IICs can sustain seven of the main hallmarks of cancer: the promotion of proliferative signaling, the resistance to cell death, the escape of growth suppressors, the activation of invasion and metastasis, the induction of angiogenesis, the reprogramming of energy metabolism, and the capability of evading immune destruction. IICs supply direct and indirect mitogenic growth mediators that stimulate proliferation of tumor cells and stromal cells. The main released mediators are: epidermal growth factor (EGF), transforming growth factor- β (TGF- β), tumor necrosis factor- α (TNF- α), fibroblast growth factors (FGFs), various interleukins (ILs), chemokines, histamine, and heparins (Balkwill et al. 2005). IICs express and secrete a variety of proteolytic enzymes (metallo, serine, and cysteine proteinases and heparanase) that, in addition to liberating mitogenic growth factors, can selectively cleave cell-cell and cell-ECM adhesion molecules, and ECM molecules, thereby disabling growth suppressing adhesion complexes maintaining homeostasis (Lu et al. 2011). Moreover, another mechanism used by cancer cells to become resistant to cell detachment-induced apoptosis that involves IICs, is the binding IICs-cancer cells. Thus, IICs can enable cancer cells the ability to survive in ectopic microenvironments by suppressing the triggering of cell death pathways. For instance, α 4-integrin-expressing TAMs promote survival of metastatic breast cancer cells in lung by binding vascular cell adhesion molecule-1 (VCAM-1) expressed on breast cancer cells (Chen et al. 2011). TAMs also protect breast cancer cells from chemotherapy (taxol, etoposide, and doxorubicin)-induced cell death by a cathepsin protease-dependent mechanism (Shree et al. 2011). Furthermore, IICs have a crucial role in the induction of angiogenesis. In fact, while endothelial cells mediate leukocyte recruitment by expressing many leukocyte adhesion molecules, IICs produce a diverse assortment of soluble factors that influence endothelial cell behavior. The main soluble mediators produced by IICs are: VEGF, FGF, TNF- α , TGF- β , platelet-derived growth factor (PDGF), chemokines, matrix metalloproteinases (MMPs), proteases, DNA-damaging molecules, histamine. All of these effectors have capabilities to regulate vascular cell survival, proliferation, and motility, along with tissue remodeling, culminating in new vessel formation. In particular, TAMs regulate tumor angiogenesis largely through their production of VEGF-A (Lin et al. 2007), and also mast cells, that are reservoirs of potent vascular mediators including VEGF, are important promoter of tumor angiogenesis (Kessler et al. 1976). Furthermore, neutrophils and their myeloid progenitors, which produce MMP-9, are demonstrably involved in angiogenic switching in some tumors (Pahler et al. 2008). Platelets release distinctive granules containing either pro- or antiangiogenic regulatory molecules, and have been implicated in

angiogenesis for decades (Sabrkhany et al. 2011). Moreover, platelets and macrophages can be added to the roster of tumor-promoting hematopoietic cells that facilitate invasion and metastasis. Interestingly, mast cells and macrophages, in primary tumor TMs, provide a wide range of proteases, that foster ectopic tissue invasion by remodeling structural components of ECM which in turn provide conduits for malignant cell egress, as well as by generating ECM fragments with pro-invasive signaling activities (Kessenbrock et al. 2010). Furthermore, macrophages are the primary source of EGF, that promotes invasion/chemotaxis and intravasation of breast carcinoma cells through a paracrine loop operative between tumor cells and macrophages (Wyckoff et al. 2004). Finally, functional genetic studies demonstrated that also platelets, through platelet-derived TGF- β ligand, have an invasion- and metastasis-promoting activity (Labelle et al. 2011).

Notably, the most important IICs involved in anti-tumor immunity resistance are T regulatory cells. In fact, T regulatory cells typically play an important physiological role in suppressing responses to self-antigens, thereby preventing autoimmunity. MDSCs, TAMs and mast cells can indirectly foster immune suppression through recruitment or promotion of the generation of T regulatory cells (Ruffell et al. 2010, Wasiuk et al. 2009).

Finally, TAMs are implicated in the altered metabolism of tumors, as well as in the development of metabolic pathologies (Biswas et al. 2012).

Cancer-associated fibroblastic cells

Connective tissue fibroblasts proximal to neoplastic growths can be activated, and mesenchymal progenitors—in particular, mesenchymal stem cells (MSCs), both local and bone marrow derived—can be recruited and induced to differentiate into myofibroblasts defined in part by expression of alpha smooth muscle actin (α -SMA) (Paunescu et al. 2011), or into adipocytes defined by expression of fatty acid binding protein-4 (FABP4) (Rosen et al. 2006). Each of these subtypes can contribute to a variety of tumor-promoting functions, with the potential to impact on multiple hallmark capabilities. Thus, for example, cancer-associated fibroblastic cells can express and secrete signaling proteins that include mitogenic epithelial growth factors—hepatocyte growth factor (HGF), EGF family members, insulin-like growth factor-1 (IGF-1), stromal cell-derived factor-1 (SDF-1), and a variety of FGFs—with the capability to stimulate cancer cell proliferation (Cirri et al. 2011). In addition, both activated adipocytes and activated fibroblasts can express many mediators, thereby recruiting and activating IICs that, in turn, provide mitogenic signals to cancer cells, as well as other cell types in the TM (Dirat et al. 2011). Furthermore, cancer-associated fibroblastic cells have also the capability to limit the impact on tumor growth and progression of cancer cell apoptosis through the secretion of diffusible paracrine survival factors such as IGF-1 and IGF-2 (Kalluri et al. 2006) and of ECM molecules and of ECM-remodeling proteases (Lu et al. 2011). Moreover, cancer-associated adipocytes, analogous to IICs, confer a radioresistant phenotype to breast cancer cells dependent on adipocyte-derived IL-6 (Bochet et al. 2011). Notably, cancer-

associated fibroblastic cells, in different TMs, can produce a large amount of proangiogenic signaling proteins, including VEGF, FGFs, and IL-8/CXCL8, a variety of ECM-degrading enzymes, and they can also produce chemo-attractants for proangiogenic IICs, thereby indirectly orchestrating tumor angiogenesis (Vong et al. 2011). Interestingly, these cells modulate the capability of cancer cells to invade locally or establish secondary tumors at distant metastatic site through two important hormones, HGF, which stimulates c-Met, and TGF- β , that is involved in activating EMT programs in certain cancer cells, thereby enabling their capability for invasion and metastasis (Chaffer et al. 2011). Another important role of cancer-associated fibroblastic cells is the immune destruction resistance through the inhibition cytotoxic T cells and NK/T cells, in part by producing TGF- β (Stover et al. 2007). Finally, recent data have also revealed a remarkable symbiotic relationship in energy metabolism between cancer-associated fibroblastic cells and cancer cells. The nature of the symbiosis can evidently vary depending on the TM. In some cases, the cancer-associated fibroblastic cells switch on aerobic glycolysis, utilizing glucose and secreting lactate that is taken up by cancer cells (Balliet et al. 2011). In other cases, the symbiosis is opposite: cancer cells switch on aerobic glycolysis, utilizing glucose and exporting lactate, which the cancer-associated fibroblastic cells then take up and use as fuel to drive their tumor-promoting functional activities (Rattigan et al. 2012) (Figure 7).

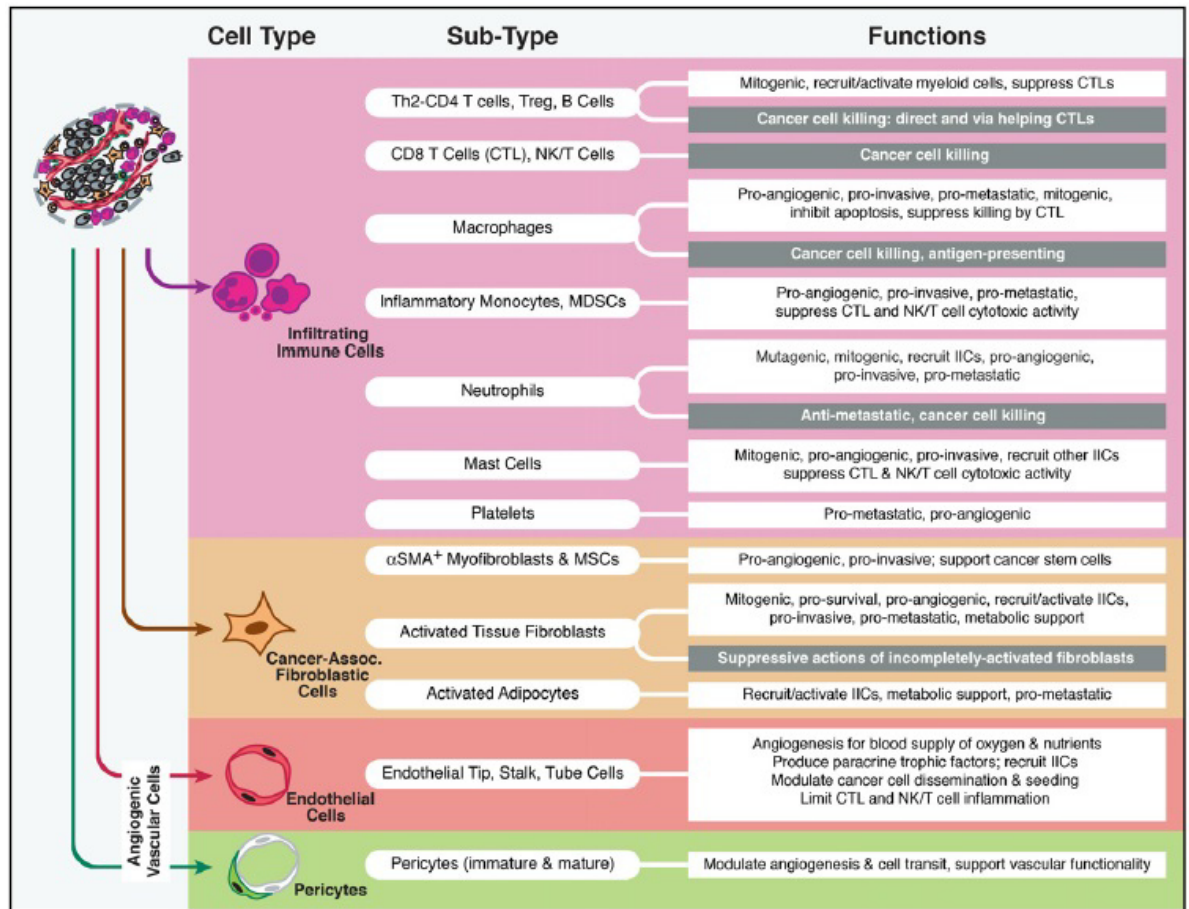


Figure 7. Multiple stromal cell types and subcell types of the tumor microenvironment can variably contribute to, or in some cases oppose, acquisition of the hallmarks of cancer

1.2.3 Cancer-associated fibroblasts (CAFs)

In the early growth of tumors, cancer cells form a neoplastic lesion, called carcinoma in situ (CIS), that is separated from the surrounding tissue and contained within the boundary of a basement membrane. CIS is associated with a stroma similar to that observed during wound healing, and it is commonly referred to as “reactive stroma”. During cancer progression from CIS to invasive carcinoma, the tumor cells invade the reactive stroma. During ductal carcinoma in situ (DCIS) the basement membrane, although intact, is altered, while during invasive ductal carcinoma it is degraded, thus, enabling the direct contact between reactive stroma and cancer cells (Kalluri and Zeisberg 2006) (Figure 8).

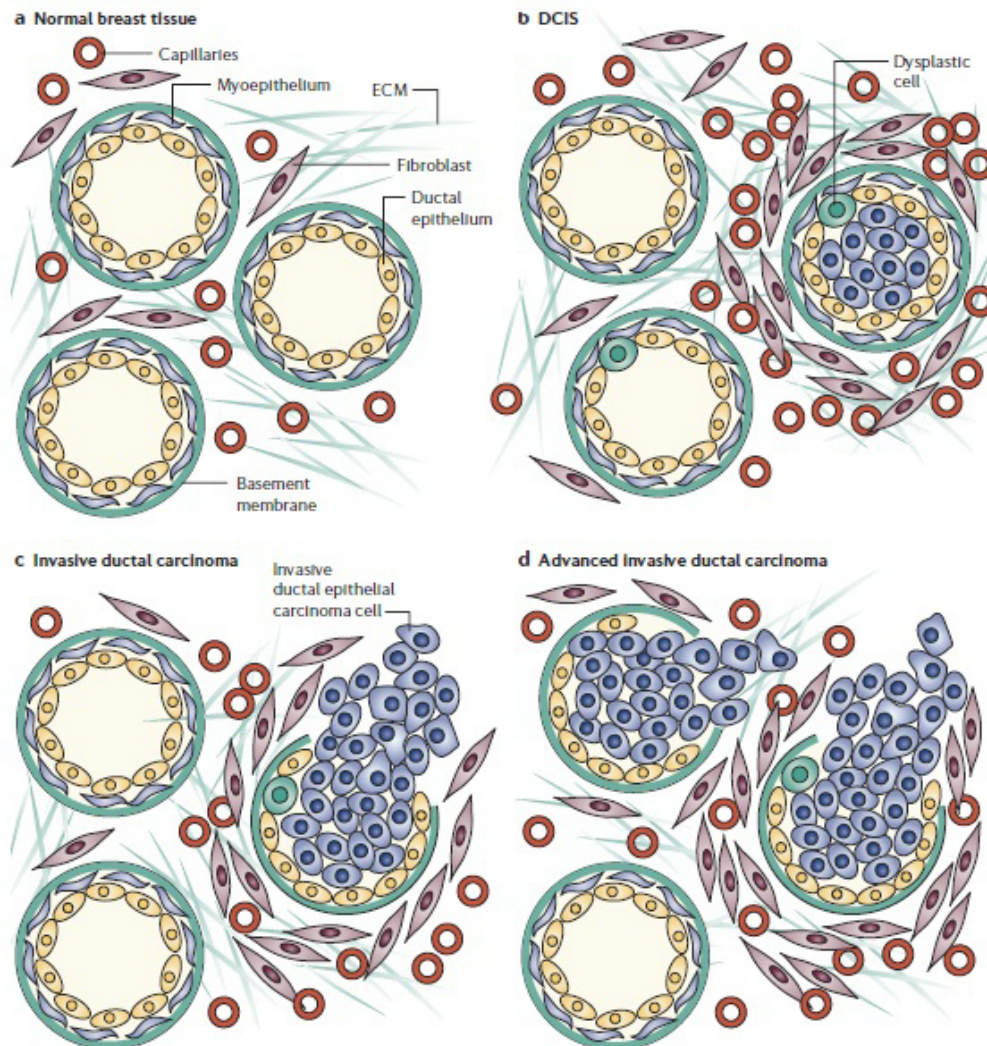


Figure 8. Tumor-stroma interactions during different stages of mammary ductal carcinoma progression

It is becoming increasingly clear that a subpopulation of fibroblasts, the so-called cancer-associated fibroblasts (CAFs), are prominent modifiers of cancer progression.

Activation of fibroblasts

Fibroblasts are non-vascular, non-epithelial and non-inflammatory cells that form the basic cellular component of connective tissue and contribute to its structural integrity. Typically, normal fibroblasts (NFs) appear as fusiform cells, are embedded within the fibrillar ECM of the connective tissue and constitutively express vimentin and fibroblast-specific protein 1 (FSP1). They can interact with their surrounding microenvironment through integrins such as the $\alpha1\beta1$ integrin (Figure 9). In normal conditions, fibroblasts are in an inactive

quiescent state with a low proliferation index and minimum metabolic capacity. Fibroblasts become activated in wound healing and fibrosis, both conditions requiring tissue remodeling. These activated fibroblasts, myofibroblasts, were originally described by Giulio Gabbiani in 1971 during wound healing in granulation tissues. Myofibroblasts differ morphologically and functionally from quiescent fibroblasts. In response to mechanical stress, myofibroblasts acquire contractile stress fibers (microfilament bundles), start to express α -smooth muscle actin (α -SMA), which is instrumental in the force generation, and ED-A splice variant of fibronectin, and form direct cell–cell contacts through gap junctions. Once the wound healing process is completed, most of the myofibroblasts are removed by apoptosis from the granulation tissue (Gabbiani et al. 1971). Active fibroblasts play similar roles in wound healing and in cancer, which is considered as a wound that does not heal (Svoboda et al. 1986). In fact, during wound healing and in cancers, fibroblasts become activated, start to proliferate, secrete higher amounts of ECM components, such as type I collagen, tenascin C, EDA-fibronectin and secreted protein acidic and rich in cysteine (SPARC). Moreover CAFs, like myofibroblasts, are highly heterogeneous, acquire contractile features, and express α -smooth-muscle actin (Polyak and Kalluri 2010) (Figure 9). However, while in normal wounds active fibroblasts are transient, CAFs are persistent in tumors.

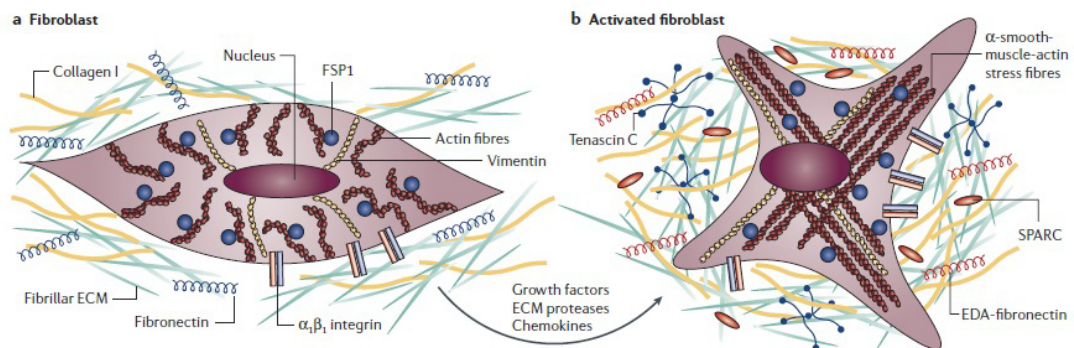


Figure 9. Fibroblast activation

Numerous growth factors such as transforming growth factor- β (TGF- β), chemokines such as monocyte chemotactic protein 1 (MCP1), and ECM-degrading proteases have been shown to mediate the activation of fibroblasts (Kalluri and Zeisberg 2006).

In more detail, three alternative models for the evolution of the stromal fibroblasts present within invasive human carcinomas are:

- **SELECTION:** acquisition of genetic alterations (for instance p53 loss) may allow clonal selection of a small population of fibroblasts or progenitors that have undergone such alterations,

- **TRANS-DIFFERENTIATION:** populations of normal stromal fibroblasts recruited into a tumor may trans-differentiate into CAFs without acquiring any genetic alterations, presumably through TM interaction (suggesting the possibility that CAFs are essentially equivalent to the myofibroblasts present in sites of wound healing and chronic inflammation),
- **DIFFERENTIATION:** stromal myofibroblasts are recruited from specialized circulating progenitor cell types (Orimo and Weinberg 2006) (Figure 10).

The main precursors for activated fibroblasts seem to be the local residing fibroblasts; they can also originate from pericytes and smooth muscle cells from the vasculature or from bone marrow-derived mesenchymal cells. Importantly, CAFs can derive from cancer cells (CCs) or endothelial cells, respectively via epithelial/endothelial–mesenchymal transition (EMT/EndMT), that are biological processes relevant in development, tissue regeneration and cancer progression (Räsänen and Vaheri 2010).

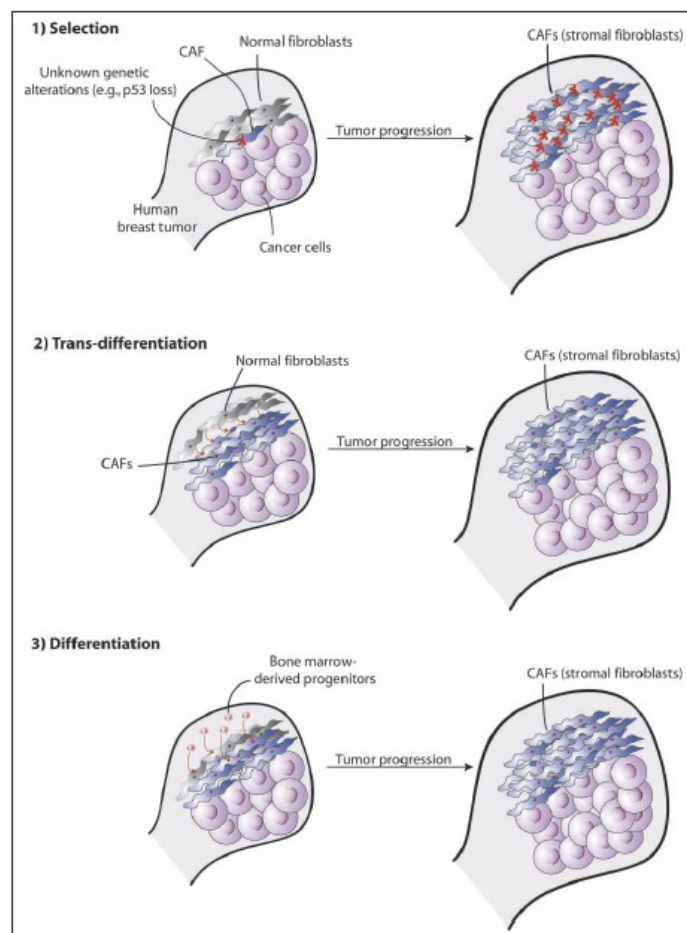


Figure 10. Models for evolution of the stromal fibroblasts in human carcinomas

CAFs in Breast Cancer (BC)

According to Orimo and Weinberg (2006), CAFs, present in human invasive breast carcinoma, release SDF-1, that is responsible for recruiting endothelial progenitor cells (EPCs) into a tumor mass, thereby promoting tumor angiogenesis. In addition, SDF-1 secreted from CAFs enhances tumor growth by direct paracrine stimulation via the chemokine (C-X-C motif) receptor 4 (CXCR4) displayed by human breast carcinoma cells, thereby revealing a second role for stromal SDF-1 in promoting tumor progression in vivo (Figure 11). *Interestingly, both the tumor-enhancing and myofibroblastic properties of CAFs are stably retained by these cells in the absence of ongoing contact with breast carcinoma cells. Accordingly, even though the CAFs appear to have initially acquired a myofibroblastic phenotype under the influence of carcinoma cells, once it is acquired, they display this trait in the absence of further signaling from the carcinoma cells (Orimo et al. 2005).*

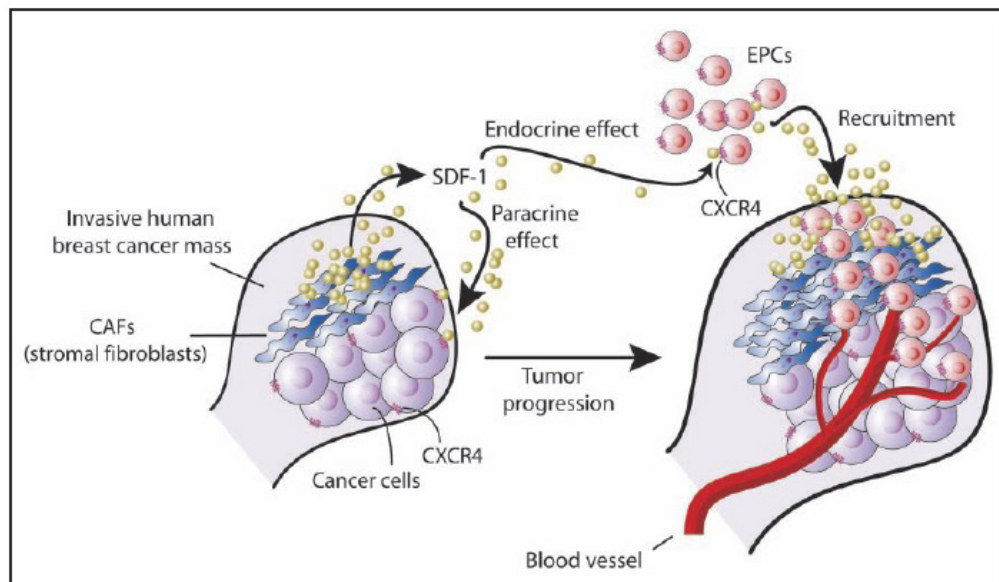


Figure 11. Stromal SDF-1 enhances tumor growth and tumor angiogenesis

In breast tumors, 80% of fibroblasts are in active form. Breast carcinomas can activate stromal fibroblasts through secretion of TGF- β . Consequently, CAFs enhance tumor growth and angiogenesis via secreted mediators such as VEGF-A, MMPs, HGF, SDF-1 and TGF- β too. Importantly, SDF-1 and TGF- β cytokines maintain the active state of stromal fibroblasts through autocrine signaling loops. (Casey et al. 2008, Kojima et al. 2010, Aboussekhra 2011) (Figure 12). CAFs have an important role in progression, invasion and metastasis of BC (Mao et al. 2012). According to Adams (1988), CAFs significantly enhance tumor growth in estrogen receptor (ER)-positive BC through the secretion of higher estradiol levels. Moreover, CAFs can promote

migration in MDA-MB-231 cells and induce EMT in ER-positive cell lines (Hugo et al. 2012). Notably, the inactivation of phosphatase and tensin homolog (PTEN) in CAFs allows BC onset and invasion (Trimboli et al. 2009). Furthermore, it has been shown that CAFs promote breast cancer metastasis through chemokine (C-C motif) ligand 2 (CCL2) secretion (Tsuyada et al. 2012). Recently, it has been shown that Snail1-expressing fibroblasts in the tumor microenvironment display mechanical properties that support metastasis (Stanisavljevic et al. 2015). Finally, breast CAFs have also an important role in therapy resistance. According to Mao et al. (2015), CAFs induce trastuzumab resistance in HER2 positive breast cancer cells.

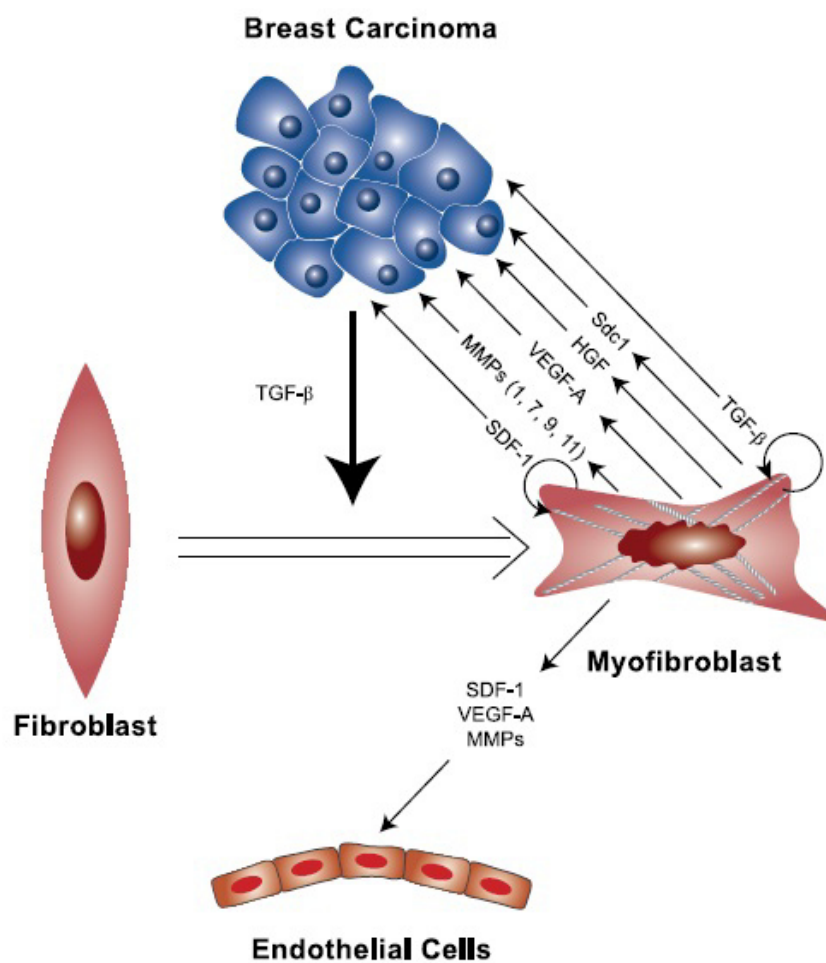


Figure 12. Breast carcinoma-mediated activation of fibroblasts

1.3 Exosomes

1.3.1 Biogenesis and secretion of exosomes

Exosomes were first observed in 1983 in differentiating reticulocytes. It was shown that during reticulocyte maturation, the transferrin receptor and many membrane-associated proteins were shed in small membrane vesicles via an unknown secretory process (Harding et al. 1983). Only in 1987, the word “exosome” was proposed for these extracellular vesicles (EVs) of endosomal origin (Johnstone et al. 1987). Firstly, this process was considered as a way for cells to eliminate unwanted proteins and molecules. However, in recent years, exosomes have emerged as important mediators of cellular communication that are involved in both normal physiological processes, such as lactation, immune response and neuronal function, and also in the development and progression of diseases, such as liver disease, neurodegenerative diseases and cancer. Exosomes have been identified in most bodily fluids, including urine, amniotic fluid, serum, saliva, breast-milk, cerebrospinal fluid, and nasal secretions. Importantly, cancer cells have been shown to secrete exosomes in greater amounts than normal cells, indicating their potential use as biomarkers for diagnosis of disease (Hannafon and Ding 2013).

Exosomes have a diameter of 30-100 nm, and are generally discriminated by size from other EVs: microvesicles, also called ectosomes, (with a diameter of 100–1000 nm), and apoptotic bodies (>1 μm in diameter) (Mittelbrunn and Sánchez-Madrid 2012). Exosomes are formed as intra-luminal vesicles (ILVs) by budding into early endosomes and multi-vesicular bodies (MVBs). In particular, the main mechanisms involved in the biogenesis of ILVs are: the endosomal-sorting complex required for transport (ESCRT) machinery and ESCRT-independent mechanisms. ESCRT consists of four complexes plus associated proteins: ESCRT-0 is responsible for cargo clustering in a ubiquitin-dependent manner, ESCRT-I and ESCRT-II induce bud formation, ESCRT-III drives vesicle scission, and the accessory proteins allow dissociation and recycling of the ESCRT machinery. The main members of the ESCRT family are TSG101 and ALIX (Baietti et al. 2012). Recent studies have shown that also ESCRT-independent mechanisms are involved in ILV formation: these mechanisms involve lipids, tetraspanins, or heat shock proteins. Of note, mammalian cells depleted for key ESCRT components still form MVBs. Exosome biogenesis can be mediated by lipids such as ceramide, cholesterol, phosphatidic acid (Trajkovic et al. 2008, Ghossoub et al. 2014). On the other hand, four-transmembrane domain proteins of the tetraspanin family (for instance CD63, CD81) have recently been proposed as instrumental in selecting cargoes for exosome secretion (van Niel et al. 2011, Perez-Hernandez et al. 2013). Finally, recent studies have shown that the chaperone HSC70 allows the selective transfer of cytosolic proteins containing a KFERQ-motif to ILVs (Sahu et al. 2011). It is still unknown whether these mechanisms act

simultaneously on the same MVB or on different MVBs. The fate of MVBs can be either fusion with lysosomes or fusion with the plasma membrane, which allows the release of their content to the extracellular milieu. Several RAB proteins (RAB11, RAB27 and RAB35) have been shown to be involved in the transport of MVBs to the plasma membrane and in exosome secretion (Stenmark 2009, Savina et al. 2005, Hsu et al. 2010). Interestingly, the involvement of RAB27A in vesicle secretion was confirmed in numerous tumor cell lines: murine melanoma (Peinado et al. 2012) and mammary carcinoma (Bobrie et al. 2012). The last and least characterized step of exosome biogenesis consists of the fusion of the MVBs with the plasma membrane, with consequent release of the EVs into the extracellular space. The soluble NSF-attachment protein receptor (SNARE) complex has been implicated in this process, and the Ca²⁺-regulated vesicle-associated membrane protein 7 (VAMP7), a member of the SNARE complex, appears to be necessary for MVB fusion with the plasma membrane in leukemic cells, but not in MDCK cells (Fader et al. 2009, Proux-Gillardeaux et al. 2007, Kowal et al. 2014) (Figure 13).

Once secreted, exosomes can bind to cells through receptor–ligand interactions, similar to cell–cell communication mediating, for example, antigen presentation. Alternatively, exosomes could putatively attach or fuse with the target-cell membrane, delivering exosomal surface proteins and perhaps cytoplasm to the recipient cell. Finally, exosomes may also be internalized by the recipient cells by mechanisms such as endocytosis (Valadi et al. 2007).

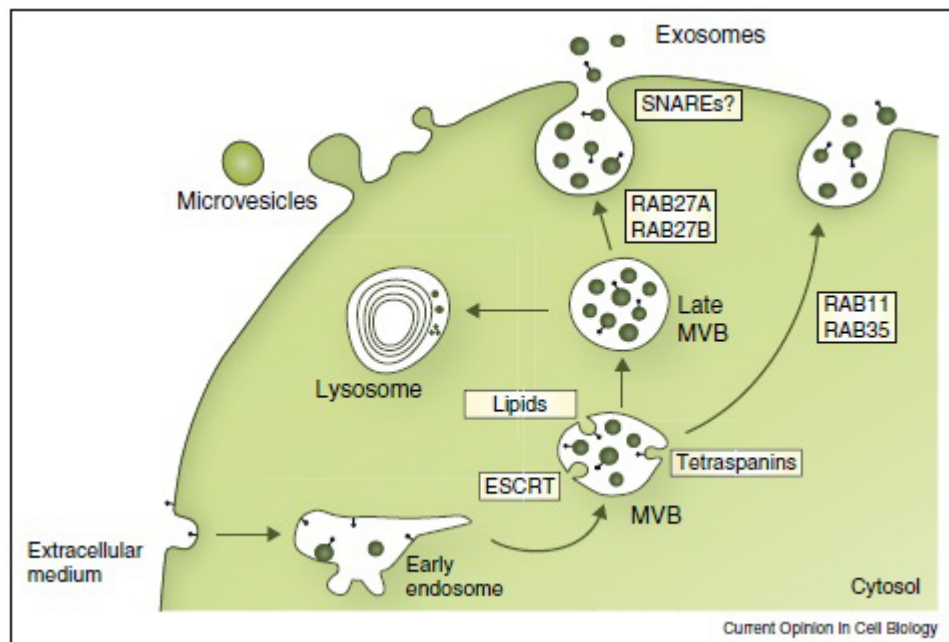


Figure 13. Exosome biogenesis and secretion

1.3.2 Exosome composition

Over the years, it has been recognized that not only the contents inside the exosomes but also the components in exosome structure can influence distant cell signaling. Primarily, exosomes carry proteins: membrane transport proteins and fusion proteins, such as RAB GTPases, annexins, flotillins, and MVB biogenesis proteins, such as Alix and tumor susceptibility gene Tsg101. Additionally, the protein families that are associated with lipid micro-domains, such as integrins and tetraspanins, such as CD9, CD81, CD82, CD83, and CD63 are also important part of exosome. The pool of exosome proteins are both conserved and also cell type specific, depending on the cells from where exosomes are secreted. Heat shock proteins (Hsp), CD63 and tetraspanins are the most prominent evolutionary conserved proteins in exosomes. Cytoskeleton and metabolism-related proteins form the pool of other frequently found proteins that include β -actin, tubulins, myosin, cofilin, glyceraldehyde 3-phosphate dehydrogenase, and major histocompatibility complex (MHC) classes I and II molecules. The lipid content of exosomes can be categorized into two types either conserved or matching the characteristics of the cell from where they are originating. These structural lipids do not only give shape to exosomes, but have also shown to take part in cell communication. Exosomes are enriched in lipids that are associated with lipid rafts: sphingolipids, cholesterol, glycerophospholipids, and ceramide that have characteristic elongated saturated fatty-acyl chains. Exosomal signaling mediators include prostaglandins, arachidonic acid, phospholipase A2, phospholipases C and D (Azmi et al. 2013). In 2007, Valadi and colleagues have elucidated that exosomes contain also mRNA and microRNAs. Recently, Sato-Kuwabara and colleagues (2015) have demonstrated that exosomes contain also non-coding RNAs and Melo and colleagues (2014) have shown that breast cancer associated exosomes contain miRs associated with RNA-induced silencing complex(RISC)-laoding complex, thus displaying cell-indipendent capacity to process precursor microRNAs (Figure 14).

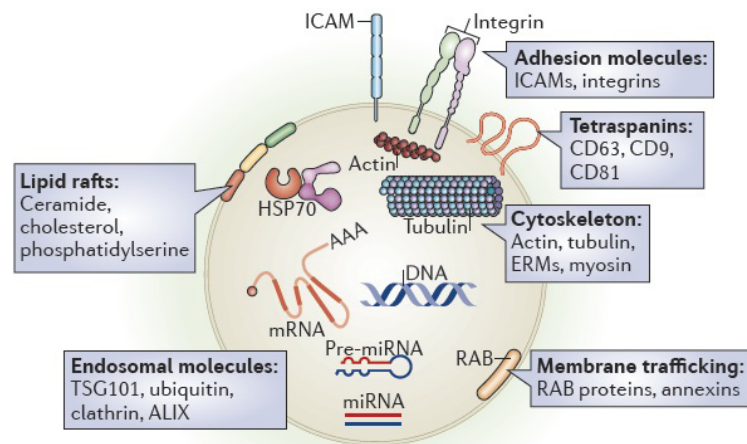


Figure 14. Exosome composition

1.3.3 The sorting mechanisms and the function of exosomal miRs

Recently, mRNAs and microRNAs have been identified in exosomes, which can be taken up by neighboring or distant cells and subsequently modulate recipient cells. microRNAs are a class of 17–24 nucleotides small, non coding RNAs, which mediate post-transcriptional gene silencing by binding to the 3'-untranslated region or open reading frame region of target mRNAs. miRs are involved in many biological activities such as cell proliferation, cell differentiation, cell migration, disease initiation, and disease progression. Their dysregulation plays an essential role in the development and progression of cancer: miRs are up- or down-regulated in malignant tissues compared to the normal counterpart, thereby they can be considered as oncogenes or tumor-suppressors, respectively. Accumulating evidence has shown that miRs can stably exist in body fluids, including saliva, urine, breast milk, and blood. In addition to being packed into exosomes or microvesicles, extracellular miRs can be loaded into high-density lipoprotein, or bound by AGO2 protein outside of vesicles (Garofalo et al. 2014). All these three modes of action protect miRs from degradation and guarantee their stability.

There are *four potential modes for sorting of miRs into exosomes*, although the underlying mechanisms remain largely unclear. These include:

- the neural sphingomyelinase 2 (nSMase2)-dependent pathway (Kosaka et al. 2013),
- the miR motif and sumoylated heterogeneous nuclear ribonucleoproteins (hnRNPs)-dependent pathway (the GGAG motif in the 3' portion of miR sequences causes specific miRs to be packed into exosomes) (Villarroya-Beltri et al. 2013),
- the 3'-end (uridylylated or adenylated) of the miR sequence-dependent pathway (Koppers-Lalic et al. 2014),
- the miR induced silencing complex (miRISC)-related pathway (AGO2 could act in exosomal miR sorting) (Melo et al. 2014).

In summary, specific sequences present in certain miRs may guide their incorporation into exosomes, whereas some enzymes or other proteins may control sorting of exosomal miRs as well in a miR sequence-independent fashion.

According to Goldie and colleagues (2014), among small RNAs, the proportion of miRs is higher in exosomes than in their parent cells. As some profiling studies have shown, miRs are not randomly incorporated into exosomes. Guduric-Fuchs and colleagues (2012) have analyzed miR expression levels in a variety of cell lines and their respective derived exosomes, and have found that a subset of miRs (miR-150, miR-142-3p, and miR-451) preferentially entered exosomes. Similarly, Ohshima and colleagues (2010) have found that members of the let-7 miR family were abundant in exosomes derived from gastric cancer cell lines, but were less abundant in exosomes derived from other cancer cells. Moreover, some reports have shown that exosomal miR expression levels are altered under different physiological conditions. The level of miR-21 was lower in exosomes from the serum of healthy donors than those glioblastoma

patients (Skog et al. 2008). Levels of let-7f, miR-20b, and miR-30e-3p were lower in vesicles from the plasma of non small-cell lung carcinoma patients than normal controls (Silva et al. 2011). *All these studies show that parent cells possess a sorting mechanism that guides specific intracellular miRs to enter exosomes.*

The miRs in cell-released exosomes can circulate with the associated vehicles to reach neighboring cells and distant cells. After being delivered into acceptor cells, exosomal miRs play functional roles. The *functions of exosomal miRs* can be generally classified into two types. One is the conventional function: the negative regulation of target genes. For example, exosomal miR-105 released from breast cancer cell lines reduced ZO-1 gene expression in endothelial cells and promoted metastases to the lung and brain (Zhou et al. 2014). Another example is the exosomal miR-92a, derived from leukemia cells. miR-92a significantly reduced the expression of integrin $\alpha 5$ in endothelial cells and enhanced endothelial cell migration and tube formation (Umezu et al. 2012). The other function is a novel mechanism that has been identified in some miRs such as exosomal miR-21 and miR-29a, that in addition to the classic role of targeting mRNAs, were first discovered to have the capacity to act as ligands that bind to toll-like receptors (TLRs) and activate immune cells (Fabbri et al. 2012). In summary, *the transfer of exosomal miRs is a new mechanism of intercellular communication that can initiate and promote tumor progression.* Finally, the amount and composition of exosomal miRs released in biologic fluid, such as urine and blood, can differ between patients with disease and healthy individuals. Thus, *exosomal miRs have a potential role as noninvasive biomarkers to indicate disease states* (Lin et al. 2015).

1.3.4 Exosomes in cancer development and metastasis

Over the last decade, a number of studies have revealed that *exosomes influence major tumor-related pathways, such as hypoxia-driven epithelial-to-mesenchymal transition, cancer stemness, angiogenesis, and metastasis* (Azmi et al. 2013) (Figure 15). Grange and colleagues (2011) have shown that exosomes released from human renal cancer stem cells stimulated angiogenesis and formation of lung pre-metastatic niche. A number of studies have indicated that hypoxia promotes exosome secretion in different tumor types. In a breast model, King and colleagues (2012) showed that hypoxia-mediated activation of HIF-1 α enhanced the release of exosomes and resulted in aggressive cell phenotype. While in a kidney tumor model, Borges and colleagues (2013) showed that TGF- β 1-containing (a promoter of EMT) exosomes from injured epithelial cells activated fibroblasts to initiate tissue regenerative response and fibrosis. In 2012, Peinado and colleagues have demonstrated that exosomes from highly metastatic melanomas increased the metastatic behavior of primary tumors by permanently ‘educating’ bone marrow progenitors through the receptor tyrosine kinase MET. Moreover, Luga and colleagues (2012) have

shown that fibroblast-derived exosomes promoted breast cancer cell protrusive activity and motility via Wnt-planar cell polarity signaling. Interestingly, tumor derived exosomes can reprogram fibroblasts to CAFs through TGF- β , thereby enhancing tumor progression (Webber et al. 2015). Recently, Khokha's group has demonstrated that cancer cell motility was induced by exosomes released from CAFs silenced for tissue inhibitor of metalloproteinases (TIMP). In this system, TIMP knock down resulted in increased expression of the metalloproteinase ADAM10 in the exosomes (Shimoda et al. 2014).

Notably, *exosomes regulate also immune response*. For instance, Zhang and colleagues (2006) have demonstrated that membrane form of TNF-alpha secreted in exosomes prevented cytotoxic T cell activation induced cell death. Finally, *exosomes have an important role in therapy resistance too*. Khan and colleagues (2009) have shown that exosomal secretion of survivin suppressed the efficacy of proton irradiation in a cellular model. In another study, Safaei and colleagues (2005) have shown that exosomes mediated cisplatin resistance in ovarian cancer. More recently, Ciravolo and colleagues (2012) have elucidated a potential role of HER-2-overexpressing exosomes in trastuzumab resistance.

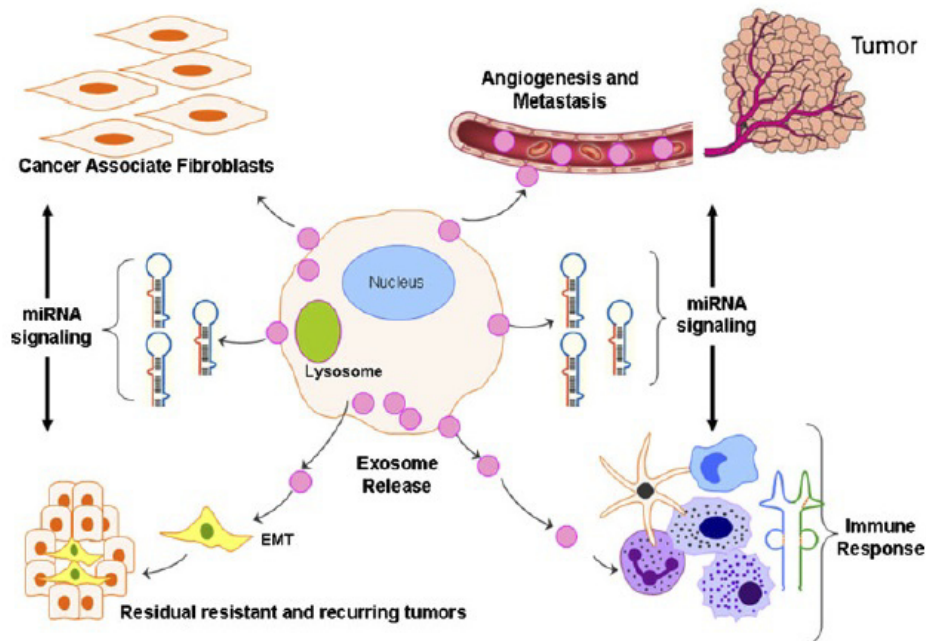


Figure 15. Role of exosomes in cancer progression

2. AIM OF THE STUDY

Despite many novel therapeutic approaches, breast cancer remains one of the leading cause of cancer mortality among women. Recent findings indicate that cancer-associated fibroblasts (CAFs), the major components of the tumor microenvironment (TM), play a crucial role in breast cancer progression, but how they promote tumorigenesis is poorly understood. Increasing evidence indicates that exosomes and their cargo, including microRNAs (miRs), may vehiculate between cells and affect the biological behavior of recipient cells. Therefore, one alternative mechanism of the promotion of breast cancer progression by CAFs may be through CAF-secreted exosomes, which would deliver oncogenic miRs (oncomiRs) to breast cancer cells. Thus, the aim of this study is to analyze the tumor-stroma interactions mediated by exosomes within the TM. In particular, we aim to identify the oncomiRs up-regulated in CAF exosomes that could have a significant role in breast cancer. Finally, we intend to clarify the mechanisms underlying protumorigenic actions of CAF exosomes and exosomal miRs in breast cancer.

3. MATERIALS AND METHODS

3.1 Primary and continuous cells and mammosphere cultures

Breast cancer cell line T47D, from ATCC, was grown in RPMI-1640. Primary cultures of fibroblasts, from “Clinica Mediterranea” (NA), were grown in Dulbecco’s Modified Eagle’s Medium/Nutrient F12-Ham (DMEM-F12). Media were supplemented with 10% heat-inactivated fetal bovine serum (FBS) and 100 U/ml penicillin/streptomycin. All media and supplements were from Sigma-Aldrich (Milan, Italy).

For mammosphere cultures, single cell suspensions were plated at a density of 1,000 cells/ml in Corning ultra-low attachment multiwell plates. Cells were grown in *stem medium*: a serum-free DMEM-F12 (Sigma, Milan, Italy), supplemented with B27 (Life technologies, Milan, Italy), 10 ng/ml EGF (Sigma, Milan, Italy) and 20 ng/ml bFGF (BD Biosciences, Milan, Italy) and 1X antibiotic-antimycotics (Life technologies, Milan, Italy). After 4-7 days, mammospheres appeared as spheres of floating viable cells.

3.2 Isolation of primary cell cultures from human breast biopsies

Human breast biopsies (samples from “Clinica Mediterranea”, NA) were cut by mechanical fragmentation with sterile scissors and tongs. Then, the tissue extracellular matrix was digested through enzymatic digestion (treatment with collagenase (Sigma-Aldrich), overnight, in continuous agitation, at 37°C). The drawn cellular suspensions were separated on the basis of their weights by two different centrifugations: the first one at 500 rpm for 5 minutes to obtain epithelial cell pellets, the second one at 1200 rpm 5 minutes to obtain fibroblast pellets.

3.3 Immunocytochemistry

The separation between epithelial cells and fibroblasts from human breast biopsies was confirmed by using the cell block technique (Shandon cytoblock kit) followed by immunocytochemistry, in collaboration with Professor Terracciano. A primary antibody was used for CK22 (pan-keratin), a known epithelial marker, in order to discriminate epithelial cells from fibroblasts.

3.4 Exosome isolation

Exosomes were isolated from cell culture media of primary fibroblasts that were grown in DMEM-F12 (Sigma-Aldrich), supplemented with 10% Exo-FBS (FBS depleted of exosomes, SBI, System Biosciences) and 1X antibiotic-antimycotics (Life technologies, Milan, Italy). The appropriate culture media were centrifuged at 3000 g 15 minutes at 4°C or RT to remove cellular debris. The supernatants were transferred into sterile tubes and an appropriate volume of the ExoQuick-TC™ Exosome Isolation Reagent (SBI, System Biosciences) was added, considering 2 ml of ExoQuick-TC™ solution every 10 ml of cell culture medium. Then, the tubes were subjected to mild agitation until the separation between the two phases was no longer visible. Finally, the tubes were kept at 4°C O/N (12 hours at least were necessary). The following day the solutions with the ExoQuick™ Reagent and cell media were centrifuged firstly at 1500 g for 30 minutes, and then at 1500 g for 5 minutes, both centrifugations at 4°C or RT. At the end of the steps, white/beige exosomal pellets appeared.

3.5 Cell transfection

For miR transient overexpression/downregulation, cells at 50% confluence were transfected using Oligofectamine (Invitrogen, Milan, Italy) and 100nM of pre-miR-21, pre-miR-143-3p, pre-miR-378e, scrambled pre-miR, or 200nM of anti-miR-21, anti-miR-143-3p, anti-miR-378e, scrambled anti-miR (Ambion®, Life Technologies).

Transfection of CAFs with Cy3-labeled-miRs

CAFs were transfected with 10nM of Cy3-labeled-miRs (miR-21-5p, miR-143-3p, miR-378e, Tebu-bio, San Diego, CA) using Oligofectamine (Invitrogen, Milan, Italy). Six hours after transfection, cells were washed two times with PBS, and the culture media were switched to fresh DMEM-F12 1% A/A, 10% exo-FBS. After incubation for a day, the culture media were collected and used for exosome preparation.

3.6 RNA extraction and Real Time PCR

Total RNAs (microRNAs and mRNAs) were extracted using Trizol (Invitrogen, Milan, Italy) according to the manufacturer's protocol. Reverse transcription of total RNA was performed starting from equal amounts of total RNA/sample (150/500ng) using miScript reverse Transcription Kit (Qiagen, Milan, Italy) for miR analysis, and using SuperScript® III Reverse Transcriptase (Invitrogen, Milan, Italy) for mRNA analysis. Quantitative analysis of miR-21, miR-143, miR-378e and RNU6A (as an internal reference) was performed by Real Time PCR using specific primers (Qiagen, Milan, Italy) and miScript SYBR Green PCR Kit (Qiagen, Milan, Italy). Real Time

PCR was also used to assess the mRNAs of NANOG, OCT3/4, SOX2, SNAIL and β -ACTIN (as an internal reference), using iQTM SYBR Green Supermix (Bio-Rad, Milan, Italy). The primer sequences were:

NANOG-FW: 5'-CAAAGGCAAACAACCCACTT-3',
NANOG-RV: 5'-TCTGGAACCAGGTCTTCACC-3',
OCT3/4-FW: 5'-CGAAAGAGAAAGCGAACCAG-3',
OCT3/4-RV: 5'-GCCGGTTACAGAACCACACT-3',
SOX2-FW: 5'-GCACATGAACGGCTGGAGCAACG-3',
SOX2-RV: 5'-TGCTGCGAGTAGGACATGCTGTAGG-3',
SNAIL-FW: 5'-AGTGGTTCTTCTGCGCTACT-3',
SNAIL-RV: 5'-GGGCTGCTGGAAGGTAAACT-3',
ACTIN-FW: 5'-TGCGTGACATTAAGGAGAAG-3',
ACTIN-RV: 5'-GCTCGTAGCTCTTCTCCA-3'.

The reaction for detection of mRNAs was performed in this manner: 95 °C for 5', 40 cycles of 95 °C for 30'', 62 °C for 30'' and 72 °C for 30''. The reaction for detection of miRs was performed in this manner: 95 °C for 15', 40 cycles of 94 °C for 15'', 55 °C for 30'' and 70 °C for 30''. All reactions were run in triplicate. The threshold cycle (CT) is defined as the fractional cycle number at which the fluorescence passes the fixed threshold. For relative quantization, the $2^{(-\Delta\Delta CT)}$ method was used. Experiments were carried out in triplicate for each data point, and data analysis was performed by using Applied Biosystems StepOnePlusTM Real-Time PCR Systems.

3.7 NCounter miRNA assay

Exosomes were isolated from four different samples of primary fibroblasts: two normal and two cancer-associated fibroblasts. Then, exosomal RNA was extracted in order to perform an “nCounter miRNA assay” (nanoString Technologies, OSU, Columbus, OHIO). Eight-hundred human miRs were digitally detected and counted in a singol reaction without amplification. System performance consisted of 6 positive miRNA assay controls, 6 negative miRNA assay controls, and 5 mRNA housekeeping controls. 100ng of purified total RNA was used as starting material. miR expression levels were measured calculating the ratio of geom. means (Normal fibroblast exosomes vs CAF exosomes).

3.8 Protein isolation and Western blotting

Cells were washed twice in ice-cold PBS, and lysed in JS buffer (50mM HEPES ph 7.5 containing 150mM NaCl, 1% Glycerol, 1% Triton X100, 1.5mM MgCl₂, 5mM EGTA, 1mM Na₃VO₄, and 1X protease inhibitor cocktail). Exosomes were lysed in RIPA lysis buffer (Sigma-Aldrich) containing protease and phosphatase inhibitors (Roche Diagnostics GmbH,

Mannheim, Germany). Protein concentration was determined by the Bradford assay (Bio-Rad, Milan, Italy) using bovine serum albumin (BSA) as the standard, and equal amounts of proteins were analysed by SDS-PAGE (12% or 15% acrylamide). Gels were electroblotted onto nitrocellulose membranes (GE Healthcare, Milan, Italy). For immunoblot experiments, membranes were blocked for 1 hour with 5% non-fat dry milk in Tris Buffered Saline (TBS) containing 0,1% Tween-20, and incubated at 4°C overnight with primary antibodies. Detection was performed by peroxidase-conjugated secondary antibodies using the enhanced chemiluminescence system (Thermo, Euroclone, Milan, Italy). Primary antibodies used were: anti- β -actin and anti- α -tubulin from Sigma-Aldrich (Milan, Italy), anti- α -SMA, anti-E-cadherin, anti-ZEB, anti-OCT3/4, anti-NANOG, anti-SNAIL, anti-CD63, anti-hsp70, anti-ALIX, anti-TSG101 from Santa Cruz Biotechnology (CA, USA).

3.9 Immunofluorescence analysis

Uptake of fibroblast exosomes by T47D cells

Once isolated, exosomes were labeled with PKH26, a red fluorescent cell membrane linker (Sigma-Aldrich). For immunofluorescence, cells grown on glass coverslips were treated at different incubation times with PKH26-exosomes, washed six times with PBS and fixed with 4% paraformaldehyde in PBS for 20 minutes at room temperature. The coverslips were washed three times in PBS. Then, cells were permeabilized with PBS 0.5% Triton X-100 for 15 minutes at room temperature, and blocked in PBS 1% bovine serum albumin (BSA) for 15 minutes. Cells were incubated with anti-tubulin antibody (Santa Cruz), diluted in PBS 1% BSA, for 1 hour at 37°C. Coverslips were washed 3 times with PBS and treated with Alexa Fluor 488 Goat Anti-Mouse IgG (Invitrogen) for 30 minutes at 37°C. Coverslips were washed and mounted with Gold antifade reagent with DAPI (Invitrogen). The cells were visualized by confocal microscopy.

Shuttling assays for fluorescently-labeled miRNAs

After a day from the transfection of CAFs with Cy3-labeled-miRs, exosomes were isolated from cell media, and T47D cells grown on glass coverslips were treated for 24 hours with the isolated exosomes. For immunofluorescence, it was used the same protocol as above, but cells were incubated with anti-CD63 primary antibody (Santa Cruz), then with Alexa Fluor 488 Goat Anti-Rabbit IgG (Invitrogen).

3.10 TGF- β treatment

TGF- β 2 human recombinant (SRP3170-5UG, Sigma-Aldrich) was used at a final concentration of 10ng/ml for 48 hours. It was added every 24 hours to fibroblast primary cultures grown in DMEM-F12 1% A/A, 10% exo-FBS.

3.11 Mammosphere formation assay

T47D cells were suspended 1000 cells/well in 1 ml of stem medium and plated into ultra-low attachment 48-well plates in presence of normal fibroblast or CAF exosomes. Alternatively, T47D cells were transfected with miRs or anti-miRs for 48 hours or 24 hours, respectively. Then, 1000 cells/well were suspended in 1 ml of stem medium and plated into ultra-low attachment 48-well plates. After 4-7 days, the formed mammospheres were counted, and the diameters were measured.

3.12 Statistical analysis

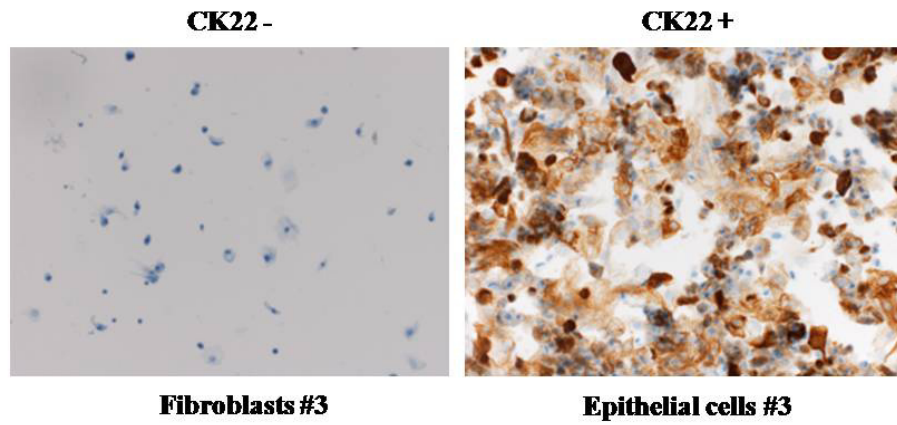
All experiments were repeated at least three times. Continuous variables are given as mean \pm standard deviation. For comparisons between two groups, the Student's t test was used to determine differences between mean values for normally distributed. Comparisons among more than three groups were determined by one-way ANOVA followed by Bonferroni's *post hoc* testing. All data were analyzed for significance using GraphPad Prism 6 software (San Diego, CA, USA). *P* values less than 0.05 were considered significant.

4. RESULTS

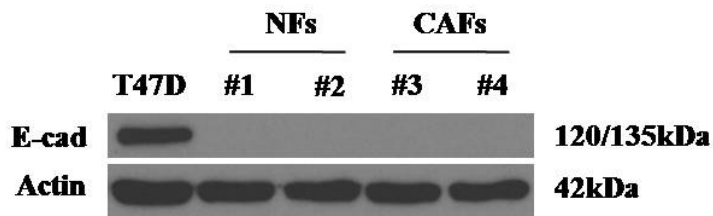
4.1 Isolation and characterization of primary fibroblasts from human breast biopsies

Derivate primary cultures of breast fibroblasts is an important starting point for studying the interactions between the microenvironment and breast cancer. In order to obtain primary fibroblast cultures, we cut human breast biopsies by mechanical fragmentation with sterile scissors and pliers. Then, we subjected the tissue extracellular matrix to enzymatic digestion. The next day, we separated the drawn cellular suspensions on the basis of their weights by two different centrifugations: with the first centrifugation (500 rpm 5') we obtained pellets of epithelial cells, then, with the centrifugation of the obtained supernatants (1200 rpm 5') we isolated fibroblasts. The correct separation of these two different cell populations was confirmed by using the cell block technique (Shandon cytoblock kit) followed by immunocytochemistry for CK22 (pan-keratin), a known epithelial marker (in collaboration with Professor Terracciano's lab) (Figure 16a). Moreover, we verified that fibroblast cultures were negative for E-cadherin by western blot analysis. Since α -SMA is a known CAF marker, we evaluated whether this protein was overexpressed in CAFs respect to normal fibroblasts by western blot analysis. As expected, fibroblasts were negative for E-cadherin (Figure 16b) and CAFs overexpressed the protein α -SMA as compared to normal fibroblasts (NFs) (Figure 16c).

a



b



c

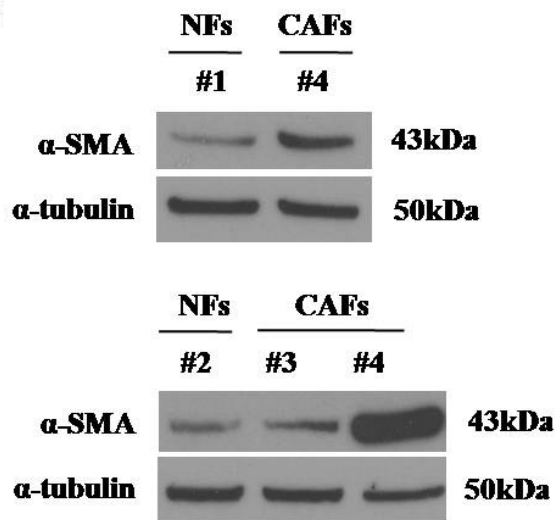


Figure 16. Characterization of human breast fibroblasts. The correct separation of cell populations of the patient #3 biopsy was confirmed: fibroblasts were CK22 negative (CK22-), whereas epithelial cells resulted CK22 positive (CK22+) (a). Cancer-associated fibroblasts (CAFs), patients #3 and #4, overexpressed α -SMA as compared to normal fibroblasts (NFs), patients #1 and #2 (c). All the fibroblasts were E-cadherin (E-cad) negative as compared to the positive control, T47D cells (b). Actin (b) and α -tubulin (c) were used as loading controls.

4.2 Identification of exosomal proteins in breast fibroblast exosomes

To characterize breast fibroblast exosomes, isolated with ExoQuick-TC™ solution, we performed a western blot analysis for different types of exosomal proteins: the tetraspanin CD63, the heat shock protein Hsp70 and the endosomal proteins, Alix and Tsg101. As shown in Figure 17, we confirmed that these exosomal markers were expressed both in normal fibroblast exosomes (patients #5, #6 and #10) and in CAF exosomes (patients #7, #9 and #11).

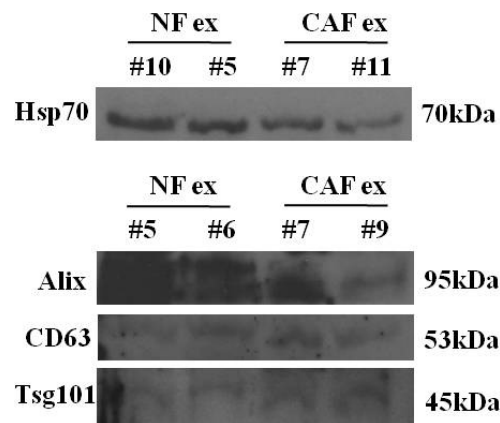


Figure 17. Exosomal markers. Exosomal proteins (Hsp70, Alix, CD63, Tsg101) were expressed in breast fibroblast exosomes, both in normal fibroblast exosomes (NF ex) and in CAF exosomes (CAF ex).

4.3 Identification of oncogenic miRs in CAF exosomes

To identify oncogenic miRs in CAF exosomes, we set up a genome-wide expression profiling of miRs (nCounter miRNA assay, nanoString Technologies, OSU) comparing exosomal miRs derived from two breast CAFs (patients #3 and #4) and two normal fibroblasts (patients #1 and #2). We found that three miRs were significantly up-regulated in CAF exosomes respect to normal fibroblast exosomes: miR-21-5p, miR-378e, and miR-143-3p (Table 1). Then, we validated the array data by Real Time PCR. As shown in Figure 18, we confirmed that these miRs were up-regulated in CAF exosomes respect to NF exosomes. Notably, we found an up-regulation of miR-143-3p also in CAF cells as compared to NF cells, but we did not observe the same for both miR-21-5p and miR-378e (Figure 18).

	Ratio of geom means: NF exosomes vs CAF exosomes	Unique id
1	0,537960845	hsa-miR-21-5p
2	0,703937608	hsa-miR-378e
3	0,768350227	hsa-miR-143-3p
4	0,795360008	hsa-miR-1246
5	0,813311489	hsa-miR-1253
6	0,880781514	hsa-miR-155-5p
7	0,938786077	hsa-miR-549
8	1,032793771	hsa-miR-125b-5p
9	1,228928787	hsa-miR-1283
10	1,256584027	hsa-miR-25-3p
11	1,294286206	hsa-miR-302d-3p

Table 1. miRNA expression profiles in NF exosomes vs CAF exosomes. Three miRs were significantly up-regulated in CAF exosomes as compared to NF exosomes.

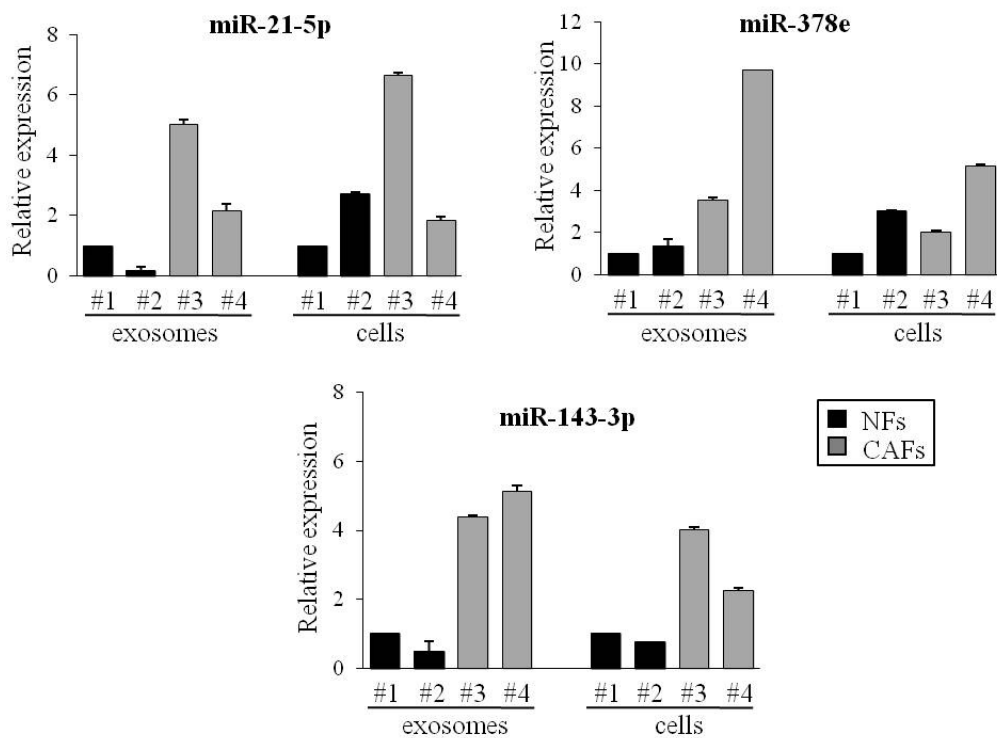


Figure 18. Array validation. Real Time PCR of miR-21, miR-378e, and miR-143 expression levels in fibroblast exosomes and cells.

4.4 TGF- β increases miR-21, miR-143, and miR-378e levels in normal fibroblast exosomes

We wondered whether TGF- β , in addition to its direct role in the activation of normal fibroblasts to CAFs, could play a role in the overexpression of these miRs. To this aim, we treated two normal fibroblasts (patients #2 and #5) with TGF- β at the final concentration of 10ng/mL for 48 hours. Then, we performed a Real Time PCR to evaluate the exosomal levels of miR-21, miR-143 and miR-378e. We found that exosomes isolated from TGF- β -treated-fibroblasts exhibited increased levels of these miRs as compared to exosomes isolated from non treated-fibroblasts (Figure 19).

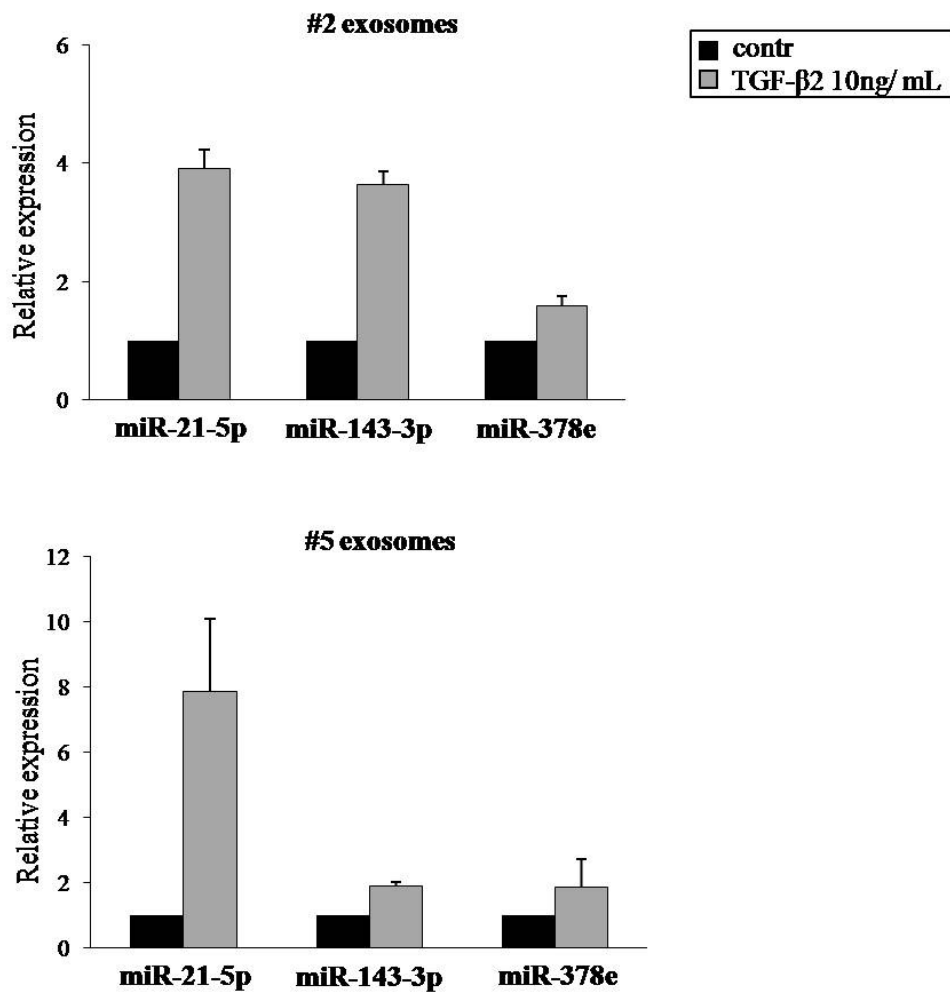


Figure 19. TGF- β increases miR-21, miR-143, and miR-378e levels in normal fibroblast exosomes. Real Time PCR of miR-21, miR-378e, and miR-143 expression levels in exosomes isolated from normal fibroblasts (patients #2 and #5) treated or not with TGF- β (10ng/mL).

4.5 Breast fibroblast-derived exosomes are transferred to T47D cells

To examine whether fibroblast exosomes could be transferred to breast cancer cells (T47D), we isolated exosomes from both normal and cancer-associated fibroblast conditioned media and we fluorescently labeled them with PKH26. Then, we cultured T47D cells with PKH26 fluorescently labeled exosomes for different times (30 minutes and 24 hours). Then, we stained the treated T47D cells using blue DAPI (nuclei) and green ALEXA488-conjugated anti-tubulin antibody. As shown in Figure 20, we confirmed the ability of T47D cells to uptake NF- (patients #2 and #6) and CAF- (patient #3) exosomes using a confocal microscopy. Notably, as shown in Figure 20b, we observed the best uptake after 24 hours of exosome treatment. To get further evidence for exosome uptake, we collected a z-stack of six images (Figure 21). NF exosomes (patient #6, Figure 21a) and CAF exosomes (patient #3, Figure 21b) were clearly uptaken from T47D cells after 24 hours of treatment, as demonstrated by the co-localization of ALEXA488 and PKH26 signals. These results indicate that NF- and CAF- derived exosomes can be transferred into T47D cells, suggestive of a potential role in regulating breast cancer biology.

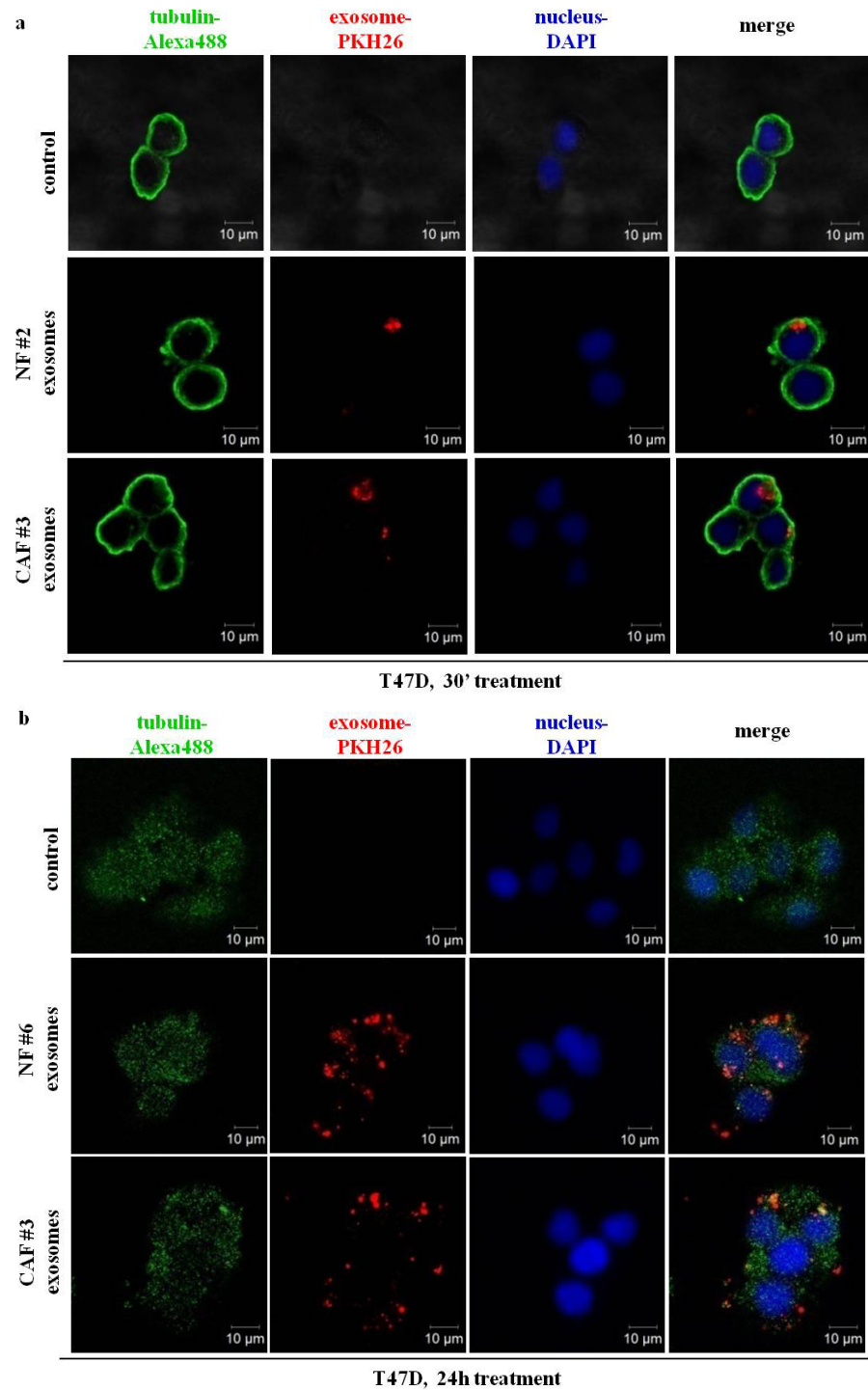


Figure 20. Breast fibroblast-derived exosomes are transferred to T47D cells. T47D cells were cultured in absence (control) or in presence of NF- (patients #2 and #6) or CAF- (patient #3) derived PKH26-labeled exosomes for 30 minutes (a) or 24 hours (b). Exosomes were uptaken from T47D cells, as shown using a confocal microscope (original magnification, $\times 60$). T47D cells

were stained using DAPI (nuclei) and ALEXA488-conjugated anti-tubulin antibody. Scale bar: 10 μ m.

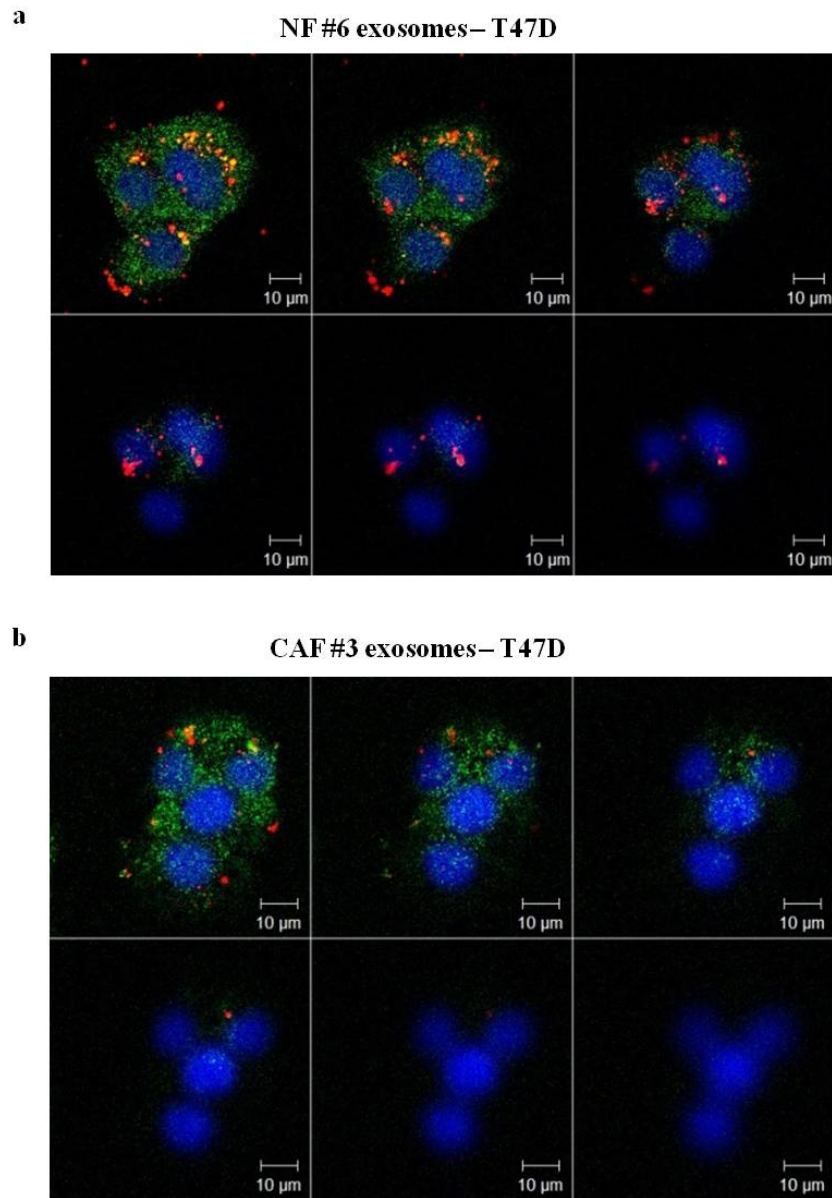
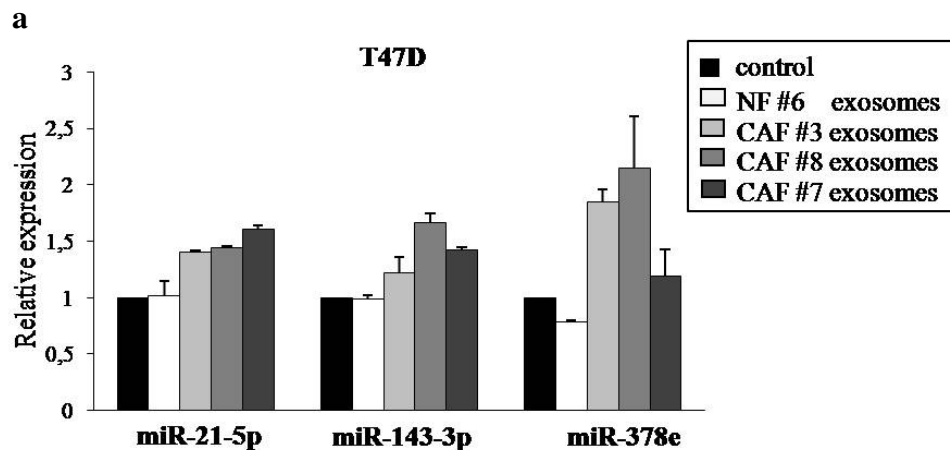


Figure 21. Z stack images of exosome uptake. T47D cells were cultured in presence of fibroblast PKH26-labeled exosomes for 24 hours. T47D cells were stained using DAPI (nuclei) and ALEXA488-conjugated anti-tubulin antibody. Six images for each point were acquired, and slice thickness was 1 μ m. NF exosomes (patient #6, a) and CAF exosomes (patient #3, b) were uptaken from T47D cells, as demonstrated by the co-localization of ALEXA488 and PKH26 signals. Confocal microscope (original magnification, $\times 60$). Scale bar: 10 μ m.

4.6 miRs released by CAFs are shuttled into breast cancer cells via exosomes

In order to demonstrate that CAFs could transfer via exosomes miR-21, miR-143 and miR-378e in T47D cells, we treated T47D cells with CAF- or NF- isolated exosomes (CAF patients #3, #7 and #8, NF patient #6) for 24 hours. Then, we performed a Real Time PCR to evaluate miR levels in T47D cells. As shown in Figure 22a, T47D cells treated with CAF exosomes exhibited increased levels of these miRs as compared to both non treated T47D cells and T47D cells treated with NF exosomes. In addition, to visualize the transport of extracellular miRs derived from CAFs into T47D cells, we transfected CAFs (patient #11) with cy3-labeled miRs (cy3-miR-21-5p, cy3-miR-143-3p, cy3-miR-378e). The next day, we isolated exosomes from CAF cell media and we cultured T47D cells with them. Twenty-four hours after the treatment, we stained the treated cells using blue DAPI (nuclei) and green ALEXA488-conjugated anti-CD63 antibody. As shown in Figure 22b, we detected the signals of cy3-miRs in the cytoplasm of T47D cells, using a confocal microscopy. Notably, as shown in z-stack images (Figure 23), cy3-miRs co-localized with the signals of an exosomal marker, CD63. Taken together, these results suggest that CAF-secreted exosomes mediate miR-21, miR-143 and miR-378e shuttling into T47D cells.



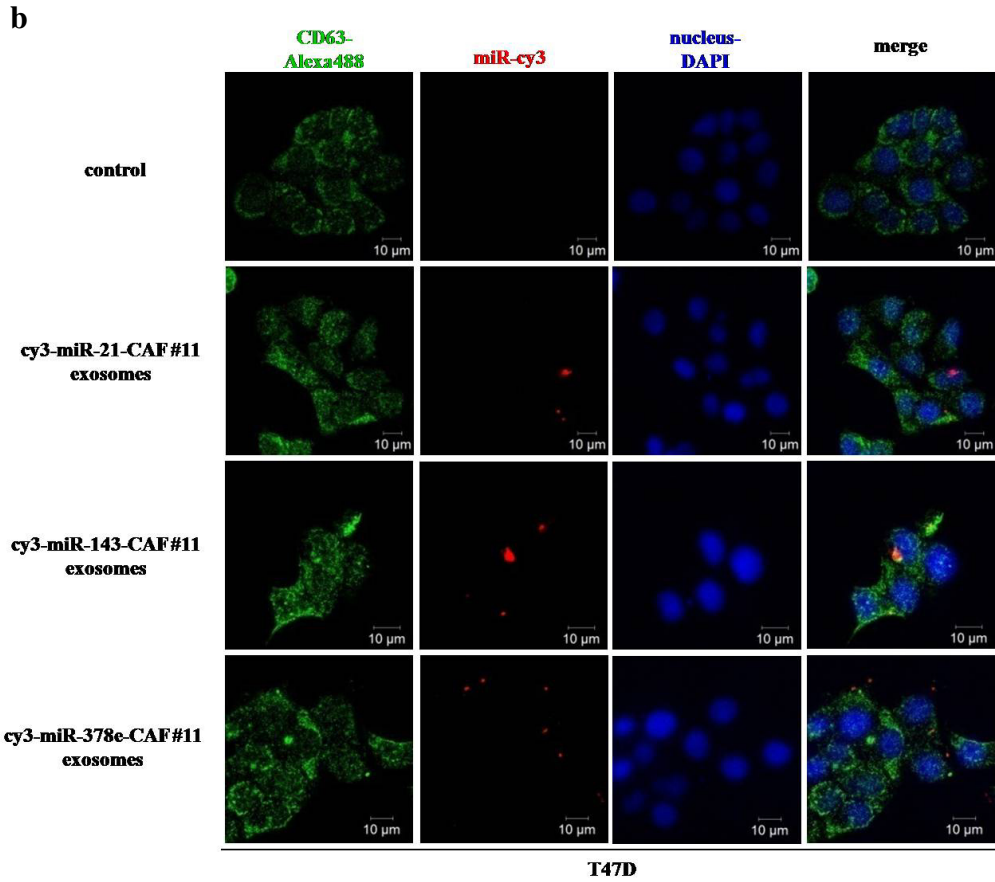


Figure 22. miR-21, miR-143, miR-378e are shuttled from CAF exosomes into breast cancer cells. T47D cells were treated 24 hours in absence (control) or in presence of NF exosomes (patient #6) or CAF exosomes (patients #3, #7 and #8). Then, a Real Time PCR was performed to evaluate miR-21, miR-143, and miR-378e levels in T47D cells. T47D cells treated with CAF exosomes exhibited increased levels of these miRs as compared to both non treated T47D cells and T47D cells treated with NF exosomes (a). T47D cells were cultured in absence (control) or in presence of exosomes isolated from cy3-miR-CAF#11 (cy3-miR-21, cy3-miR-143, cy3-miR-378e) for 24 hours. Cy3-miRs were shuttled from CAF#11 exosomes into T47D cells, as shown using a confocal microscope (original magnification, $\times 60$). T47D cells were stained using DAPI (nuclei) and ALEXA488-conjugated anti-CD63 antibody. Scale bar: 10 μ m.

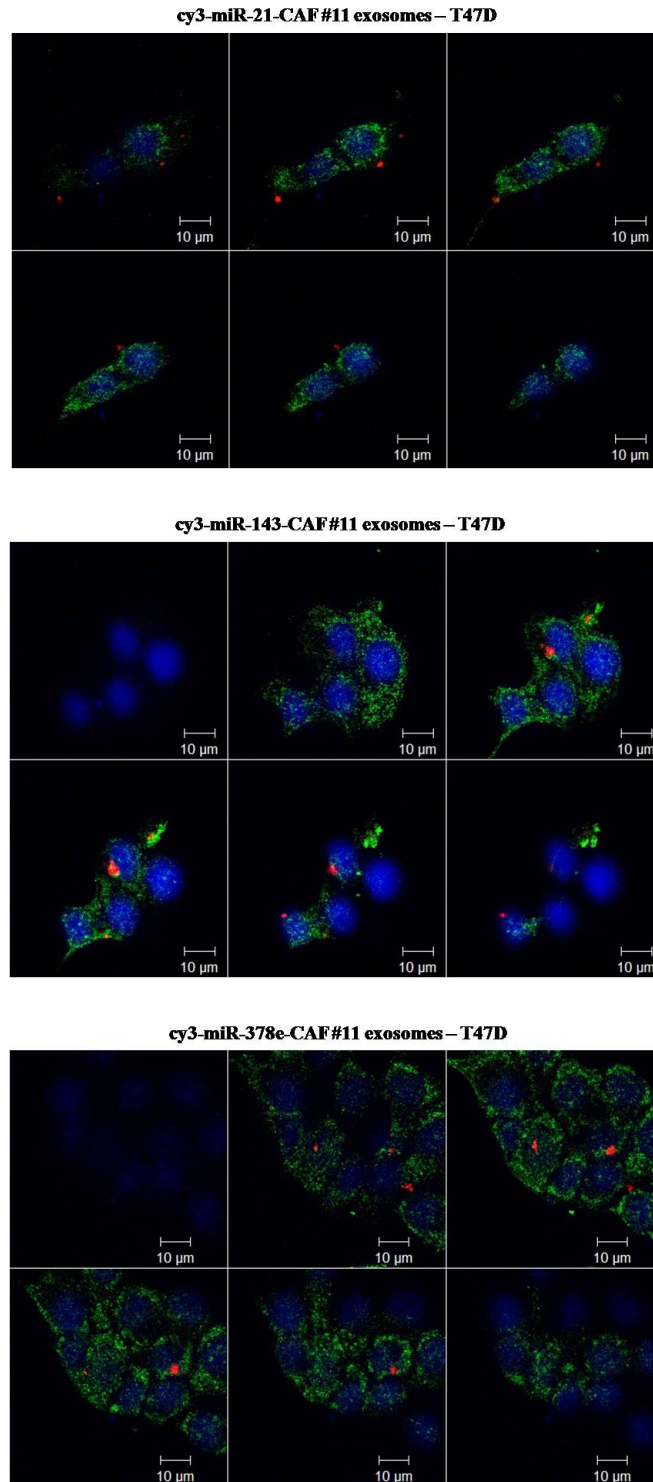


Figure 23. Z stack images of cy3-miRs shuttled from CAF exosomes to T47D cells. T47D cells were cultured with exosomes isolated from cy3-miR-CAF#11 (cy3-miR-21, cy3-miR-143, cy3-miR-378e). The treated cells were stained using DAPI (nuclei) and ALEXA488-conjugated anti-CD63 antibody. Six

images for each point were acquired, and slice thickness was 1 μ m. Cy3-miRs were shuttled from CAF#11 exosomes into T47D cells, as shown by the co-localization of cy3-miRs and Alexa488-CD63 signals. Confocal microscope (original magnification, $\times 60$). Scale bar: 10 μ m.

4.7 CAF exosomes increase stem cell and EMT markers in breast cancer cells

We investigated the oncogenic role of CAF exosomes in T47D cells. Firstly, we tested the role of CAF conditioned medium on different biologic processes, such as proliferation and epithelial-mesenchymal transition (EMT). Notably, we found that the treatment of T47D cells with CAF conditioned medium enriched in exosomes increased stemness and EMT markers, whereas did not affect proliferation (data not shown). Thus, we decided to isolate exosomes from CAF (patients #3, #7 and #9) or NF (patients #5, #6 and #10) conditioned media to test their effects on cancer cell features such as the expression of stemness markers. We treated T47D cells with NF exosomes or CAF exosomes for 72 hours. Then, we performed a Real Time PCR to evaluate NANOG, OCT3/4, SOX2 (stemness genes) and SNAIL (EMT gene) levels in T47D cells. Interestingly, T47D cells treated with CAF exosomes displayed increased levels of these markers as compared to both non treated T47D cells and T47D cells treated with NF exosomes (Figure 24a,b,c). In addition, we performed a Western Blot analysis for NANOG and for E-cadherin and Zeb (genes involved in EMT). As shown in Figure 24a, T47D cells treated with CAF#3 exosomes exhibited increased levels of NANOG protein as compared to both non treated T47D cells and T47D cells treated with NF#5 exosomes. Furthermore, as shown in Figure 24b, T47D cells treated with CAF#9 exosomes exhibited increased levels of Zeb protein and decreased levels of E-cadherin protein as compared to both non treated T47D cells and T47D cells treated with NF#10 exosomes. Taken together, these data suggest that CAF exosomes promote EMT phenotype and stemness proprieties in breast cancer cells.

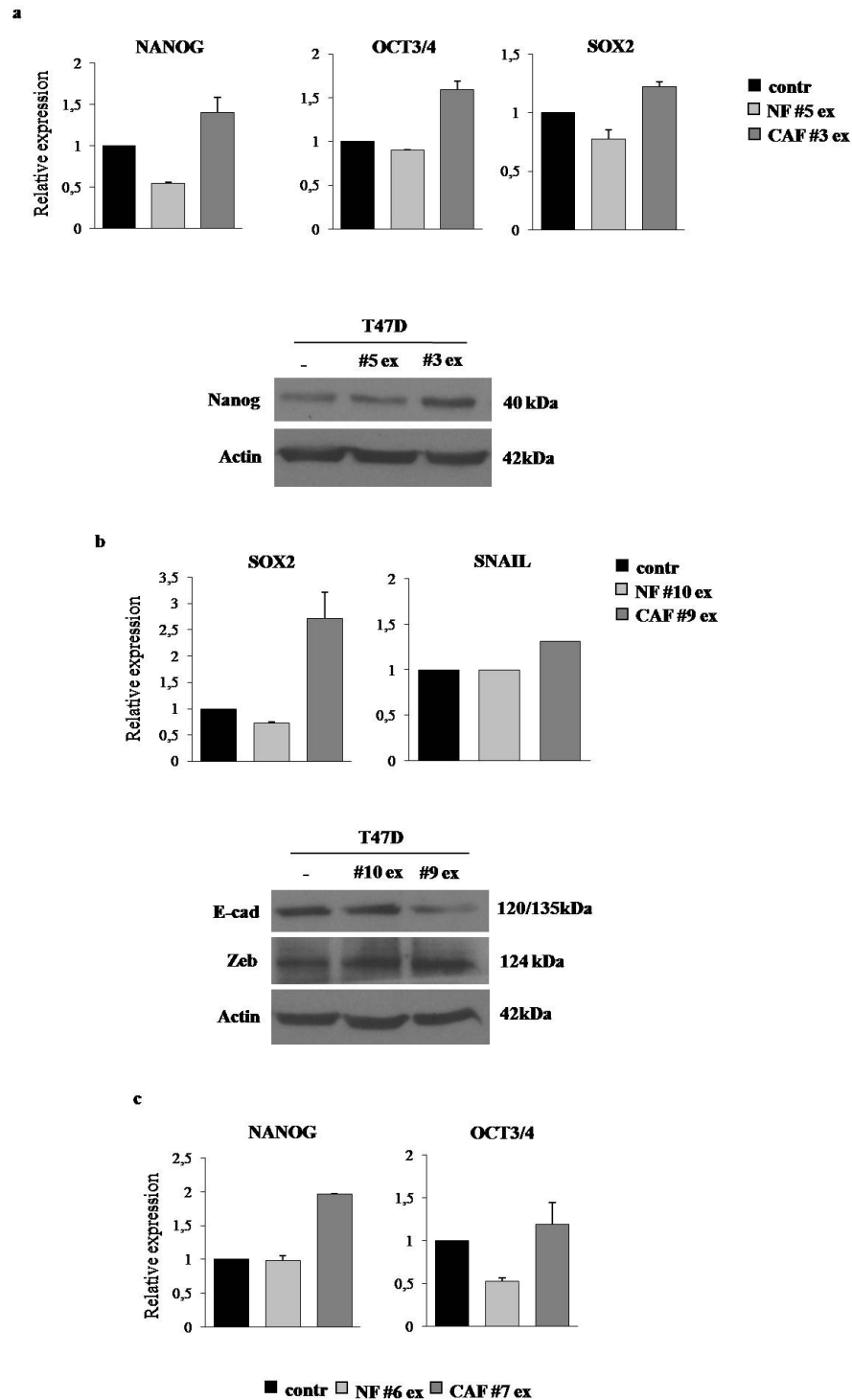


Figure 24. CAF exosomes increase stemness and EMT markers in T47D cells. T47D cells were cultured in absence (control) or in presence of NF#5 exosomes (NF#5 ex) or CAF#3 exosomes (CAF#3 ex) for 72h. T47D cells exhibited increased levels of NANOG, OCT3/4 and SOX2 mRNAs when cells

were treated with CAF#3 ex respect to both non treated T47D cells and T47D cells treated with NF#5 ex. In addition, T47D cells displayed increased levels of NANOG protein only when treated with CAF#3 ex (a). T47D cells were cultured in absence (control) or in presence of NF#10 exosomes (NF#10 ex) or CAF#9 exosomes (CAF#9 ex) for 72h. T47D cells exhibited increased levels of SOX2 and SNAIL mRNAs when cells were treated with CAF#9 ex as compared to both non treated T47D cells and T47D cells treated with NF#10 ex. Additionally, T47D cells displayed increased levels of Zeb protein and decreased levels of E-cadherin (E-cad) protein only when treated with CAF#9 ex (b). T47D cells were cultured in absence (control) or in presence of NF#6 exosomes (NF#6 ex) or CAF#7 exosomes (CAF#7 ex) for 72h. T47D cells exhibited increased levels of NANOG and OCT3/4 mRNAs when cells were treated with CAF#7 ex respect to both non treated T47D cells and T47D cells treated with NF#6 ex (c).

4.8 CAF exosomes increase mammosphere formation ability

To investigate the role of CAF exosomes on the stemness phenotype, we adopted a suspension culture of T47D cells. Briefly, we seeded T47D cells in non-adherent conditions (low attachment plates) and we cultured them in stem medium (medium supplemented with EGF, bFGF, B27) in absence or in presence of NF exosomes (patients #5, #6 and #10) or CAF exosomes (patients #3, #7 and #9). After four days, we assessed the ability of cells to form spheres. We observed a significant increase in the number of spheres (Figure 25a,b,c) and in their diameter (Figure 25d) in T47D cells treated with CAF exosomes compared with both non treated T47D cells and T47D cells treated with NF exosomes, thus indicating that CAF exosomes increase mammosphere formation ability.

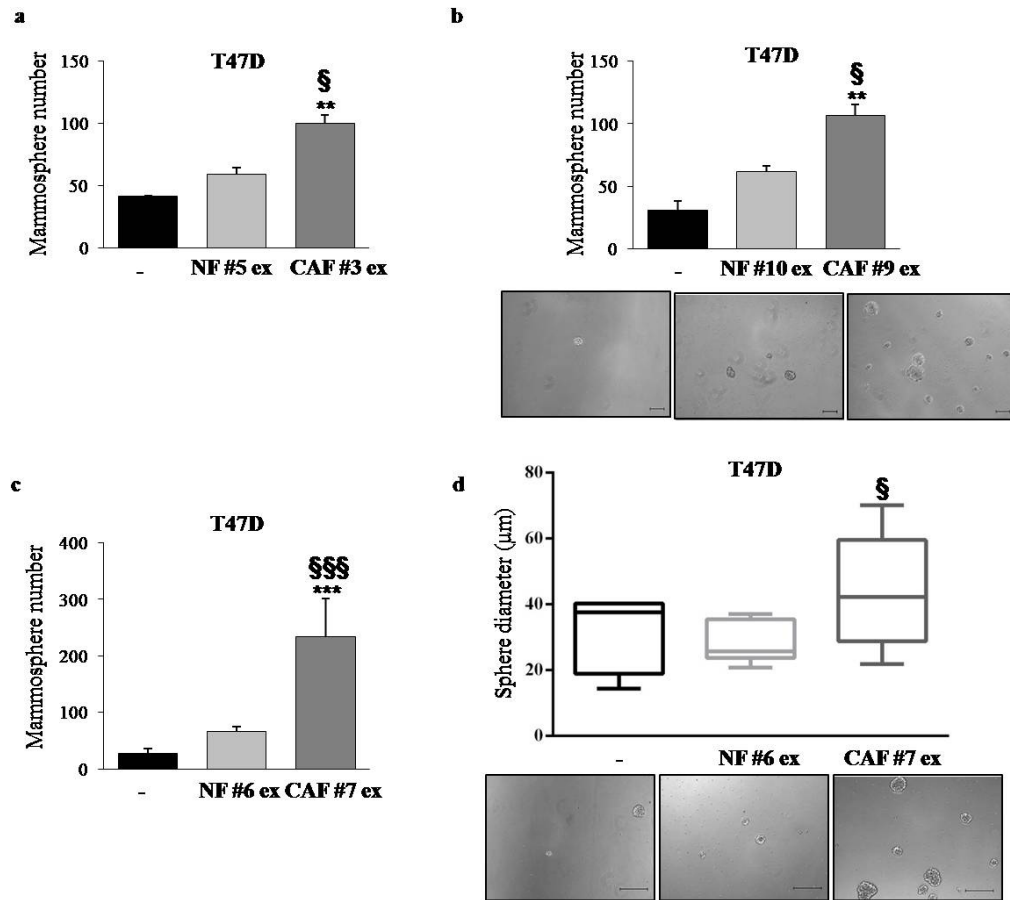


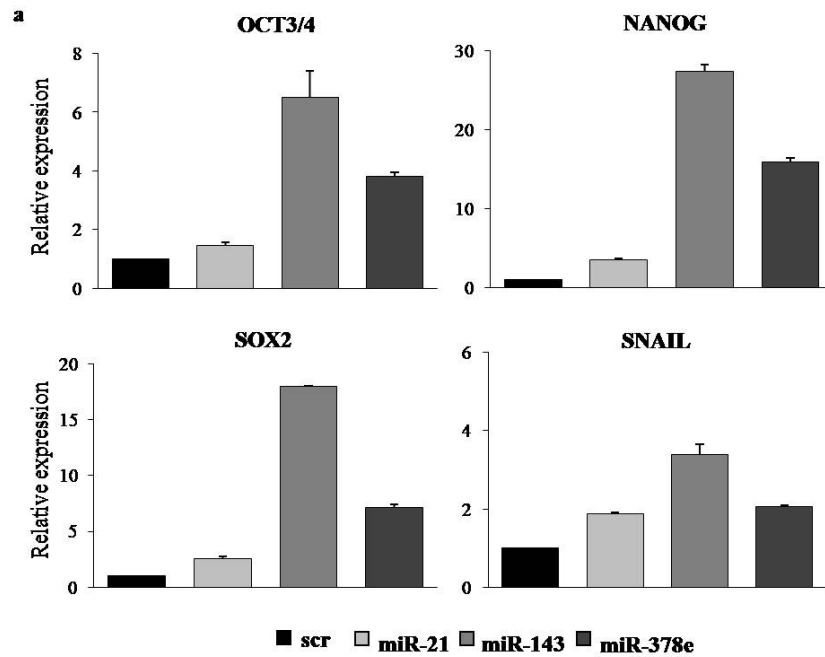
Figure 25. CAF exosomes increase stemness phenotype. T47D cells were cultured in non-adherent conditions and in stem medium in absence (control) or in presence of NF exosomes (NF ex) or CAF exosomes (CAF ex). After four days, the capacity of cells to form spheres was assessed. T47D cells treated with CAF ex formed increased number of spheres as compared to both control and T47D cells treated with NF ex (CAF#3ex vs NF#5ex, (a), CAF#9ex vs NF#10ex, (b), and CAF#7ex vs NF#6ex, (c)). Diagram showing the sphere diameter distribution in T47D cells (control, T47D treated with NF#6ex or CAF#7ex) found in 10 representative fields (d). Scale bar: 100μm. Data were obtained from three independent experiments and are presented as mean value \pm SD. P value was calculated using one-way ANOVA followed by Bonferroni's *post hoc* testing.

* $p < 0.05$; ** $p < 0.01$; *** $p < 0.001$ (over control).

§ $p < 0.05$; §§ $p < 0.01$; §§§ $p < 0.001$ (over NF ex).

4.9 miR-21, miR-143 and miR-378e increase stem cell and EMT markers in breast cancer cells

To investigate whether CAF exosomes increased stemness and EMT expression through their cargo miRs, we transfected T47D cells with miRs: scrambled (control), -21, -143, -378e, for 48 hours. Then, we performed a Real Time PCR to evaluate NANOG, OCT3/4, SOX2 and SNAIL mRNA levels in the transfected cells. Interestingly, T47D cells transfected with miRs -21, -143, and -378e displayed increased levels of these markers as compared to scrambled control (Figure 26a). In addition, we performed a Western Blot analysis for Nanog, Oct3/4, Zeb and Snail. As shown in Figure 26b, T47D cells transfected with miRs -21, -143, and -378e showed increased levels of Nanog, Oct3/4, Zeb and Snail proteins as compared to scrambled control. Taken together, these data suggest that miR-21, miR-143 and miR-378e, similarly to CAF exosomes, induce EMT phenotype and stemness proprieties in breast cancer cells.



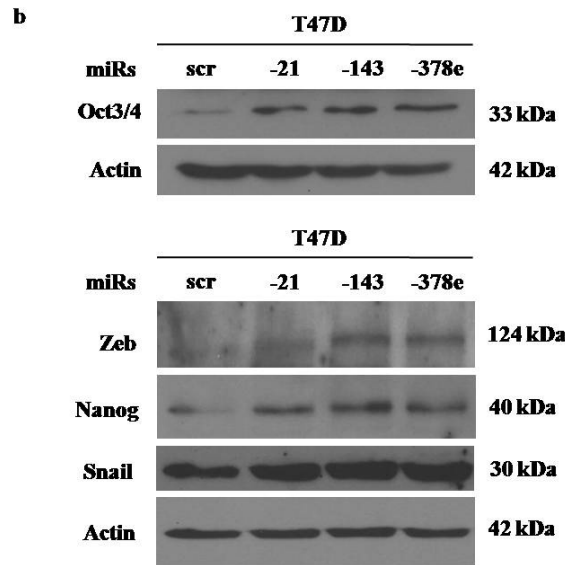


Figure 26. miR-21, miR-143 and miR-378e increase stemness and EMT markers in T47D cells. T47D cells were transfected with miRs: scrambled (scr, control), -21, -143, and -378e, for 48h. T47D cells transfected with these miRs exhibited increased levels of NANOG, OCT3/4, SOX2 and SNAIL mRNAs as compared to scrambled control (a). In addition, T47D cells transfected with these miRs displayed increased levels of Oct3/4, Zeb, Nanog and Snail proteins as compared to scrambled control. Actin was used as loading control (b).

4.10 miR-21, miR-143 and miR-378e increase mammosphere formation ability

To investigate the role of miR-21, miR-143 and miR-378e on the stemness phenotype, we performed a mammosphere formation assay. Briefly, we transfected T47D cells with miRs: scrambled (control), -21, -143, -378e, for 48 hours. Since these miRs are present together in CAF exosomes, we decided to co-transfect cells with combinations of them (miRs -21 + -143 or -21 + -378e or -143 + -378e or -21 + -143 + -378e, final concentration: 100nM) to evaluate synergic effects. We seeded the transfected cells in non-adherent conditions and in stem medium. After four days, we assessed the ability of cells to form spheres. We observed a significant increase in the number of spheres (Figure 27a) and in their diameter (Figure 27b) in T47D cells transfected with miRs as compared to scrambled control. Notably, T47D cells transfected with miRs -21 + -143 + -378e exhibited the best significant capacity to form mammospheres (increased number and diameter), thus indicating that these miRs together increase mammosphere formation ability.

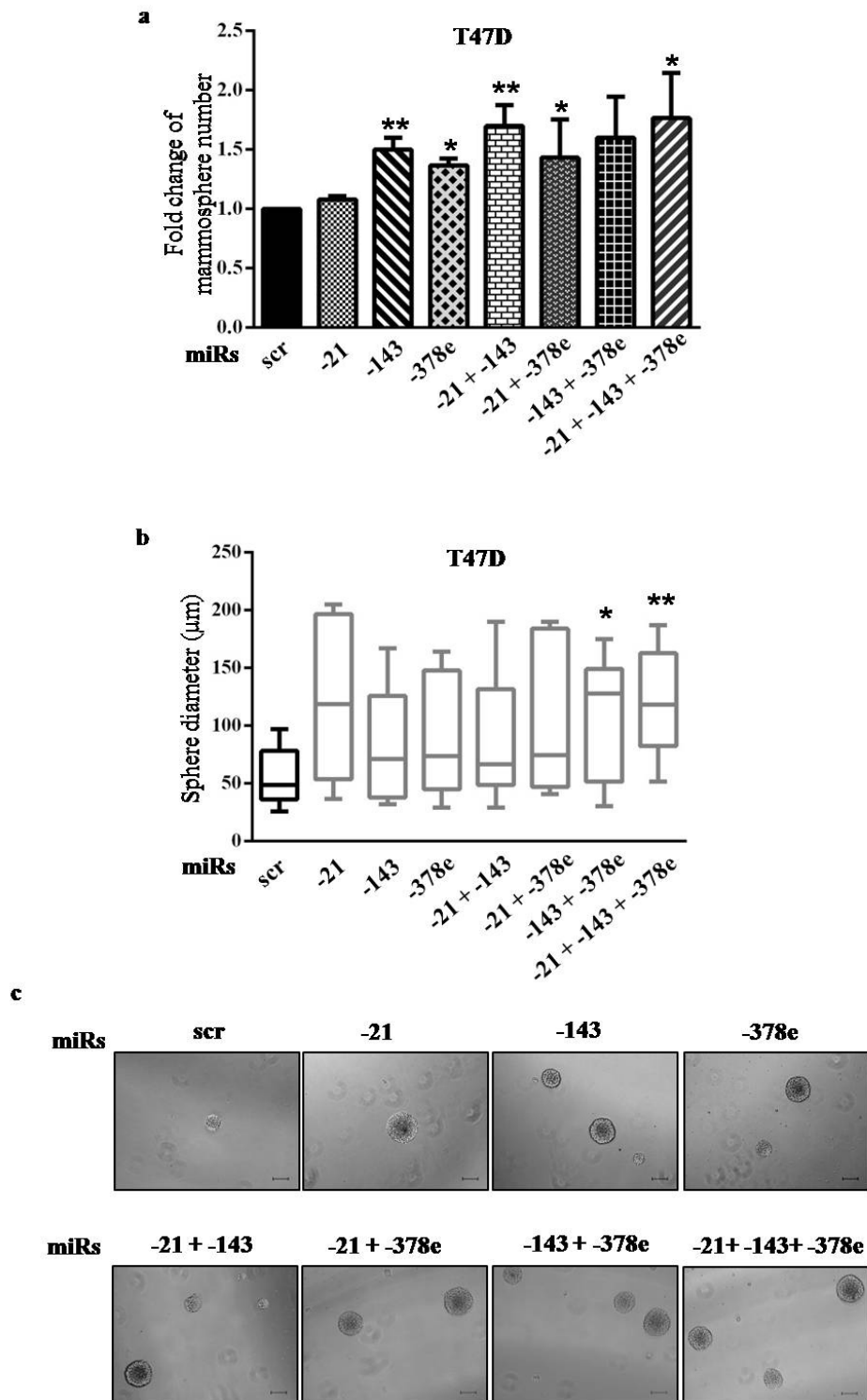


Figure 27. miR-21, miR-143 and miR-378e increase stemness phenotype. T47D cells were transfected with miRNAs: scrambled (scr, control), -21, -143, -378e, alone or in combinations (final concentration: 100nM). After four days,

the capacity of cells to form spheres was assessed. T47D cells transfected with miRs formed increased number of spheres as compared to scrambled control. The best effects were observed when cells were transfected with combinations of miRs. In addition, among these miRs, the best effective in the induction of mammosphere formation was miR-143 (a). Diagram showing the sphere diameter distribution in T47D cells, found in 10 representative fields (b). Scale bar: 100µm (c). Data were obtained from three independent experiments and are presented as mean value \pm SD. P value was calculated using Student's t test. * $p < 0.05$; ** $p < 0.01$.

4.11 Anti-miRs -21, -143 and -378e decrease stemness phenotype

To further confirm the role of miRs -21, -143 and -378e in promoting the stemness phenotype, we transfected T47D cells with Anti-miRs: scrambled (control), -21, -143, -378e or -21 + -143 + -378e. As described above, we performed a mammosphere formation assay and observed that T47D cells transfected with Anti-miRs displayed a decreased ability to grow as stem-like aggregates (Figure 28a). Furthermore, we performed a Real Time PCR for SOX2 and a Western Blot analysis for genes involved in EMT, E-cadherin, Zeb, Snail. We found that T47D cells transfected with Anti-miRs exhibited decreased levels of SOX2 mRNAs respect to Anti-miR-scrambled control (Figure 28b). In addition, T47D cells transfected with Anti-miRs displayed increased levels of E-cadherin protein as compared to the control, whereas only the cells co-transfected with all the Anti-miRs exhibited decreased levels of Zeb protein. Finally, the cells transfected with Anti-miR-143 or with Anti-miRs -21 + -143 + -378e exhibited decreased levels of Snail protein respect to the control (Figure 28c). Taken together, these data strongly confirm the role of these miRs in breast cancer stemness phenotype.

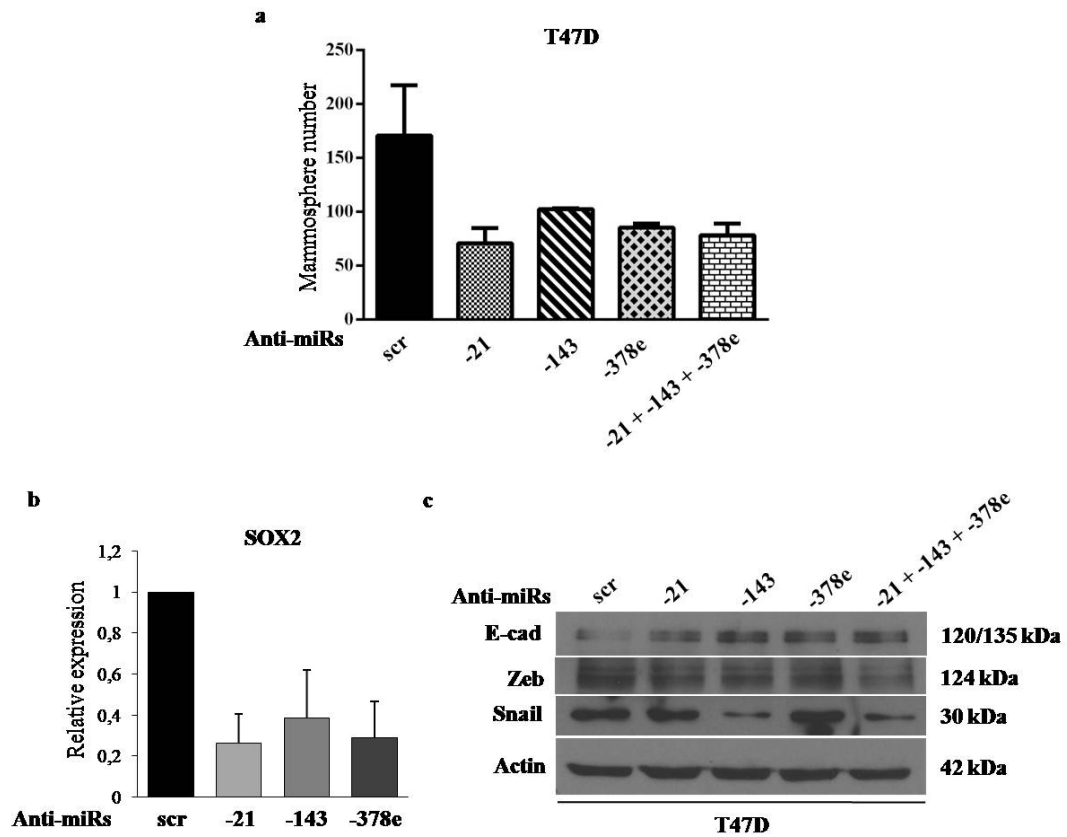


Figure 28. Anti-miRs -21, -143 and -378e decrease mammosphere formation ability and stem cell and EMT markers. T47D cells were transfected with Anti-miRs (alone or in combinations, final concentration: 200nM) or Anti-miR-scrambled (Anti-miRs scr, control). The cells transfected with Anti-miRs exhibited decreased mammosphere number as compared to the control (a). The cells transfected with Anti-miRs displayed decreased SOX2 mRNA levels (b) and increased levels of E-cadherin protein as compared to the control (c). The cells co-transfected with Anti-miRs -21 + -143 + -378e exhibited decreased levels of Zeb and Snail proteins. In addition, the cells transfected with Anti-miR-143 showed decreased levels of Snail protein as compared to the control. Actin was used as loading control (c).

5. DISCUSSION

Breast cancer is the most common cause of cancer death among women. Prognosis for most patients with early breast cancer is generally very good, however, a significant proportion (20–30%) of chemotherapy-treated early breast cancer patients relapses with metastatic disease (Forman et al. 2013, Albain et al. 2012, Tjensvoll et al. 2012). Advances in standard treatments of BC, such as surgery, radiotherapy and chemotherapy, have increased patient survival, but BC incidence and the death related to this cancer are still high.

Accumulating evidence indicates that signals driving tumorigenesis are not simply cancer cell-autonomous but involve the tumor stroma. Cancer-associated fibroblasts represent the major components of tumor stroma and play an important role in promoting tumorigenic processes such as angiogenesis, metastasis, immune response suppression, therapy resistance in several solid tumors. The metastatic potential of non-small cell lung cancer cells has been shown to be associated with the tumor microenvironment. CAF-induced EMT led to an increase in motility and a decrease in proliferation of non-small cell lung cancer cells through SMAD3-dependent up-regulation of the growth inhibitory gene p21CIP1 and α -SMA (Kim et al. 2013). Another study has demonstrated that myofibroblasts of pancreatic ductal adenocarcinoma had a crucial role in the immune response, innate and adaptive. In fact, they showed that myofibroblast-depleted tumors were associated with a decreased Teff/Treg ratio and a significant elevation in Ctl4 expression (Ozdemir et al. 2014). Furthermore, a recent study has reported that two subtypes of CAFs of oral squamous cell carcinoma promoted cell invasion via different mechanisms (Costea et al. 2013). More recently, it has been demonstrated that cancer-associated fibroblasts induced trastuzumab resistance in HER2+ breast cancer (Mao et al. 2015).

The intercommunication between tumor cells and their surrounding microenvironment is essential for the tumor to progress and metastasize. Many examples of heterotypic signaling within the tumor microenvironment involve classical paracrine signaling loops of cytokines or growth factors and their receptors. Although these signaling mechanisms undoubtedly operate as key means of intercellular communication within the TM, more recently, exosomes, membrane-derived vesicles, have been recognized as important mediators of intercellular communication. In fact, they carry lipids, proteins, mRNAs and microRNAs that can be transferred to recipient cells, thereby modulating cell biology. In the context of cancer, this process entails the transfer of cancer-promoting cellular contents between cancer cells and stromal cells within the tumor microenvironment or into the circulation to act at distant sites, thereby enabling cancer progression. For instance, it has been demonstrated that exosomes released by human melanoma and colorectal

carcinoma cells could promote the differentiation of monocytes to myeloid-derived suppressor cells, thus supporting tumoral growth and immune escape (Valenti et al. 2007). An interesting work has shown that melanoma-derived exosomes from the primary tumor “educated” their environment to form a protumorigenic niche and programmed bone marrow-derived progenitors at the pre-metastatic site to assume a proangiogenic phenotype, thereby enhancing metastatic dissemination. This effect was dependent on the receptor tyrosine kinase MET, as its inhibition in exosomes impaired pro-metastatic effects (Peinado et al. 2012). Not only cancer cells, but also various stromal cells are capable of exosome release. For instance, Luga and colleagues (2012) have shown that fibroblast-secreted exosomes promoted breast cancer cell migration through WNT-PCP signaling. More recently, Shimoda and colleagues (2014) have reported that human CAFs secreted ADAM10-rich exosomes that promoted cell motility and activated RhoA and Notch signaling in several cancer cells. Taken together, these studies provide evidence of how it is useful to investigate the exosome-mediated communication to better understand the underlying mechanisms of tumorigenesis.

In order to understand the basic biology of cancer progression and to develop therapeutic approaches, it is interesting to analyze the transfer of exosomal microRNAs to recipient cells where they can regulate tumorigenic processes. microRNAs are small noncoding RNAs that typically inhibit the translation and stability of messenger RNAs (mRNAs), controlling genes involved in cellular processes such as inflammation, cell-cycle regulation, stress response, differentiation, apoptosis, and migration. Their deregulation has been shown to play an essential role in the development and progression of cancer. Compared with those in normal tissue, miRNAs in malignant tissue are up- or down-regulated; these miRNAs can be considered oncogenes or tumor suppressors, respectively, and can affect all the hallmarks of cancer. Extensive analyses have highlighted the causative roles of many miRNAs in cancer by using either human cancer cells or genetically engineered animal models. For example, transgenic expression of miR-155 or miR-21 and deletion of miR-15/16 are sufficient to initiate lymphoma-genesis in mice. Conversely, systemic delivery of selected miRNAs, including let-7, miR-26a, miR-34a, and miR-143/145, inhibits tumor progression in vivo (Garofalo et al. 2014). Recently, it has emerged that, in addition to cellular miRNA deregulation, exosomal miRNA deregulation could play a crucial role in cancer. For example, a study has shown that leukemia cells could release miR-92a via exosomes into human umbilical vein endothelial cells, leading to increased cell migration and tube formation (Umezu et al. 2013). Another study has elucidated how miR-223 secreted by tumor-associated macrophages promoted the invasion of breast cancer cells, through the disruption of the Mef2c- β -catenin pathway (Yang et al. 2011). Moreover, it has been reported that miR-21 and miR-29a secreted by lung cancer exosomes bound to murine TLR7 and human TLR8 and triggered a Toll-like receptor (TLR)-mediated prometastatic inflammatory response that could lead to tumor growth and metastasis (Fabbri

et al. 2012). More recently, an interesting work has demonstrated that CAF-derived miR-409 induced tumorigenesis, epithelial-to-mesenchymal transition and stemness of the epithelial prostate cancer cells in vivo (Josson et al. 2014).

Therefore, these works strongly suggest that one alternative mechanism of the promotion of breast cancer progression by CAFs may be through cancer-associated fibroblast-secreted exosomes, which would deliver oncogenic miRs to breast cancer cells. To this aim, for the first time, we characterized exosomal miRs of breast cancer-associated fibroblasts. Notably, we found that in CAF exosomes the levels of miR-21-5p, miR-378e, and miR-143-3p were increased as compared to normal fibroblast exosomes, whereas we did not observe an up-regulation of these miRs in CAF cells as compared to NF cells, indicating a selective mechanism of exosomal miRNA sorting. We visualized, by immunofluorescence experiments, the transfer of PKH26-labeled-exosomes from fibroblasts to breast cancer cells. Furthermore, we confirmed the transfer of these miRs from CAF exosomes to T47D breast cancer cells in our system with two different approaches: we visualized cy3-labeled-miRs (cy3-miR-21-5p, cy3-miR-143-3p, cy3-miR-378e) shuttling from CAF exosomes into T47D cells, and we observed the increase of these miR levels in breast cancer cells treated with CAF exosomes. Then, we demonstrated that TGF- β , in addition to its direct role in the activation of normal fibroblasts to CAFs, could increase the levels of these miRs in normal fibroblast exosomes, suggesting that the up-regulation of these miRs is a signature of TGF- β activated fibroblasts. Taken together, these data strongly show a crosstalk between CAFs and BC cells mediated by miR-21-5p, miR-143-3p and miR-378e.

miR-21 is a well characterized oncogenic miR. In our group, we have found that miR-21 regulates therapy resistance in glioma cells (Quintavalle et al. 2013). Several works have demonstrated the role of miR-21 in cancer progression and diagnosis. In particular, in breast cancer, it has been reported that miR-21 correlates with poor prognosis, regulates EMT phenotype and promotes cancer cell proliferation and invasion (Han et al. 2012, Dong et al. 2014, Song et al. 2010). It has also been found up-regulated in the serum of breast cancer patients (Li et al. 2014). The tumorigenic role of miR-143-3p depends on cancer types. miR-143-3p have been found up-regulated in a large cohort of patients including 88 colorectal cancer tumors, suggesting that have an oncogenic role (Schee et al. 2013). On the contrary, it has been shown down-regulated in gastric cancer, indicating a tumor suppressive role (Wu et al. 2013). miR-378e has not been studied, so far for oncogenic/oncosuppressive role.

Many tumors, including breast cancer, are maintained by a subpopulation of cells that display stem cell properties, known as cancer stem cells (CSCs). CSCs are defined by their ability to initiate tumors in immune-compromised mice upon serial passage, a demonstration of self renewal, as well as their ability to differentiate into the non-self-renewing cells forming the tumor bulk (Korkaya et al. 2008, Ginestier et al. 2007). Analogous to the regulation of normal stem cells by their “niche”, CSCs are regulated by, and in

turn regulate, cells within the tumor microenvironment. Several studies have provided evidence that these CSCs mediate tumor metastasis and contribute to treatment resistance and relapse (Li et al. 2008, Liu et al. 2010). Bi-directional paracrine signals coordinately regulate tumorigenic cell populations including CSCs. Tumorigenic cells in turn produce factors that attract and regulate the diverse variety of cell types that constitute the tumor microenvironment. For instance, in human breast cancers, mesenchymal stem cells may be recruited from the bone marrow to sites of growing tumor, where they interact with breast CSCs through cytokine loops involving IL-6 and CXCL7, thereby promoting breast cancer metastasis (Liu et al. 2011, Karnoub et al. 2007). Therefore, strategies designed to specifically target the interaction between the CSCs and their microenvironment represent an important approach to improving patient outcome. Recent findings have shown that hierarchically organized cell populations are more plastic than previously imagined (Chaffer et al. 2011, Chaffer et al. 2013, He et al. 2011). Thus, epithelial cells may dedifferentiate and thereby enter back into the stem cell pool. Moreover, this plastic model of tumorigenicity suggests that the pool of cells capable of successfully seeding a metastatic outgrowth is not restricted to the existing pool of CSCs within a primary tumor. Instead, the more differentiated progeny of these CSCs may also initiate metastases if it is capable of reverting to the tumor-initiating CSC state at distant sites of dissemination. Thus, therapies aimed at targeting the CSCs within a tumor will not be curative if the pool of CSCs can be continuously regenerated from plastic non cancer stem cells that are capable of dedifferentiating and reentering the CSC state. In this scenery, to discover the underlying mechanisms that promote dedifferentiation processes could provide new targets for therapeutic strategies.

In our study, we wondered whether CAF exosomes and the identified exosomal miRs could promote dedifferentiation process of BC cells. For the first time, we provided evidence of the role of CAF exosomes and their miR contents in the induction of stemness phenotype in breast cancer cells. In fact, T47D cells exposed to CAF exosomes or transfected with the identified miRs exhibited a significantly increased capacity to form mammospheres (breast cancer cells enriched in stem-like cells that grown as spheres).

Notably, accumulating evidence indicates that the expression of Oct3/4, Nanog, and Sox2 transcription factors has a strong correlation with CSCs: knockdown of these genes decreased tumor sphere formation and inhibited tumor formation in xenograft tumor models (Leis et al 2012, Wang et al. 2014). The transdifferentiation of epithelial cells into mesenchymal cells, a process known as epithelial-mesenchymal transition (EMT), is integral in development, wound healing and stem cell behavior, and contributes pathologically to fibrosis and cancer progression. This switch in cell differentiation and behavior is mediated by key transcription factors, including Snail and Zeb, and is characterized by the loss of epithelial marker expressions, such as E-cadherin. Epithelial-mesenchymal transition and mesenchymal-epithelial transition have been closely linked to ‘stemness’ in development and cancer. EMT has also

been associated with epithelial and carcinoma stem cell properties. Expression of Snail in breast epithelial cells induces a mesenchymal cell population marked with a stem-like phenotype, which is similar to that observed in epithelial stem cells. The correlation of EMT with stemness extends to carcinomas. In breast carcinomas, induction of EMT promotes the generation of CSCs that are able to form mammospheres, and, similarly, CSCs isolated from tumors express EMT markers (Mani et al. 2008, Scheel et al. 2012).

Interestingly, we found that T47D cells exposed to CAF exosomes or transfected with the identified miRs also displayed increased stem cell markers, such as SOX2, Nanog and Oct3/4, and promoted EMT markers, decreased E-cadherin and increased Snail and Zeb. Our findings showed that, among these miRs, the most effective was miR-143-3p, whereas the best effect in promoting mammosphere formation was observed when breast cancer cells were co-transfected with combinations of these miRs, thus indicating that they act together. On the contrary, breast cancer cells co-transfected with combinations of the Anti-miRs displayed a strong reduction of mammosphere formation capacity, EMT and stemness markers, thereby underlying a good strategy to prevent dedifferentiation of breast cancer cells.

In summary, we conclude that CAF exosomes regulate the stemness phenotype of breast cancer cells and our data suggest that this effect could be fostered by exosome-mediated delivery of oncogenic miRs, as they together promote stem-like phenotype. Our data clearly provide insights into the mechanisms underlying the stemness maintenance in breast cancer and propose miR-21-5p, miR-143-3p and miR-378e as new therapeutic molecular targets.

6. CONCLUSIONS

In conclusion, this study demonstrates that functional miRNAs can be transferred from cancer-associated fibroblasts to breast cancer cells. Exosomes secreted from CAFs shuttle miR-21-5p, miR-143-3p and miR-378e into breast cancer cells. Interestingly, CAF exosomes promote the dedifferentiation of breast cancer cells through the up-regulation of stemness and EMT markers, thereby enabling stemness maintenance. Furthermore, the overexpression of the identified miRs in breast cancer cells enhances the stemness phenotype and increases stemness and EMT markers. On the contrary, the down-regulation of these miRs, through specific Anti-miRs, prevents the dedifferentiation of breast cancer cells through the down-regulation of stemness and EMT markers. Thus, our study provides insights into the mechanisms of cell-cell interactions through which CAFs regulate breast cancer progression via the exosomal-mediated delivery of oncogenic miRNAs. In addition, our data strongly provide evidence of new therapeutic molecular targets.

7. REFERENCES

- Aboussekhra A. Role of cancer-associated fibroblasts in breast cancer development and prognosis. *Int J Dev Biol.* 2011; 55(7-9):841-9.
- Adam Sharp and Catherine Harper-Wynne. Treatment of Advanced Breast Cancer (ABC): The Expanding Landscape of Targeted Therapies. *J Cancer Biol Res.* 2014; 2(1): 1036.
- Adams EF, Newton CJ, Braunsberg H, Shaikh N, Ghilchik M, James VH. Effects of human breast fibroblasts on growth and 17 beta-estradiol dehydrogenase activity of MCF-7 cells in culture. *Breast Cancer Res Treat.* 1988; 11(2):165-72.
- Anderson KN, Schwab RB, Martinez ME. Reproductive risk factors and breast cancer subtypes: a review of the literature. *Breast Cancer Res Treat.* 2014; 144(1):1-10.
- Azmi AS, Bao B, Sarkar FH. Exosomes in cancer development, metastasis, and drug resistance: a comprehensive review. *Cancer Metastasis Rev.* 2013; 32(3-4):623-42.
- Baietti MF, Zhang Z, Mortier E, Melchior A, Degeest G, Geeraerts A, Ivarsson Y, Depoortere F, Coomans C, Vermeiren E, Zimmermann P, David G. Syndecan-syntenin-ALIX regulates the biogenesis of exosomes. *Nat Cell Biol.* 2012; 14(7):677-85.
- Balkwill F, Charles KA, Mantovani A. Smoldering and polarized inflammation in the initiation and promotion of malignant disease. *Cancer Cell* 2005; 7(3):211-7.
- Balliet RM, Capparelli C, Guido C, Pestell TG, Martinez-Outschoorn UE, Lin Z, Whitaker-Menezes D, Chiavarina B, Pestell RG, Howell A, Sotgia F, Lisanti MP. Mitochondrial oxidative stress in cancer-associated fibroblasts drives lactate production, promoting breast cancer tumor growth: understanding the aging and cancer connection. *Cell Cycle* 2011; 10(23):4065-73.
- Biswas SK, Mantovani A. Orchestration of metabolism by macrophages. *Cell Metab.* 2012; 15(4):432-7.
- Bobrie A, Krumeich S, Reyat F, Recchi C, Moita LF, Seabra MC, Ostrowski M, Théry C. Rab27a supports exosome-dependent and -independent mechanisms that modify the tumor microenvironment and can promote tumor progression. *Cancer Res.* 2012; 72(19):4920-30.

Bochet L, Meulle A, Imbert S, Salles B, Valet P, Muller C. Cancer-associated adipocytes promotes breast tumor radioresistance. *Biochem Biophys Res Commun*. 2011; 411(1):102-6.

Borges FT, Melo SA, Özdemir BC, Kato N, Revuelta I, Miller CA, Gattone VH 2nd, LeBleu VS, Kalluri R. TGF- β 1-containing exosomes from injured epithelial cells activate fibroblasts to initiate tissue regenerative responses and fibrosis. *J Am Soc Nephrol*. 2013; 24(3):385-92.

Branco-Price C, Zhang N, Schnelle M, Evans C, Katschinski DM, Liao D, Ellies L, Johnson RS. Endothelial cell HIF-1 α and HIF-2 α differentially regulate metastatic success. *Cancer Cell* 2012; 21(1):52-65.

Casey TM, Eneman J, Crocker A, White J, Tessitore J, Stanley M, Harlow S, Bunn JY, Weaver D, Muss H, Plaut K. Cancer associated fibroblasts stimulated by transforming growth factor beta1 (TGF-beta 1) increase invasion rate of tumor cells: a population study. *Breast Cancer Res Treat*. 2008; 110(1):39-49.

Chaffer CL, Brueckmann I, Scheel C, Kaestli AJ, Wiggins PA, Rodrigues LO, Brooks M, Reinhardt F, Su Y, Polyak K, Arendt LM, Kuperwasser C, Bieri B, Weinberg RA. Normal and neoplastic nonstem cells can spontaneously convert to a stem-like state. *Proc Natl Acad Sci USA* 2011; 108(19):7950-5.

Chaffer CL, Marjanovic ND, Lee T, Bell G, Kleer CG, Reinhardt F, D'Alessio AC, Young RA, Weinberg RA. Poised chromatin at the ZEB1 promoter enables breast cancer cell plasticity and enhances tumorigenicity. *Cell* 2013; 154(1):61-74.

Chaffer CL, Weinberg RA. A perspective on cancer cell metastasis. *Science* 2011; 331(6024):1559-64.

Chen Q, Zhang XH, Massagué J. Macrophage binding to receptor VCAM-1 transmits survival signals in breast cancer cells that invade the lungs. *Cancer Cell* 2011; 20(4):538-49.

Ciravolo V, Huber V, Ghedini GC, Venturelli E, Bianchi F, Campiglio M, Morelli D, Villa A, Della Mina P, Menard S, Filipazzi P, Rivoltini L, Tagliabue E, Pupa SM. Potential role of HER2-overexpressing exosomes in countering trastuzumab-based therapy. *J Cell Physiol*. 2012; 227(2):658-67.

Cirri P, Chiarugi P. Cancer associated fibroblasts: the dark side of the coin. *Am J Cancer Res*. 2011; 1(4):482-97.

Costea DE, Hills A, Osman AH, Thurlow J, Kalna G, Huang X, Pena Murillo C, Parajuli H, Suliman S, Kulasekara KK, Johannessen AC, Partridge M. Identification of two distinct carcinoma-associated fibroblast subtypes with differential tumor-promoting abilities in oral squamous cell carcinoma. *Cancer Res*. 2013; 73(13):3888-901.

Czerwinska P, Kaminska B. Regulation of breast cancer stem cell features. *Contemp Oncol (Pozn)*. 2015; 19(1A):A7-A15.

Di Leva G, Garofalo M, Croce CM. MicroRNAs in cancer. *Annu Rev Pathol*. 2014; 9:287-314.

Dirat B, Bochet L, Dabek M, Daviaud D, Dauvillier S, Majed B, Wang YY, Meulle A, Salles B, Le Gonidec S, Garrido I, Escourrou G, Valet P, Muller C. Cancer-associated adipocytes exhibit an activated phenotype and contribute to breast cancer invasion. *Cancer Res*. 2011; 71(7):2455-65.

Dong G, Liang X, Wang D, Gao H, Wang L, Wang L, Liu J, Du Z. High expression of miR-21 in triple-negative breast cancers was correlated with a poor prognosis and promoted tumor cell in vitro proliferation. *Med Oncol*. 2014; 31(7):57.

Early Breast Cancer Trialists' Collaborative Group (EBCTCG), Peto R, Davies C, Godwin J, Gray R, Pan HC, Clarke M, Cutter D, Darby S, McGale P, Taylor C, Wang YC, Bergh J, Di Leo A, Albain K, Swain S, Piccart M, Pritchard K. Comparisons between different polychemotherapy regimens for early breast cancer: meta-analyses of long-term outcome among 100,000 women in 123 randomised trials. *Lancet* 2012; 379(9814):432-44.

Fabbri M, Paone A, Calore F, Galli R, Gaudio E, Santhanam R, Lovat F, Fadda P, Mao C, Nuovo GJ, Zanesi N, Crawford M, Ozer GH, Wernicke D, Alder H, Caligiuri MA, Nana-Sinkam P, Perrotti D, Croce CM. MicroRNAs bind to Toll-like receptors to induce prometastatic inflammatory response. *Proc Natl Acad Sci U S A* 2012; 109(31):E2110-6.

Fader CM, Sánchez DG, Mestre MB, Colombo MI. TI-VAMP/VAMP7 and VAMP3/cellubrevin: two v-SNARE proteins involved in specific steps of the autophagy/multivesicular body pathways. *Biochim Biophys Acta* 2009; 1793(12):1901-16.

Folkman J, Watson K, Ingber D, Hanahan D. Induction of angiogenesis during the transition from hyperplasia to neoplasia. *Nature* 1989; 339(6219):58-61.

Forman D, Bray F, Brewster DH, Gombe Mbalawa C, Kohler B, Piñeros M, et al., editors. *Cancer Incidence in Five Continents (CI5)*. Lyon: IARC Scientific Publications; 2013.

Gabbiani G, Ryan GB, Majne G. Presence of modified fibroblasts in granulation tissue and their possible role in wound contraction. *Experientia* 1971; 27(5):549-50.

Ghossoub R, Lembo F, Rubio A, Gaillard CB, Bouchet J, Vitale N, Slavík J, Machala M, Zimmermann P. Syntenin-ALIX exosome biogenesis and budding

into multivesicular bodies are controlled by ARF6 and PLD2. *Nat Commun.* 2014; 5:3477.

Goldie BJ, Dun MD, Lin M, Smith ND, Verrills NM, Dayas CV, Cairns MJ. Activity-associated miRNA are packaged in Map1b-enriched exosomes released from depolarized neurons. *Nucleic Acids Res.* 2014; 42(14):9195-208.

Grange C, Tapparo M, Collino F, Vitillo L, Damasco C, Deregibus MC, Tetta C, Bussolati B, Camussi G. Microvesicles released from human renal cancer stem cells stimulate angiogenesis and formation of lung premetastatic niche. *Cancer Res.* 2011; 71(15):5346-56.

Guduric-Fuchs J, O'Connor A, Camp B, O'Neill CL, Medina RJ, Simpson DA. Selective extracellular vesicle-mediated export of an overlapping set of microRNAs from multiple cell types. *BMC Genomics* 2012; 13:357.

Han M, Wang Y, Liu M, Bi X, Bao J, Zeng N, Zhu Z, Mo Z, Wu C, Chen X. MiR-21 regulates epithelial-mesenchymal transition phenotype and hypoxia-inducible factor-1 α expression in third-sphere forming breast cancer stem cell-like cells. *Cancer Sci.* 2012; 103(6):1058-64.

Hanahan D, Coussens LM. Accessories to the crime: functions of cells recruited to the tumor microenvironment. *Cancer Cell* 2012; 21(3):309-22.

Hanahan D, Weinberg RA. Hallmarks of cancer: the next generation. *Cell* 2011; 144(5):646-74.

Hannafon BN, Ding WQ. Intercellular Communication by Exosome-Derived microRNAs in Cancer. *Int J Mol Sci.* 2013; 14(7):14240-69.

Harding C, Stahl P. Transferrin recycling in reticulocytes: pH and iron are important determinants of ligand binding and processing. *Biochem Biophys Res Commun.* 1983; 113(2):650-8.

He K, Xu T, Goldkorn A. Cancer cells cyclically lose and regain drug-resistant highly tumorigenic features characteristic of a cancer stem-like phenotype. *Mol Cancer Ther.* 2011; 10(6):938-48.

Hsu C, Morohashi Y, Yoshimura S, Manrique-Hoyos N, Jung S, Lauterbach MA, Bakhti M, Grønberg M, Möbius W, Rhee J, Barr FA, Simons M. J. Regulation of exosome secretion by Rab35 and its GTPase-activating proteins TBC1D10A-C. *Cell Biol.* 2010; 189(2):223-32.

Hugo HJ, Lebre S, Tomaskovic-Crook E, Ahmed N, Blick T, Newgreen DF, Thompson EW, Ackland ML. Contribution of Fibroblast and Mast Cell (Afferent) and Tumor (Efferent) IL-6 Effects within the Tumor Microenvironment. *Cancer Microenviron.* 2012.

Johnstone RM, Adam M, Hammond JR, Orr L, Turbide C. Vesicle formation during reticulocyte maturation. Association of plasma membrane activities with released vesicles (exosomes). *J Biol Chem.* 1987; 262(19):9412-20.

Josson S, Gururajan M, Sung SY, Hu P, Shao C, Zhau HE, Liu C, Lichterman J, Duan P, Li Q, Rogatko A, Posadas EM, Haga CL, Chung LW. Stromal fibroblast-derived miR-409 promotes epithelial-to-mesenchymal transition and prostate tumorigenesis. *Oncogene* 2014.

Kalluri R, Zeisberg M. Fibroblasts in cancer. *Nat Rev Cancer* 2006; 6(5):392-401.

Kaminska B, Kulesza DW, Ramji K. Overview of Mechanisms of Cancer Stem Cell Drug Resistance. *Current Signal Transduction Therapy* 2013; 8: 180-92.

Kessenbrock K, Plaks V, Werb Z. Matrix metalloproteinases: regulators of the tumor microenvironment. *Cell* 2010; 141(1):52-67.

Kessler DA, Langer RS, Pless NA, Folkman J. Mast cells and tumor angiogenesis. *Int J Cancer* 1976; 18(5):703-9.

Khan S, Aspe JR, Asumen MG, Almaguel F, Odumosu O, Acevedo-Martinez S, De Leon M, Langridge WH, Wall NR. Extracellular, cell-permeable survivin inhibits apoptosis while promoting proliferative and metastatic potential. *Br J Cancer* 2009; 100(7):1073-86.

Kim SH, Choe C, Shin YS, Jeon MJ, Choi SJ, Lee J, Bae GY, Cha HJ, Kim J. Human lung cancer-associated fibroblasts enhance motility of non-small cell lung cancer cells in co-culture. *Anticancer Res.* 2013; 33(5):2001-9.

King HW, Michael MZ, Gleadle JM. Hypoxic enhancement of exosome release by breast cancer cells. *BMC Cancer* 2012; 12:421.

Kojima Y, Acar A, Eaton EN, Mellody KT, Scheel C, Ben-Porath I, Onder TT, Wang ZC, Richardson AL, Weinberg RA, Orimo A. Autocrine TGF-beta and stromal cell-derived factor-1 (SDF-1) signaling drives the evolution of tumor-promoting mammary stromal myofibroblasts. *Proc Natl Acad Sci U S A.* 2010; 107(46):20009-14.

Koppers-Lalic D, Hackenberg M, Bijnsdorp IV, van Eijndhoven MA, Sadek P, Sie D, Zini N, Middeldorp JM, Ylstra B, de Menezes RX, Würdinger T, Meijer GA, Pegtel DM. Nontemplated nucleotide additions distinguish the small RNA composition in cells from exosomes. *Cell Rep.* 2014; 8(6):1649-58.

Kosaka N, Iguchi H, Hagiwara K, Yoshioka Y, Takeshita F, Ochiya T. Neutral sphingomyelinase 2 (nSMase2)-dependent exosomal transfer of angiogenic microRNAs regulate cancer cell metastasis. *J Biol Chem.* 2013; 288(15):10849-59.

Kowal J, Tkach M, Théry C. Biogenesis and secretion of exosomes. *Curr Opin Cell Biol.* 2014; 29:116-25.

Labelle M, Begum S, Hynes RO. Direct signaling between platelets and cancer cells induces an epithelial-mesenchymal-like transition and promotes metastasis. *Cancer Cell* 2011; 20(5):576-90.

Leis O, Eguiara A, Lopez-Arribillaga E, Alberdi MJ, Hernandez-Garcia S, Elorriaga K, Pandiella A, Rezola R, Martin AG. Sox2 expression in breast tumors and activation in breast cancer stem cells. *Oncogene* 2012; 31(11):1354-65.

Li S, Yang X, Yang J, Zhen J, Zhang D. Serum microRNA-21 as a potential diagnostic biomarker for breast cancer: a systematic review and meta-analysis. *Clin Exp Med.* 2014 Dec 17.

Lin EY, Li JF, Bricard G, Wang W, Deng Y, Sellers R, Porcelli SA, Pollard JW. Vascular endothelial growth factor restores delayed tumor progression in tumors depleted of macrophages. *Mol Oncol.* 2007; 1(3):288-302.

Lin J, Li J, Huang B, Liu J, Chen X, Chen XM, Xu YM, Huang LF, Wang XZ. Exosomes: Novel Biomarkers for Clinical Diagnosis. *Scientific World Journal.* 2015; 2015:657086.

Lu P, Takai K, Weaver VM, Werb Z. Extracellular matrix degradation and remodeling in development and disease. *Cold Spring Harb Perspect Biol.* 2011; 3(12).

Luga V, Zhang L, Vitoria-Petit AM, Ogunjimi AA, Inanlou MR, Chiu E, Buchanan M, Hosein AN, Basik M, Wrana JL. Exosomes mediate stromal mobilization of autocrine Wnt-PCP signaling in breast cancer cell migration. *Cell* 2012; 151(7):1542-56.

Malhotra GK, Zhao X, Band H, Band V. Histological, molecular and functional subtypes of breast cancers. *Cancer Biol Ther.* 2010; 10(10): 955–960.

Mani SA, Guo W, Liao MJ, Eaton EN, Ayyanan A, Zhou AY, Brooks M, Reinhard F, Zhang CC, Shipitsin M, Campbell LL, Polyak K, Briskin C, Yang J, Weinberg RA. The epithelial-mesenchymal transition generates cells with properties of stem cells. *Cell* 2008; 133(4):704-15.

Mao Y, Keller ET, Garfield DH, Shen K, Wang J. Stromal cells in tumor microenvironment and breast cancer. *Cancer Metastasis Rev.* 2013; 32(1-2):303-15.

Mao Y, Zhang Y, Qu Q, Zhao M, Lou Y, Liu J, Huang O, Chen X, Wu J, Shen K. Cancer-associated fibroblasts induce trastuzumab resistance in HER2 positive breast cancer cells. *Mol Biosyst.* 2015. [Epub ahead of print]

Melo SA, Sugimoto H, O'Connell JT, Kato N, Villanueva A, Vidal A, Qiu L, Vitkin E, Perelman LT, Melo CA, Lucci A, Ivan C, Calin GA, Kalluri R. Cancer exosomes perform cell-independent microRNA biogenesis and promote tumorigenesis. *Cancer Cell* 2014; 26(5):707-21.

Miller E, Lee HJ, Lulla A, Hernandez L, Gokare P, Lim B. Current treatment of early breast cancer: adjuvant and neoadjuvant therapy. *F1000Res.* 2014; 3:198.

Mittelbrunn M, Sánchez-Madrid F. Intercellular communication: diverse structures for exchange of genetic information. *Nat Rev Mol Cell Biol.* 2012; 13(5):328-35.

Morel AP, Lièvre M, Thomas C, Hinkal G, Ansieau S, Puisieux A. Generation of breast cancer stem cells through epithelial-mesenchymal transition. *PLoS One* 2008; 3(8):e2888.

Muñoz P, Iliou MS, Esteller M. Epigenetic alterations involved in cancer stem cell reprogramming. *Mol Oncol.* 2012; 6(6):620-36.

Ohshima K, Inoue K, Fujiwara A, Hatakeyama K, Kanto K, Watanabe Y, Muramatsu K, Fukuda Y, Ogura S, Yamaguchi K, Mochizuki T. Let-7 microRNA family is selectively secreted into the extracellular environment via exosomes in a metastatic gastric cancer cell line. *PLoS One* 2010; 5(10):e13247.

Orimo A, Gupta PB, Sgroi DC, Arenzana-Seisdedos F, Delaunay T, Naeem R, Carey VJ, Richardson AL, Weinberg RA. Stromal fibroblasts present in invasive human breast carcinomas promote tumor growth and angiogenesis through elevated SDF-1/CXCL12 secretion. *Cell* 2005; 121(3):335-48.

Orimo A, Weinberg RA. Stromal fibroblasts in cancer: a novel tumor-promoting cell type. *Cell Cycle* 2006; 5(15):1597-601.

Özdemir BC, Pentcheva-Hoang T, Carstens JL, Zheng X, Wu CC, Simpson TR, Laklai H, Sugimoto H, Kahlert C, Novitskiy SV, De Jesus-Acosta A, Sharma P, Heidari P, Mahmood U, Chin L, Moses HL, Weaver VM, Maitra A, Allison JP, LeBleu VS, Kalluri R. Depletion of carcinoma-associated fibroblasts and fibrosis induces immunosuppression and accelerates pancreas cancer with reduced survival. *Cancer Cell* 2014; 25(6):719-34.

Pahler JC, Tazzyman S, Erez N, Chen YY, Murdoch C, Nozawa H, Lewis CE, Hanahan D. Plasticity in tumor-promoting inflammation: impairment of

macrophage recruitment evokes a compensatory neutrophil response. *Neoplasia* 2008; 10(4):329-40.

Paunescu V, Bojin FM, Tatu CA, Gavriluc OI, Rosca A, Gruia AT, Tanasie G, Bunu C, Crisnic D, Gherghiceanu M, Tatu FR, Tatu CS, Vermesan S. Tumor-associated fibroblasts and mesenchymal stem cells: more similarities than differences. *J Cell Mol Med*. 2011; 15(3):635-46.

Peinado H, Alečković M, Lavotshkin S, Matei I, Costa-Silva B, Moreno-Bueno G, Hergueta-Redondo M, Williams C, García-Santos G, Ghajar C, Nitadori-Hoshino A, Hoffman C, Badal K, Garcia BA, Callahan MK, Yuan J, Martins VR, Skog J, Kaplan RN, Brady MS, Wolchok JD, Chapman PB, Kang Y, Bromberg J, Lyden D. Melanoma exosomes educate bone marrow progenitor cells toward a pro-metastatic phenotype through MET. *Nat Med*. 2012; 18(6):883-91.

Peinado H, Lavotshkin S, and Lyden D. The secreted factors responsible for pre-metastatic niche formation: Old sayings and new thoughts. *Semin. Cancer Biol*. 2011.

Perez-Hernandez D, Gutiérrez-Vázquez C, Jorge I, López-Martín S, Ursa A, Sánchez-Madrid F, Vázquez J, Yáñez-Mó M. The intracellular interactome of tetraspanin-enriched microdomains reveals their function as sorting machineries toward exosomes. *J Biol Chem*. 2013; 288(17):11649-61.

Pinto CA, Widodo E, Waltham M, Thompson EW. Breast cancer stem cells and epithelial mesenchymal plasticity - Implications for chemoresistance. *Cancer Lett*. 2013; 341(1):56-62.

Polyak K, Kalluri R. The role of the microenvironment in mammary gland development and cancer. *Cold Spring Harb Perspect Biol*. 2010; 2(11):a003244.

Proux-Gillardeaux V, Raposo G, Irinopoulou T, Galli T. Expression of the Longin domain of TI-VAMP impairs lysosomal secretion and epithelial cell migration. *Biol Cell*. 2007; 99(5):261-71.

Quintavalle C, Donnarumma E, Iaboni M, Roscigno G, Garofalo M, Romano G, Fiore D, De Marinis P, Croce CM, Condorelli G. Effect of miR-21 and miR-30b/c on TRAIL-induced apoptosis in glioma cells. *Oncogene* 2013; 32(34):4001-8.

Räsänen K, Vaheri A. Activation of fibroblasts in cancer stroma. *Exp Cell Res*. 2010; 316(17):2713-22.

Rattigan YI, Patel BB, Ackerstaff E, Sukenick G, Koutcher JA, Glod JW, Banerjee D. Lactate is a mediator of metabolic cooperation between stromal

carcinoma associated fibroblasts and glycolytic tumor cells in the tumor microenvironment. *Exp Cell Res*. 2012; 318(4):326-35.

Rivenbark AG, O'Connor SM, Coleman WB. Molecular and cellular heterogeneity in breast cancer: challenges for personalized medicine. *Am J Pathol*. 2013; 183(4):1113-24.

Rosen ED, MacDougald OA. Adipocyte differentiation from the inside out. *Nat Rev Mol Cell Biol*. 2006; 7(12):885-96.

Ruffell B, DeNardo DG, Affara NI, Coussens LM. Lymphocytes in cancer development: polarization towards pro-tumor immunity. *Cytokine Growth Factor Rev*. 2010; 21(1):3-10.

Rupninder Sandhu, MBBS, Joel S. Parker, MS, Wendell D. Jones, PhD, Chad A. Livasy, MD, William B. Coleman, PhD. Microarray-Based Gene Expression Profiling for Molecular Classification of Breast Cancer and Identification of New Targets for Therapy. *LabMed* 2010; vol. 41 no. 6 364-372.

Sabrkhany S, Griffioen AW, Oude Egbrink MG. The role of blood platelets in tumor angiogenesis. *Biochim Biophys Acta* 2011; 1815(2):189-96.

Safaei R, Larson BJ, Cheng TC, Gibson MA, Otani S, Naerdemann W, Howell SB. Abnormal lysosomal trafficking and enhanced exosomal export of cisplatin in drug-resistant human ovarian carcinoma cells. *Mol Cancer Ther*. 2005; 4(10):1595-604.

Sahu R, Kaushik S, Clement CC, Cannizzo ES, Scharf B, Follenzi A, Potolicchio I, Nieves E, Cuervo AM, Santambrogio L. Microautophagy of cytosolic proteins by late endosomes. *Dev Cell*. 2011; 20(1):131-9.

Sato-Kuwabara Y, Melo SA, Soares FA, Calin GA. The fusion of two worlds: non-coding RNAs and extracellular vesicles--diagnostic and therapeutic implications (Review). *Int J Oncol*. 2015; 46(1):17-27.

Savina A, Fader CM, Damiani MT, Colombo MI. Rab11 promotes docking and fusion of multivesicular bodies in a calcium-dependent manner. *Traffic*. 2005; 6(2):131-43.

Schee K, Lorenz S, Worren MM, Günther CC, Holden M, Hovig E, Fodstad O, Meza-Zepeda LA, Flatmark K. Deep Sequencing the MicroRNA Transcriptome in Colorectal Cancer. *PLoS One* 2013; 8(6):e66165.

Scheel C, Weinberg RA. Cancer stem cells and epithelial-mesenchymal transition: concepts and molecular links. *Semin Cancer Biol*. 2012; 22(5-6):396-403.

Shimoda M, Principe S, Jackson HW, Luga V, Fang H, Molyneux SD, Shao YW, Aiken A, Waterhouse PD, Karamboulas C, Hess FM, Ohtsuka T, Okada Y, Ailles L, Ludwig A, Wrana JL, Kislinger T, Khokha R. Loss of the Timp gene family is sufficient for the acquisition of the CAF-like cell state. *Nat Cell Biol.* 2014; 16(9):889-901.

Shree T, Olson OC, Elie BT, Kester JC, Garfall AL, Simpson K, Bell-McGuinn KM, Zabor EC, Brogi E, Joyce JA. Macrophages and cathepsin proteases blunt chemotherapeutic response in breast cancer. *Genes Dev.* 2011; 25(23):2465-79.

Silva J, García V, Zaballos Á, Provencio M, Lombardía L, Almonacid L, García JM, Domínguez G, Peña C, Diaz R, Herrera M, Varela A, Bonilla F. Vesicle-related microRNAs in plasma of nonsmall cell lung cancer patients and correlation with survival. *Eur Respir J.* 2011; 37(3):617-23.

Skog J, Würdinger T, van Rijn S, Meijer DH, Gainche L, Sena-Esteves M, Curry WT Jr, Carter BS, Krichevsky AM, Breakefield XO. Glioblastoma microvesicles transport RNA and proteins that promote tumor growth and provide diagnostic biomarkers. *Nat Cell Biol.* 2008; 10(12):1470-6.

Song B, Wang C, Liu J, Wang X, Lv L, Wei L, Xie L, Zheng Y, Song X. MicroRNA-21 regulates breast cancer invasion partly by targeting tissue inhibitor of metalloproteinase 3 expression. *J Exp Clin Cancer Res.* 2010; 29:29.

Stanisavljevic J, Loubat-Casanovas J, Herrera M, Luque T, Peña R, Lluch A, Albanell J, Bonilla F, Rovira A, Peña C, Navajas D, Rojo F, García de Herreros A, Baulida J. Snail1-expressing fibroblasts in the tumor microenvironment display mechanical properties that support metastasis. *Cancer Res.* 2015; 75(2):284-95.

Stenmark H. Rab GTPases as coordinators of vesicle traffic. *Nat Rev Mol Cell Biol.* 2009; 10(8):513-25.

Stover DG, Bierie B, Moses HL. A delicate balance: TGF-beta and the tumor microenvironment. *J Cell Biochem.* 2007; 101(4):851-61.

Svoboda J, Dvorák M, Guntaka R, Geryk J. Transmission of (LTR, v-src, LTR) without recombination with a helper virus. *Virology* 1986; 153(2):314-7.

Takahashi K, Yamanaka S. Induction of pluripotent stem cells from mouse embryonic and adult fibroblast cultures by defined factors. *Cell* 2006; 126(4):663-76.

Talmadge JE, and Fidler IJ. AACR centennial series: the biology of cancer metastasis: historical perspective. *Cancer Res.* 2010; 70, 5649–5669.

Tjensvoll K, Oltedal S, Heikkilä R, Kvaløy JT, Gilje B, Reuben JM, Smaaland R, Nordgård O. Persistent tumor cells in bone marrow of non-metastatic breast cancer patients after primary surgery are associated with inferior outcome. *BMC Cancer* 2012; 12:190.

Trajkovic K, Hsu C, Chiantia S, Rajendran L, Wenzel D, Wieland F, Schwille P, Brügger B, Simons M. Ceramide triggers budding of exosome vesicles into multivesicular endosomes. *Science*. 2008; 319(5867):1244-7.

Trimboli AJ, Cantemir-Stone CZ, Li F, Wallace JA, Merchant A, Creasap N, Thompson JC, Caserta E, Wang H, Chong JL, Naidu S, Wei G, Sharma SM, Stephens JA, Fernandez SA, Gurcan MN, Weinstein MB, Barsky SH, Yee L, Rosol TJ, Stromberg PC, Robinson ML, Pepin F, Hallett M, Park M, Ostrowski MC, Leone G. Pten in stromal fibroblasts suppresses mammary epithelial tumors. *Nature* 2009; 461(7267):1084-91.

Tsuyada A, Chow A, Wu J, Somlo G, Chu P, Loera S, Luu T, Li AX, Wu X, Ye W, Chen S, Zhou W, Yu Y, Wang YZ, Ren X, Li H, Scherle P, Kuroki Y, Wang SE. CCL2 mediates cross-talk between cancer cells and stromal fibroblasts that regulates breast cancer stem cells. *Cancer Res.* 2012; 72(11):2768-79.

Umezu T, Ohyashiki K, Kuroda M, Ohyashiki JH. Leukemia cell to endothelial cell communication via exosomal miRNAs. *Oncogene* 2013; 32(22):2747-55.

Valadi H, Ekström K, Bossios A, Sjöstrand M, Lee JJ, Lötvall JO. Exosome-mediated transfer of mRNAs and microRNAs is a novel mechanism of genetic exchange between cells. *Nat Cell Biol.* 2007; 9(6):654-9.

Valenti R, Huber V, Iero M, Filipazzi P, Parmiani G, Rivoltini L. Tumor-released microvesicles as vehicles of immunosuppression. *Cancer Res.* 2007; 67(7):2912-5.

van Niel G, Charrin S, Simoes S, Romao M, Rochin L, Saftig P, Marks MS, Rubinstein E, Raposo G. The tetraspanin CD63 regulates ESCRT-independent and -dependent endosomal sorting during melanogenesis. *Dev Cell.* 2011; 21(4):708-21.

Villarroya-Beltri C, Gutiérrez-Vázquez C, Sánchez-Cabo F, Pérez-Hernández D, Vázquez J, Martín-Cofreces N, Martínez-Herrera DJ, Pascual-Montano A, Mittelbrunn M, Sánchez-Madrid F. Sumoylated hnRNPA2B1 controls the sorting of miRNAs into exosomes through binding to specific motifs. *Nat Commun.* 2013; 4:2980.

Vong S, Kalluri R. The role of stromal myofibroblast and extracellular matrix in tumor angiogenesis. *Genes Cancer* 2011; 2(12):1139-45.

Wang D, Lu P, Zhang H, Luo M, Zhang X, Wei X, Gao J, Zhao Z, Liu C. Oct-4 and Nanog promote the epithelial-mesenchymal transition of breast cancer stem cells and are associated with poor prognosis in breast cancer patients. *Oncotarget* 2014; 5(21):10803-15.

Wasiuk A, de Vries VC, Hartmann K, Roers A, Noelle RJ. Mast cells as regulators of adaptive immunity to tumors. *Clin Exp Immunol.* 2009; 155(2):140-6.

Webber JP, Spary LK, Sanders AJ, Chowdhury R, Jiang WG, Steadman R, Wymant J, Jones AT, Kynaston H, Mason MD, Tabi Z, Clayton A. Differentiation of tumor-promoting stromal myofibroblasts by cancer exosomes. *Oncogene* 2015; 34(3):290-302.

Wu XL, Cheng B, Li PY, Huang HJ, Zhao Q, Dan ZL, Tian DA, Zhang P. MicroRNA-143 suppresses gastric cancer cell growth and induces apoptosis by targeting COX-2. *World J Gastroenterol.* 2013; 19(43):7758-65.

Wyckoff J, Wang W, Lin EY, Wang Y, Pixley F, Stanley ER, Graf T, Pollard JW, Segall J, Condeelis J. A paracrine loop between tumor cells and macrophages is required for tumor cell migration in mammary tumors. *Cancer Res.* 2004; 64(19):7022-9.

Yang M, Chen J, Su F, Yu B, Su F, Lin L, Liu Y, Huang JD, Song E. Microvesicles secreted by macrophages shuttle invasion-potentiating microRNAs into breast cancer cells. *Mol Cancer* 2011; 10:117.

Zhang HG, Liu C, Su K, Yu S, Zhang L, Zhang S, Wang J, Cao X, Grizzle W, Kimberly RP. A membrane form of TNF-alpha presented by exosomes delays T cell activation-induced cell death. *J Immunol.* 2006; 177(3):2025.

Zhou W, Fong MY, Min Y, Somlo G, Liu L, Palomares MR, Yu Y, Chow A, O'Connor ST, Chin AR, Yen Y, Wang Y, Marcusson EG, Chu P, Wu J, Wu X, Li AX, Li Z, Gao H, Ren X, Boldin MP, Lin PC, Wang SE. Cancer-secreted miR-105 destroys vascular endothelial barriers to promote metastasis. *Cancer Cell* 2014; 25(4):501-15.

miR-221/222 Target the DNA Methyltransferase MGMT in Glioma Cells

Cristina Quintavalle^{1,2}*, Davide Mangani¹*, Giuseppina Roscigno^{1,2}, Giulia Romano³, Angel Diaz-Lagares⁴, Margherita Iaboni¹, Elvira Donnarumma³, Danilo Fiore¹, Pasqualino De Marinis⁵, Ylmeri Soini⁶, Manel Esteller⁴, Gerolama Condorelli^{1,2}*

1 Department of Molecular Medicine and Medical Biotechnology, "Federico II" University of Naples, Naples, Italy, **2** IEOS, CNR, Naples, Italy, **3** Fondazione IRCCS SDN, Naples, Italy, **4** Epigenetic and Cancer Biology Program (PEBC) IDIBELL, Hospital Duran i Reynals, Barcelona, Spain, **5** Ospedale Cardarelli, Naples, Italy, **6** Department of Pathology and Forensic Medicine, Institute of Clinical Medicine, Pathology and Forensic Medicine, School of Medicine, Cancer Center of Eastern Finland, University of Eastern Finland, Kuopio, Finland

Abstract

Glioblastoma multiforme (GBM) is one of the most deadly types of cancer. To date, the best clinical approach for treatment is based on administration of temozolomide (TMZ) in combination with radiotherapy. Much evidence suggests that the intracellular level of the alkylating enzyme O⁶-methylguanine–DNA methyltransferase (MGMT) impacts response to TMZ in GBM patients. MGMT expression is regulated by the methylation of its promoter. However, evidence indicates that this is not the only regulatory mechanism present. Here, we describe a hitherto unknown microRNA-mediated mechanism of MGMT expression regulation. We show that miR-221 and miR-222 are upregulated in GBM patients and that these paralogues target MGMT mRNA, inducing greater TMZ-mediated cell death. However, miR-221/miR-222 also increase DNA damage and, thus, chromosomal rearrangements. Indeed, miR-221 overexpression in glioma cells led to an increase in markers of DNA damage, an effect rescued by re-expression of MGMT. Thus, chronic miR-221/222-mediated MGMT downregulation may render cells unable to repair genetic damage. This, associated also to miR-221/222 oncogenic potential, may poor GBM prognosis.

Citation: Quintavalle C, Mangani D, Roscigno G, Romano G, Diaz-Lagares A, et al. (2013) miR-221/222 Target the DNA Methyltransferase MGMT in Glioma Cells. PLoS ONE 8(9): e74466. doi:10.1371/journal.pone.0074466

Editor: Russell O. Pieper, University of California-San Francisco, United States of America

Received: June 10, 2013; **Accepted:** July 31, 2013; **Published:** September 19, 2013

Copyright: © 2013 Quintavalle et al. This is an open-access article distributed under the terms of the Creative Commons Attribution License, which permits unrestricted use, distribution, and reproduction in any medium, provided the original author and source are credited.

Funding: This work was partially supported by funds from Associazione Italiana Ricerca sul Cancro, to GC (grant n.ro 10620), MERIT (RBNE08E8CZ_002) to GC, POR Campania FSE 2007-2013, Project CRÈME to GC. CQ and MI was supported by the "Federazione Italiana Ricerca sul Cancro" Post-Doctoral Research Fellowship. GR was supported by a MERIT project Fellowship. ADL was supported by the Angeles Alvario-2009 postdoctoral fellowship from the Xunta de Galicia and European Social Fund and at present is the recipient of a Sara Borrell postdoctoral contract (CD12/00738) from the Instituto de Salud Carlos III at the Spanish Ministry of Economy and Competitiveness. The funders had no role in study design, data collection and analysis, decision to publish, or preparation of the manuscript.

Competing interests: The authors have declared that no competing interests exist.

* E-mail: gecondor@unina.it

© These authors contributed equally to this work.

Introduction

Glioblastoma multiforme (GBM) is the most common and deadly primary tumor of the central nervous system. Despite several therapeutic advances, the prognosis for GBM remains poor, with a median survival lower than 15 months [1,2]. Currently, first-line therapy for GBM comprises surgery with the maximum feasible resection, followed by a combination of radiotherapy and treatment with the alkylating agent temozolomide (TMZ), also referred to by its brand name Temodal [3,4,5]. TMZ is a methylating agent that modifies DNA in several positions, one of them being O⁶-methylguanine MeG (O⁶MeG) [6]. If the methyl group is not removed before cell division, this modified guanine preferentially pairs with thymine

during DNA replication, triggering the DNA mismatch repair (MMR) pathway, DNA double-strand breaks, and, therefore, the apoptotic pathway [7,8]. O⁶-methylguanine–methyltransferase (MGMT) is a suicide cellular DNA repair enzyme ubiquitously expressed in normal human tissues. MGMT does not act as a part of a repair complex but works alone [9]. To neutralize the cytotoxic effects of alkylating agents, such as TMZ, it rapidly reverses alkylation at the O⁶ position of guanine, transferring the alkyl group to an internal cysteine residue in its active site. In this form, the enzyme is inactive and, thus, requires *de novo* protein synthesis. In tumors, high levels of MGMT activity are associated with resistance to alkylating agents [10]. In contrast, epigenetic silencing of MGMT gene expression by promoter methylation

results in sensitization to therapy [11,12]. However, some studies have reported that MGMT promoter methylation does not always correlate with MGMT expression and with response to therapy [13,14]. Therefore, the existence of other mechanisms of MGMT regulation should be postulated.

MicroRNAs (miRs) are small regulatory molecules that have a role in cancer progression and in tumor therapy response [15,16]. By negatively regulating the expression of their targets, miRs can act as tumor suppressors or oncogenes [17]. miRs may also regulate DNA damage response and DNA repair, interfering with the response to chemotherapy or radiotherapy [18]. Several studies have indicated that the modulation of miR expression levels is a possible therapeutic strategy for cancer.

The paralogues miR-221 and miR-222 have frequently been found to be dysregulated in glioblastoma and astrocytomas [19,20,21,22]. Their upregulation increases glioma cell proliferation, motility, and *in vivo* growth in mouse models. miR-221/222 have also been shown to be implicated in cellular sensitivity to tumor necrosis factor-related apoptosis-inducing ligand (TRAIL)-treatment [23,24,25]. In this manuscript, we provide evidence that miR-221 and miR-222 regulate MGMT expression levels in glioblastoma, increasing the response to TMZ, but due to their oncogenic potential, affect overall patient survival negatively.

Materials and Methods

Cell culture and transfection

U87MG, T98G, LN428, LN308, A172, and HEK-293 cells were grown in DMEM. LN229 were grown in Advanced DMEM (Gibco, Life technologies, Milan, Italy). T98G, U87MG, and LN229 were from ATCC (LG Standards, Milan Italy); LN428, LN308, and A172 were kindly donated by Frank Furnari (La Jolla University). Media were supplemented with 10% heat-inactivated fetal bovine serum (FBS) -5% FBS for LN229 -2 mM L-glutamine, and 100 U/ml penicillin/streptomycin. All media and supplements were from Sigma Aldrich (Milan, Italy). For overexpression of miRs, cells at 50% confluency were transfected using Oligofectamine (Invitrogen, Milan, Italy) and 100nM pre-miR-221 or pre-miR-222, a scrambled miR or anti-miR-221/222 (Applied Biosystems, Milan, Italy). For overexpression of MGMT, cells were transfected using Lipofectamine and Plus Reagent with 4 µg of MGMT cDNA (Origene, Rockville MD USA). Temozolomide was purchased from Sigma Aldrich (Milan, Italy).

Human Glioma samples

A total of 34 formalin-fixed, paraffin-embedded (FFPE) tissue samples were collected from the archives of the Department of Pathology, University Hospital of Kuopio, Finland. Permission to use the material was obtained from the National Supervisory Authority for Welfare and Health of Finland, and the study was accepted by the ethical committee of the Northern Savo Hospital District, Kuopio, Finland.

Primary cell cultures

Glioblastoma specimens were obtained as previously described [19]. Samples were mechanically disaggregated, and the lysates grown in DMEM-F12 medium supplemented with 10% FBS, 1% penicillin streptomycin, and 20 ng/ml epidermal growth factor (EGF; Sigma-Aldrich, Milan, Italy). To determine the glial origin of the isolated cells, we stained the cultures for glial fibrillary acidic protein (GFAP), a protein found in glial cells.

Protein isolation and Western blotting

Cells were washed twice in ice-cold PBS and lysed in JS buffer (50 mM HEPES pH 7.5 containing 150 mM NaCl, 1% Glycerol, 1% Triton X100, 1.5mM MgCl₂, 5mM EGTA, 1 mM Na₃VO₄, and 1X protease inhibitor cocktail). Protein concentration was determined by the Bradford assay (BioRad, Milan, Italy) using bovine serum albumin (BSA) as the standard, and equal amounts of proteins were analyzed by SDS-PAGE (12.5% acrylamide). Gels were electroblotted onto nitrocellulose membranes (GE Healthcare, Milan, Italy). For immunoblot experiments, membranes were blocked for 1 hr with 5% non-fat dry milk in Tris-buffered saline (TBS) containing 0.1% Tween-20, and incubated at 4°C overnight with primary antibody. Detection was performed by peroxidase-conjugated secondary antibodies using the enhanced chemiluminescence system (GE Healthcare, Milan, Italy). Primary antibodies used were: anti-β-actin from Sigma-Aldrich (Milan Italy); anti-caspase-3 and anti-PARP from Santa Cruz Biotechnologies (Santa Cruz, CA, USA), anti-γH2AX from Millipore (Milan, Italy), anti-p53, p^{ser15} p53, and phosphorylated-ATM from Cell Signaling Technology (Milan, Italy).

RNA extraction and Real-Time PCR

Cell culture: Total RNA (microRNA and mRNA) were extracted using Trizol (Invitrogen, Milan, Italy) according to the manufacturer's protocol.

Tissue specimens

Total RNA (miRNA and mRNA) from FFPE tissue specimens was extracted using RecoverAll Total Nucleic Acid isolation Kit (Ambion, Life Technologies, Milan, Italy) according to the manufacturer's protocol. Reverse transcription of total miRNA was performed starting from equal amounts of total RNA/sample (1µg) using miScript reverse Transcription Kit (Qiagen, Milan, Italy), and with SuperScript® III Reverse Transcriptase (Invitrogen, Milan, Italy) for mRNA. Quantitative analysis of MGMT, β-actin (as an internal reference), miR-221, miR-222, and RNU5A (as an internal reference) were performed by RealTime PCR using specific primers (Qiagen, Milan, Italy), miScript SYBR Green PCR Kit (Qiagen, Milan, Italy), and iQ™ SYBR Green Supermix (Bio-Rad, Milan, Italy), respectively. The reaction for detection of mRNAs was performed as follows: 95°C for 15', 40 cycles of 94°C for 15", 60°C for 30", and 72°C for 30". The reaction for detection of miRNAs was performed as follows: 95°C for 15', 40 cycles of 94°C for 15", 55°C for 30", and 70°C for 30". All reactions were run in triplicate. The threshold cycle (CT) is defined as the fractional cycle number

at which the fluorescence passes the fixed threshold. For relative quantization, the $2^{-\Delta CT}$ method was used as previously described [26]. Experiments were carried out in triplicate for each data point, and data analysis was performed by using a Bio-Rad software (Bio-Rad, Milan, Italy).

Luciferase assay

The 3' UTR of the human MGMT gene was PCR amplified using the following primers: MGMT-Fw: 5'TCTAGAGTATGTGCAGTAGGATGGATG3'; MGMT-Rv: 5'TCCAGAGCTACAGGTTTCCCTTCC3', and cloned downstream of the Renilla luciferase stop codon in pGL3 control vector (Promega, Milan, Italy). A deletion was introduced into the miRNA-binding sites with the QuikChange Mutagenesis Kit (Stratagene, La Jolla CA USA) using the following primers: MGMT-mut Fw: 5'CTATATCCAAAAGGGAAACCTGTAGCTCTTGC 3'. MGMT-mut Rv: 5'-GCAGAGCTACACGTTTCCCTTTGGATATAG 3'. HEK-293 cells were co-transfected with 1.2 µg of plasmid and 400 µg of a Renilla luciferase expression construct, pRL-TK (Promega, Milan, Italy), with Lipofectamine 2000 (Invitrogen, Milan, Italy). Cells were harvested 24 hrs post-transfection and assayed with Dual Luciferase Assay (Promega, Milan, Italy) according to the manufacturer's instructions. Three independent experiments were performed in triplicate.

Cell death quantification

Cell viability was evaluated with the CellTiter 96 Aqueous One Solution Cell Proliferation Assay (Promega, Milan, Italy) according to the manufacturer's protocol. Metabolically active cells were detected by adding 20 µL of MTS to each well. After 2 hrs of incubation, the plates were analyzed in a Multilabel Counter (BioTek, Milan, Italy). For caspase-3 inhibition experiments, ZVAD-Fmk was purchased from Calbiochem.

Comet assay

Alkaline comet assay was performed accordingly to manufacturer's instructions (Trevigen, Gaithersburg, Maryland, USA). Briefly, 12×10^4 glioblastoma cell lines were transfected with miRs or MGMT cDNA and then treated with TMZ in 6-well plates. Cells were collected and then combined with LMAgarose. The mixture was applied to Comet slides and kept at 4°C in the dark for 10'. The slides were immersed in pre-chilled lysis buffer for 30 min. The slides were washed and then electrophoresis was carried out. The slides were fixed in 70% ethanol for 5 min and let dry overnight. SYBR green was added and comets were photographed at 100 x microscopes (Carl Zeiss Inc., NY, USA).

γH2AX flow cytometric analysis

Treated cells were fixed with 2% paraformaldehyde for 1 hr. Fixed cells were permeabilized with 0.1% Triton-X100/PBS for 5 min on ice. Blocking was done in PBS+2% BSA. Anti-phosphorylated H2Ax antibody (Ser139, γH2Ax, Millipore, Milan, Italy) was diluted in PBS and then FITC-conjugated goat anti-mouse antibody (Santa cruz Biotechnology, CA, USA) was

used. Cells were analyzed with a Becton Dickinson FACScan flow cytometer.

Caspase Assay

The assay was performed using the Colorimetric CaspACE™ Assay System, (Promega, Milan, Italy) as reported in the instruction manual. Briefly, T98G cells were transfected with miR-221 and/or MGMT cDNA, plated in 96-well plates, and then treated with 300 µMol of temozolomide or with 10 µMol of ZVAD-Fmk. After treatments, 100 µl caspase-3/-7 reagent was added to each well for 1 hr in the dark. The plates were analyzed in a Multilabel Counter (BioTek, Milan, Italy).

MGMT Methylation Analysis

DNA methylation status in the CpG island of *MGMT* was established by PCR analysis of bisulfite modified genomic DNA, which induces chemical conversion of unmethylated, but not methylated, cytosine to uracil. DNA was extracted from cell lines using the DNeasy blood and tissue kit (Qiagen, Milan, Italy). DNA (1 µg) was modified with sodium bisulfite using the EZ DNA methylation-gold kit (Zymo Research, CA, USA) according to the manufacturer's instructions. Methylation-specific polymerase chain reaction (MSP) was performed with primers specific for either methylated or the modified unmethylated DNA. Primer sequences for the unmethylated reaction were 5'TTTGTGTTTGTAGTTTGTAGTTTGT3' (forward primer) and 5'AACTCCACACTCTTCCAAAAACAAAACA3' (reverse primer), and for the methylated reaction they were 5'TTTCGACGTTTCGTAGTTTTCGC3' (forward primer) and 5'GCACTCTTCCGAAAACGAAACG3' (reverse primer.) The annealing temperature was 59°C. The cell line SW48 and *in vitro* methylated DNA (CpGenome Universal Methylated DNA, Millipore) were used as a positive control for the methylation of MGMT and DNA from normal lymphocytes used as a negative control. Controls without DNA were used for each set of methylation-specific PCR assays. The methylation-specific PCR product was loaded directly onto 2% agarose gels, stained with syber safe, and examined under ultraviolet illumination.

Colony Assay

Cells were transfected with scrambled miR or miR-221 for 24 hrs, harvested, and 2.4×10^4 cells plated in 6-well plates. After 24 hrs, cells were treated with 300 µMol TMZ for 24 hrs, as indicated. Cells were transferred to 100-mm dishes and grown for 6 days. Finally, the cells were colored with 0.1% crystal violet dissolved in 25% methanol for 20 min at 4°C. Dishes were washed with water, left to dry on the bench, and then photographs taken.

Statistical analysis

Student's *t* test and nonparametric Mann-Whitney tests were used to determine differences between values for normally and, respectively, not normally distributed variables. A probability level <0.05 was considered significant throughout

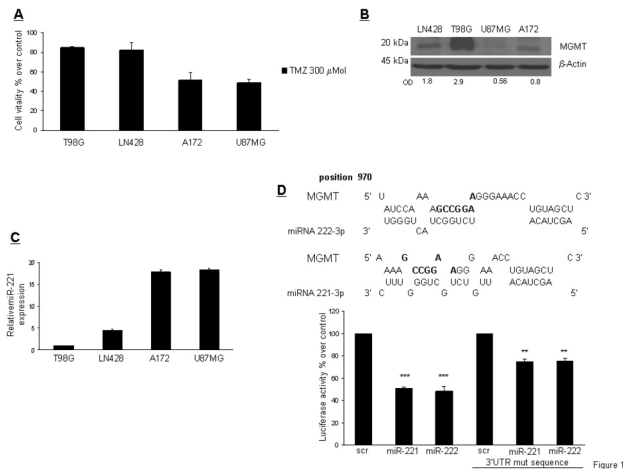


Figure 1. TMZ sensitivity and MGMT and miR-221/222 expression in glioma cells. (A) Glioma cells were treated with TMZ (300μMol) for 24 hr. Cell viability was evaluated with an MTT assay. (B) Western blot analysis of MGMT expression in glioblastoma cells. (C) Real time PCR of miR-221 expression in glioblastoma cells. (D) RNA Hybrid prediction analyzes of miR-222, miR-221, and MGMT 3' UTR. In bold are shown the mutated oligonucleotides. Luciferase activity of HEK-293 cells transiently co-transfected with the luciferase reporter containing wild-type MGMT-3'UTR or mutant MGMT-3'UTR in the presence of pre-miR-222, miR-221, or scrambled oligonucleotide. Representative of at least three independent experiments. *** $p < 0.001$ versus control, ** $p < 0.0037$ versus control.

doi: 10.1371/journal.pone.0074466.g001

the analysis. Data were analyzed with GraphPad Prism (San Diego, CA, USA) for Windows.

Results

Sensitivity of human glioma cell lines to temozolomide

We analyzed the sensitivity to TMZ of human glioma cell lines by exposing the cells to 300 μMol TMZ for 48 hours and then assessing cell viability with the MTT assay (Figure 1A). We observed different TMZ sensitivities, which correlated with MGMT levels analyzed by Western blot (Figure 1B). We also observed an inverse correlation between the level of MGMT (Figure 1B) and miR-221 expression in glioma cell lines (Figure 1C). An RNA hybrid alignment bioinformatics search identified a possible binding site for miR-221/222 at position 970 of the 3' UTR of *MGMT*.

To examine whether miR-221/222 interfered with *MGMT* expression by directly targeting the predicted 3' UTR region, we cloned this region downstream of a luciferase reporter gene in the pGL3 vector. HEK-293 cells were co-transfected with the reporter plasmid plus the negative control miR (scrambled miR), miR-221, or miR-222. Only transfection of either miR-221 or miR-222 with the wild-type *MGMT*-3'UTR reporter plasmid led to a significant decrease of luciferase activity. On the

contrary, co-expression of the scrambled miR had no effect (Figure 1D). In addition, miR-221/222's effect on the promoter of *MGMT* was reduced with the mutant *MGMT*-3'UTR reporter, in which the seed sequence was mutated. Together, these results demonstrate that miR-221/222 directly target *MGMT*-3'UTR, thereby reducing *MGMT* expression.

miR-221/222 target MGMT protein and mRNA

In order to establish a causal link between miR-221/222 and *MGMT* expression, we transfected T98G cells with either pre-miR-221 or pre-miR-222 for 72 hrs and then analyzed MGMT levels by Western blot and real time-PCR. Upon miR transfection, MGMT protein and mRNA were downregulated (Figure 2A). In contrast, MGMT expression was increased upon transfection with anti-miR-221 or -222 in U87MG cells (Figure 2B). Similarly, miR-221/222, induced downregulation of MGMT in LN428 cells, another TMZ-resistant glioma cell line (Figure 2C), and in A375 cells, a TMZ-resistant melanoma cell line (Figure 2D). Since *MGMT* expression is mainly dependent on the methylation status of its promoter [27], we determined if miR-221/222 acted by modulating *MGMT* promoter methylation. To this end, we performed a bisulfite modification assay by PCR using specific primers for both methylated and unmethylated *MGMT* promoter. As shown in Figure 2E, miR-221/222 expression in T98G cells, or anti-miR expression in U87MG cells, did not modify the methylation profile of the *MGMT* promoter.

miRs-221/222 modulate TMZ sensitivity in glioma cells

To verify if miR-221/222 play a role in the modulation of TMZ sensitivity because of their effects on MGMT expression, we characterized the viability of T98G, LN428, and A375 cells transfected with miR-221/222 and then treated with TMZ for 24 hrs. As shown in Figure 3A, miR-221/222 transfection increased the response to TMZ. These results were also confirmed by proliferation and colony assays (Figure 3B and 3C). To establish a causal link between miR-221 expression and MGMT downregulation, we performed a rescue experiment with simultaneous overexpression of miR-221 and MGMT cDNA in two different cell lines (T98G and LN428). As shown in Figure 3D, the effect of miR-221 on TMZ response was abolished by MGMT overexpression. We then verified in nine different glioblastoma primary cell lines and in six glioma cell lines any correlation between miR-221 expression and TMZ sensitivity. As shown, TMZ sensitivity positively correlated with the expression level of miR-221 (Figure 3E).

miR-221 promotes apoptotic cell death

In order to evaluate the mechanism of TMZ-induced cell death, we assessed the presence of apoptotic cells by PI staining and flow cytometry upon miR-221 transfection and TMZ treatment. We found that TMZ increased apoptotic cell death in miR-221-overexpressing cells compared with control cells. Interestingly, this effect was rescued by the co-expression of MGMT cDNA with miR-221 (Figure 4A). Caspase-3/7 activation assay further confirmed the involvement of the apoptotic machinery. As shown in Figure 4B, miR-221 expression increased caspase-3 activity upon

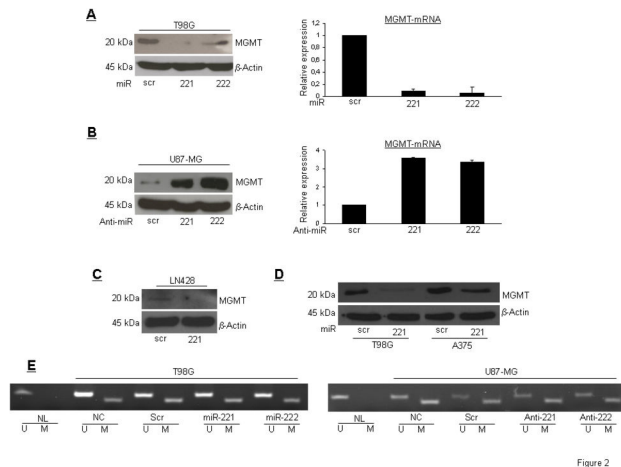


Figure 2

Figure 2. miR-221/222 target *MGMT*. (A) Western blot analysis and real time PCR of MGMT protein and RNA after miR-221/222 transfection of T98G cells. (B) Western blot analysis and real time PCR of MGMT protein and RNA after anti-miR-221 and -222 transfection of U87MG cells. (C) Western blot of MGMT expression upon miR-221 transfection of LN428 cells. (D) Western blot analysis of MGMT expression in T98G cells, as a control, and the melanoma cell line A375 upon miR-221 transfection. (E) Analysis of methylation status of MGMT promoter in T98G and U87MG upon miR- or anti-miR-221/222 transfection. U is for the un-methylated form, M for methylated form, NL is for normal lymphocytes, used as control.

doi: 10.1371/journal.pone.0074466.g002

TMZ treatment, while the co-expression of MGMT cDNA with miR-221 abolished this effect. Simultaneous treatment with the caspase inhibitor ZVAD-fmk and TMZ was able to decrease caspase activity, confirming that TMZ induced cell death by a caspase-mediated mechanism. Caspase-3 activation, observed by Western blot in miR-221-transfected cells after 24 hrs of TMZ treatment, was rescued by MGMT cDNA (Figure 4C). Coherently, we observed an increase in cell viability after miR-221 transfection and simultaneous treatment with TMZ and ZVAD-fmk (Figure 4D).

miR-221 promotes DNA damage after TMZ treatment

MGMT activity repairs DNA by removing DNA adducts caused by TMZ treatment. The absence of MGMT increases cell death upon exposure to TMZ, but, as a long-term effect, may increase DNA damage, and thus the accumulation of mutations. We investigated whether miR-221 may increase DNA damage upon TMZ treatment by down-modulating MGMT expression. This was assessed by a comet assay, which quantifies double-stranded DNA (dsDNA) breaks, in T98G cells transfected with miR-221 or a scrambled sequence and then treated with TMZ at different times. We found that miR-221 produced a significant enhancement of dsDNA breaks (Figure 5A). To strengthen our hypothesis, we looked for the phosphorylation status of histone H2AX (γ H2AX) at Ser139, which reflects dsDNA break formation. As shown in Figure 5B,

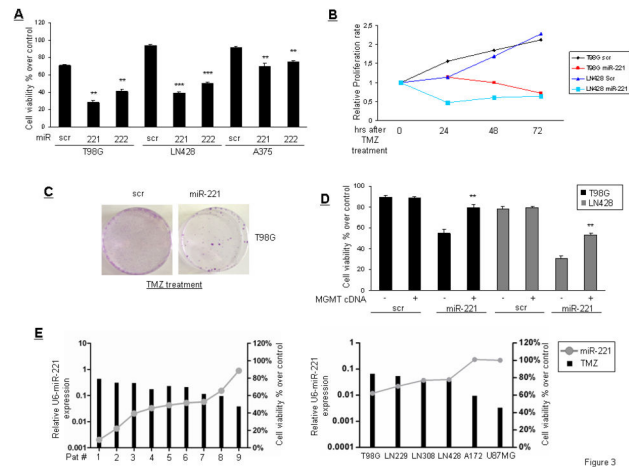


Figure 3

Figure 3. miR-221 modulates TMZ sensitivity. (A) Cell viability of T98G, LN428, and A375 cells transfected with miR-221 and miR-222 upon TMZ treatment (300 μ Mol) for 24 hrs. **p value<0.0082 versus scr column, ***p value<0.005 versus scr column. (B) Growth curve of T98G and LN428 cells transfected or not with miR-221 after 24 hrs of treatment with TMZ. (C) Colony assay of T98G and LN428 cells transfected with miR-221 and then treated for 24 hrs with TMZ (300 μ Mol). Cells were left to grow for 6 days after treatment removal. (D) MGMT expression rescues cell viability after TMZ treatment in T98G and LN428 cells overexpressing miR-221 **p value<0.0082 versus untransfected MGMT column. (E) Correlation between miR-221 expression and TMZ sensitivity in nine primary glioblastoma cell lines and in six glioblastoma cell lines.

doi: 10.1371/journal.pone.0074466.g003

miR-221 significantly increased γ H2AX, as assessed by immunocytofluorescence (upper panel) or by Western blot (lower panel), suggesting that miR overexpression may induce DNA damage. This effect was even stronger in the presence of TMZ, but was rescued by MGMT cDNA (Figure 5B, middle panel). Furthermore, we also observed an increase of other DNA damage markers, such as P-ATM, P-p53^{ser15} and PARP cleavage, upon miR-221 transfection; this was even stronger upon treatment with both miR-221 and TMZ (Figure 5C). These effects were rescued by the simultaneous expression of MGMT with miR-221. Taken together, these data suggest that the targeting of *MGMT* by miR-221 increases DNA damage. This effect was amplified by TMZ treatment.

MGMT and miR-221 expression in glioblastoma patients

We then evaluated the expression of MGMT and miR-221 in human glioblastoma samples. Patients were clustered into two separate groups: a long survival (survival >15 months) group and a short survival (survival <15 months) group, according to common classification [2].

We first analyzed the methylation profile of the *MGMT* promoter, and then *MGMT* mRNA and miR-221 levels. We performed methylation-specific PCR (MSP) on 33 human

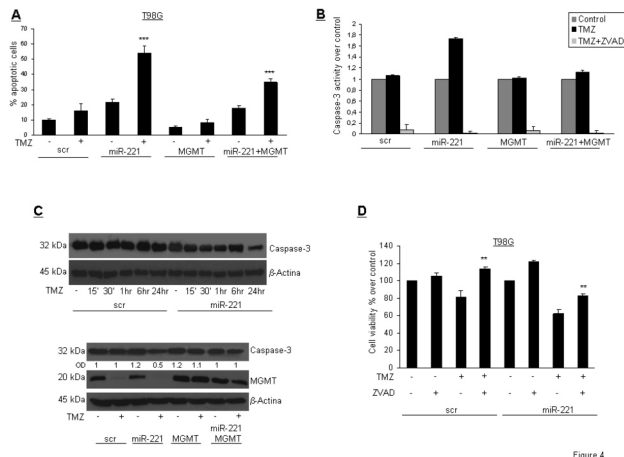


Figure 4

Figure 4. miR-221 promotes DNA damages upon TMZ treatment. (A) Apoptotic cell death assessed by FACS in T98G cells transfected with miR-221 or scrambled sequence and MGMT and treated with TMZ for 24 hrs. *** p value < 0.005 versus untransfected MGMT column. (B) Active caspase-3 quantification in T98G cells as indicated and treated with TMZ for 24 hrs in the presence or absence of 3 hrs pre-treatment with ZVAD-fmk. (C) Upper panel Time course analysis of caspase-3 activation upon TMZ treatment in T98G cells transfected with miR-221 or with scrambled sequence. Lower panel Western blot analysis of caspase-3 activation after miR-221 and MGMT transfection. (D) Cell viability of T98G cells transfected with miR-221 or with scrambled sequence treated with TMZ for 24 hrs in the presence or absence of 3 hrs pre-treatment with ZVAD-fmk. ** p value < 0.0034 versus only treated TMZ column, Student's t test.

doi: 10.1371/journal.pone.0074466.g004

glioblastoma paraffin-embedded tissues, and found 27 to be unmethylated and 4 to be methylated (samples 2, 21, 22, and 28) (Figure S1). For two samples (#31 and #32), it was not possible to define the *MGMT* promoter methylation profile. We then analyzed the effect of miR-221 on *MGMT* regulation among 15 unmethylated samples from which we obtained sufficient RNA for real time PCR analysis. We identified 4 long- (#1, #4, #10, and #14) and 11 short- (#6, #7, #8, #12, #13, #17, #18, #23, #25, #32, and #33) survival patients. We found that the short-survival group exhibited a higher miR-221 level and a lower *MGMT* level compared with the long-survival group (Figure 6 A,B). These data supports our in vitro evidence of an inverse correlation between miR-221 and *MGMT* expression. Furthermore, this observation identifies miR-221 as a negative prognostic factor for survival.

Discussion

Much evidence suggests that the intracellular level of the alkylating enzyme *MGMT* affects TMZ response in GBM patients [10,11]. Low levels of *MGMT* are associated with a better TMZ response, because in the absence of *MGMT* the cells are not able to repair the TMZ-induced base mismatch.

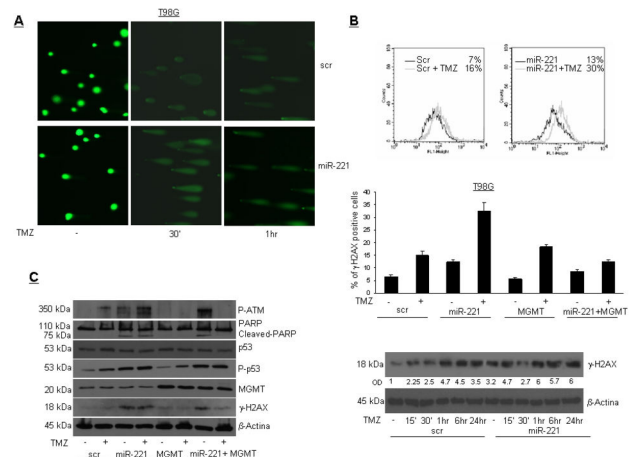


Figure 5

Figure 5. miR-221 promotes DNA damage. (A) Alkaline comet assay of T98G cells transfected with miR-221 and treated with TMZ for the indicated times. (B) Analysis of γH2AX in T98G cells transfected with scrambled control miR or miR-221, treated with TMZ in the presence or in the absence of *MGMT* cDNA, by immunocytofluorescence (upper and medium panel) or by Western blot (lower panel). (C) Western blot analysis of the indicated proteins upon transfection of T98G cells with miR-221 and *MGMT* cDNA and TMZ treatment for 24 hrs.

doi: 10.1371/journal.pone.0074466.g005

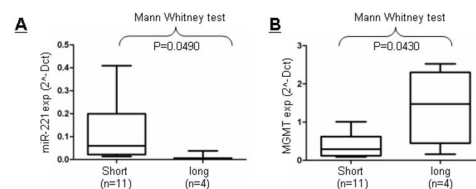


Figure 6. Association of miR-221 and *MGMT* expression. Mann-Whitney U test analysis was performed to evaluate the association between miR-221 and *MGMT* expression in long- and short-survival groups of patients. The expression of miR-221 ($2^{-\Delta C_t}$) (A-B) and *MGMT* ($2^{-\Delta C_t}$) are inversely correlated with patient survival ($p < 0.0490$ and $p = 0.043$, respectively).

doi: 10.1371/journal.pone.0074466.g006

Hence, double-strand DNA breaks, DNA mismatch repair, and the apoptotic pathway are activated. *MGMT* expression is regulated by the methylation of its promoter. *MGMT* promoter methylation lowers *MGMT* levels and accounts for a greater TMZ response when associated with radiotherapy. However, a fraction of patients with unmethylated *MGMT* show some TMZ response, suggesting that promoter methylation is not the only regulatory mechanism of *MGMT* expression [13,14].

In the present study, we addressed this specific issue by investigating the involvement of miRs in *MGMT* regulation. First, we characterized TMZ sensitivity in a subset of

glioblastoma cell lines and primary cells obtained from GBM patients. We found that the analyzed glioblastoma cell lines (T98G, LN428, U87MG, and A172) expressed different levels of miR-221/222 and displayed a consistent difference in MGMT expression. This inverse correlation was also observed in glioblastoma biopsies.

Bioinformatics identified a possible miR-221/222 binding site on *MGMT*. This was confirmed by a luciferase assay and overexpression experiments. The effect of miR-221/222 on MGMT levels was direct and not related to *MGMT* promoter methylation, since miR transfection did not alter the *MGMT* methylation profile. Instead, we found evidence that miR-221/222 regulated MGMT levels, leading to increased TMZ-induced apoptosis, reduced anchorage-independent growth, and reduced cell viability. Overexpression of MGMT cDNA with miR-221/222 rescued the effects on TMZ sensitivity. This result was not restricted to glioma cells, but was obtained also in other cancer cells sensitive to TMZ, such as human malignant melanoma.

It has been demonstrated that *MGMT* may be a target also of other miRs, such as miR-181, in GBM [28]. Zhang et al. demonstrated that miR-181d targets *MGMT* 3' UTR, and reported an inverse correlation between miR-181d and MGMT levels in human GBM samples, in particular in those samples in which the *MGMT* promoter was unmethylated [28]. However, the modest correlation between miR-181d and MGMT suggested that other miRs may regulate MGMT expression. Therefore, miR-221/222 may be part of this cohort.

MGMT expression may be regulated also thought the p53 pathway. Blough et al. provided evidence that p53 regulates MGMT expression in murine astrocytes, and presented data suggesting that p53 contributes to the regulation of MGMT gene expression in the human astrocytic glioma cell line SF767 [29].

In this manuscript, we demonstrate that miR-221 overexpression increases DNA damage in glioma cells. In fact, miR-221-overexpressing glioma cells exhibited an increase in DNA damage markers, such as P-ATM, P-p53, cleaved PARP, and γ H2AX. These markers were activated even in the absence of TMZ, and became increased upon TMZ treatment. MGMT participates in the repair of DNA. Thus, miR-221/222 induces chronic MGMT downregulation, rendering the cells unable to repair DNA damage. It is well established that miR221/222 are oncogenic microRNAs that are upregulated in a number of human tumors [30,31,32]. In GMB tissue and cell lines, upregulated miR-222 and miR-221 expression correlated with the stage of the disease, cell motility, and TRAIL response [19,23,31,33]. We found that miR-221 is a negative prognostic factor, since it is up regulated in short-survival patients and is downregulated in long-survival ones. However, we did not observe the expected correlation between miR-221 expression and response to temozolomide/survival. Arguably, overall survival and therapy response have to be linked to other factors. It therefore seems that the pro-oncogenic effect of miR-221 is more powerful than its potentiation of the response to temozolomide.

The role of MGMT in DNA damage repair has been investigated also in animal models. Reduced expression of this

repair enzyme has been thought to result in a spontaneous 'mutator' phenotype and to promote neoplastic lesions in the presence of either endogenous or exogenous sources of alkylation stress. Sakumi, et al. showed that *Mgmt*^{-/-} mice develop thymic lymphomas and lung adenomas to a greater extent when exposed to methylnitrosourea (MNU), suggesting that the DNA repair methyltransferase protected these mice from MNU-induced tumorigenesis [34]. Sandercock et al. reported that MGMT-deficient cells exhibited an increased mutational burden, but only following exposure to specific environmental mutagens [35]. Takagi et al. demonstrated that mice with mutations in *Mgmt* as well as in the DNA mismatch repair gene *Mlh1* developed numerous tumors after being administered MNU. When exposed to a sub-lethal dose of MNU (1mM), the mutation frequency in *Mgmt*^{-/-}/*Mlh1*^{-/-} cells was up to 12 times that of untreated cells; this effect was not present in control mice [36]. Walter et al. generated transgenic mice overexpressing MGMT in brain and liver, or in lung [37]. They found that expression of the transgene correlated with a reduced prevalence of MNU-induced tumors in liver and in lung and also with reduced spontaneous hepatocellular carcinoma. Reese et al. found that overexpression of MGMT decreased the incidence and increased the latency of thymic lymphoma induction in mice with both heterozygous and wild type p53 alleles [38]. This protective effect was described also by Allay et al., who reported that the incidence of lymphomas was much lower in MGMT transgenic mice compared with controls [39]. Those studies thus suggest that MGMT, other than being involved in the response to therapy, is also involved in DNA repair. Therefore, its inactivation may produce devastating effects on DNA integrity.

In summary, we have provided evidence of the existence of an adjunct mechanism of MGMT regulation, besides promoter methylation, involving miR targeting its 3' UTR. We have also shown that overexpression of miR-221/222 produces an increase in sensitivity to TMZ via a reduction in the level of MGMT. On the other hand, these miRs increase DNA damage, conferring oncogenic features to glioma cells. This may link miR-221/222 to poor GBM prognosis.

Supporting Information

Figure S1. Methylation-specific PCR analyses for MGMT methylation in glioblastoma human tumors. 33 glioblastoma samples were used for analysis. The SW48 cell line and *in vitro* methylated DNA (IVD) are shown as a positive control for methylation, normal lymphocytes (NL) as a negative control for methylation, and water (H₂O) as a negative PCR control. U and M indicate the presence of unmethylated or methylated MGMT, respectively. Red colour is for methylated samples, green for unmethylated and orange for undetermined samples. (TIF)

Acknowledgements

We wish to thank Dr. Michael Latronico for the extensive revision of the manuscript.

Author Contributions

Conceived and designed the experiments: CQ GC. Performed the experiments: G. Roscigno CQ DM ADL G. Romano.

References

- Wen PY, Kesari S (2008) Malignant Gliomas in Adults. *N Engl J Med* 359: 492-507. doi:10.1056/NEJMra0708126. PubMed: 18669428.
- Louis DN, Ohgaki H, Wiestler OD, Cavenee WK, Burger PC et al. (2007) The 2007 WHO Classification of Tumours of the Central Nervous System. *Acta Neuropathol* 114: 97-109. doi:10.1007/s00401-007-0243-4. PubMed: 17618441.
- Stupp R, Hegi ME (2013) Brain cancer in 2012: Molecular characterization leads the way. *Nat Rev Clin Oncol* 10: 69-70. doi:10.1038/nrclinonc.2012.240. PubMed: 23296110.
- Stupp R, Mason WP, van den Bent MJ, Weller M, Fisher B et al. (2005) Radiotherapy plus concomitant and adjuvant temozolomide for glioblastoma. *N Engl J Med* 352: 987-996. doi:10.1056/NEJMoa043330. PubMed: 15758009.
- Stupp R, Hegi ME, Mason WP, van den Bent MJ, Taphoorn MJB et al. (2009) Effects of radiotherapy with concomitant and adjuvant temozolomide versus radiotherapy alone on survival in glioblastoma in a randomised phase III study: 5-year analysis of the EORTC-NCIC trial. *Lancet Oncol* 10: 459-466. doi:10.1016/S1470-2045(09)70025-7. PubMed: 19269895.
- Mrugala MM, Chamberlain MC (2008) Mechanisms of Disease: temozolomide and glioblastoma-look to the future. *Nat Clin Pract Oncol* 5: 476-486. doi:10.1038/ncpgasthep1210. PubMed: 18542116.
- Roos WP, Batista LFZ, Naumann SC, Wick W, Weller M et al. (2006) Apoptosis in malignant glioma cells triggered by the temozolomide-induced DNA lesion O6-methylguanine. *Oncogene* 26: 186-197. PubMed: 16819506.
- Bignami M, O'Driscoll M, Aquilina G, Karran P (2000) Unmasking a killer. DNA O6-methylguanine and the cytotoxicity of methylating agents. *Mutat Res* 462: 71-82.
- Gerson SL (2002) Clinical Relevance of MGMT in the Treatment of Cancer. *J Clin Oncol* 20: 2388-2399. doi:10.1200/JCO.2002.06.110. PubMed: 11981013.
- Gerson SL (2004) MGMT: its role in cancer aetiology and cancer therapeutics. *Nat Rev Cancer* 4: 296-307. doi:10.1038/nrc1319. PubMed: 15057289.
- Hegi ME, Liu L, Herman JG, Stupp R, Wick W et al. (2008) Correlation of O6-Methylguanine Methyltransferase (MGMT) Promoter Methylation With Clinical Outcomes in Glioblastoma and Clinical Strategies to Modulate MGMT Activity. *J Clin Oncol* 26: 4189-4199. doi:10.1200/JCO.2007.11.5964. PubMed: 18757334.
- Dunn J, Baborie A, Alam F, Joyce K, Moxham M et al. (2009) Extent of MGMT promoter methylation correlates with outcome in glioblastomas given temozolomide and radiotherapy. *Br J Cancer* 101: 124-131. doi:10.1038/sj.bjc.6605127. PubMed: 19536096.
- Krex D, Klink B, Hartmann C, von Deimling A, Pietsch T et al. (2007) Long-term survival with glioblastoma multiforme. *Brain* 130: 2596-2606. doi:10.1093/brain/awm204. PubMed: 17785346.
- Weller M, Stupp R, Reifenberger G, Brandes AA, van den Bent MJ et al. (2010) MGMT promoter methylation in malignant gliomas: ready for personalized medicine? *Nat. Rev Neurol* 6: 39-51. doi:10.1038/nrneurol.2009.197.
- Calin GA, Croce CM (2006) MicroRNA signatures in human cancers. *Nat Rev Cancer* 6: 857-866. doi:10.1038/nrc1997. PubMed: 17060945.
- Gregory RI, Shiekhattar R (2005) MicroRNA biogenesis and cancer. *Cancer Res* 65: 3509-3512. doi:10.1158/0008-5472.CAN-05-0298. PubMed: 15867338.
- Garofalo M, Condorelli G, Croce CM (2008) MicroRNAs in diseases and drug response. *Curr Opin Pharmacol* 8: 661-667. doi:10.1016/j.coph.2008.06.005. PubMed: 18619557.
- Negrini M, Ferracin M, Sabbioni S, Croce CM (2007) MicroRNAs in human cancer: from research to therapy. *J Cell Sci* 120: 1833-1840. doi:10.1242/jcs.03450. PubMed: 17515481.
- Quintavalle C, Garofalo M, Zanca C, Romano G, Iaboni M et al. (2012) miR-221/222 overexpression in human glioblastoma increases invasiveness by targeting the protein phosphatase PTPmu. *Oncogene* 31: 858-868. doi:10.1038/onc.2011.280. PubMed: 21743492.
- Conti A, Aguenouz MH, Torre D, Tomasello C, Cardali S et al. (2009) miR-21 and 221 upregulation and miR-181b downregulation in human grade II-IV astrocytic tumors. *J Neuro Oncol* 93: 325-332. doi:10.1007/s11060-009-9797-4. PubMed: 19159078.
- Ciafrè SA, Galardi S, Mangiola A, Ferracin M, Liu CG et al. (2005) Extensive modulation of a set of microRNAs in primary glioblastoma. *Biochem Biophys Res Commun* 334: 1351-1358. doi:10.1016/j.bbrc.2005.07.030. PubMed: 16039986.
- Garofalo M, Quintavalle C, Romano G, Croce CM, Condorelli G (2012) miR221/222 in Cancer: Their Role in Tumor Progression and Response to Therapy. *Curr Mol Med* 12: 27-33. doi:10.2174/156652412798376170. PubMed: 22082479.
- Garofalo M, Di Leva G, Romano G, Nuovo G, Suh SS et al. (2009) miR-221&222 regulate TRAIL resistance and enhance tumorigenicity through PTEN and TIMP3 downregulation. *Cancer Cell* 16: 498-509. doi:10.1016/j.ccr.2009.10.014. PubMed: 19962668.
- Garofalo M, Condorelli GL, Croce CM, Condorelli G (2010) MicroRNAs as regulators of death receptors signaling. *Cell Death Differ* 2: 200-8. PubMed: 19644509.
- Garofalo M, Romano G, Di Leva G, Nuovo G, Jeon Y-J et al. (2011) EGFR and MET receptor tyrosine kinase-altered microRNA expression induces tumorigenesis and gefitinib resistance in lung cancers. *Nat Med* 18: 74-82. doi:10.1038/nm.2577. PubMed: 22157681.
- Livak KJ, Schmittgen TD (2001) Analysis of relative gene expression data using real-time quantitative PCR and the 2(-Delta Delta C(T)) Method. *Methods* 25: 402-408. doi:10.1006/meth.2001.1262. PubMed: 11846609.
- Esteller M, Hamilton SR, Burger PC, Baylin SB, Herman JG (1999) Inactivation of the DNA Repair: Gene O6-Methylguanine-DNA Methyltransferase by Promoter Hypermethylation is a Common Event in Primary Human Neoplasia. *Cancer Res* 59: 793-797.
- Zhang W, Zhang J, Hoadley K, Kushwaha D, Ramakrishnan V et al. (2012) miR-181d: a predictive glioblastoma biomarker that downregulates MGMT expression. *Neuro Oncol* 14: 712-719. doi:10.1093/neuonc/nos089. PubMed: 22570426.
- Blough MD, Zlatescu MC, Cairncross JG (2007) O6-Methylguanine-DNA Methyltransferase Regulation by p53 in Astrocytic Cells. *Cancer Res* 67: 580-584. doi:10.1158/0008-5472.CAN-06-2782. PubMed: 17234766.
- Pallante P, Visone R, Ferracin M, Ferraro A, Berlingieri MT et al. (2006) MicroRNA deregulation in human thyroid papillary carcinomas. *Endocr Relat Cancer* 13: 497-508. doi:10.1677/erc.1.01209. PubMed: 16728577.
- Conti A, Aguenouz M, La Torre D, Tomasello C, Cardali S et al. (2009) miR-21 and 221 upregulation and miR-181b downregulation in human grade II-IV astrocytic tumors. *J Neuro Oncol* 93: 325-332. doi:10.1007/s11060-009-9797-4. PubMed: 19159078.
- Pineau P, Volinia S, McJunkin K, Marchio A, Battiston C et al. (2010) miR-221 overexpression contributes to liver tumorigenesis. *Proc Natl Acad Sci U S A* 107: 264-269. doi:10.1073/pnas.0907904107. PubMed: 20018759.
- Ciafrè SA, Galardi S, Mangiola A, Ferracin M, Liu CG et al. (2005) Extensive modulation of a set of microRNAs in primary glioblastoma. *Biochem Biophys Res Commun* 334: 1351-1358. doi:10.1016/j.bbrc.2005.07.030. PubMed: 16039986.
- Sakumi K, Shiraishi A, Shimizu S, Tsuzuki T, Ishikawa T et al. (1997) Methylnitrosourea-induced Tumorigenesis in MGMT Gene Knockout Mice. *Cancer Res* 57: 2415-2418. PubMed: 9192819.
- Sandercock LE, Hahn JN, Li L, Luchman HA, Giesbrecht JL et al. (2008) Mgmt deficiency alters the in vivo mutational spectrum of tissues exposed to the tobacco carcinogen 4-(methylnitrosamino)-1-(3-pyridyl)-1-butanone (NNK). *Carcinogenesis* 29: 866-874. doi:10.1093/carcin/bgn030. PubMed: 18281247.
- Takagi Y, Takahashi M, Sanada M, Ito R, Yamaizumi M et al. (2003) Roles of MGMT and MLH1 proteins in alkylation-induced apoptosis and mutagenesis. *DNA Repair (Amst)* 2: 1135-1146. doi:10.1016/S1568-7864(03)00134-4. PubMed: 13679151.
- Walter CA, Lu J, Bhakta M, Mitra S, Dunn W et al. (1993) Brain and liver targeted overexpression of O6-methylguanine DNA methyltransferase in transgenic mice. *Carcinogenesis* 14: 1537-1543. doi:10.1093/carcin/14.8.1537. PubMed: 8353838.
- Reese JS, Allay E, Gerson SL (2001) Overexpression of human O6-alkylguanine DNA alkyltransferase (AGT) prevents MNU induced

- lymphomas in heterozygous p53 deficient mice. *Oncogene* 20: 5258-5263.
39. Allay E, Veigl M, Gerson SL (1999) Mice over-expressing human O6 alkylguanine-DNA alkyltransferase selectively reduce O6 methylguanine mediated carcinogenic mutations to threshold levels after N-methyl-N-nitrosourea. *Oncogene* 18: 3783-3787.

ORIGINAL ARTICLE

Effect of miR-21 and miR-30b/c on TRAIL-induced apoptosis in glioma cells

C Quintavalle^{1,2,7}, E Donnarumma^{3,7}, M Iaboni^{1,2}, G Roscigno^{1,2}, M Garofalo⁴, G Romano³, D Fiore¹, P De Marinis⁵, CM Croce⁴ and G Condorelli^{1,2,6}

Glioblastoma is the most frequent brain tumor in adults and is the most lethal form of human cancer. Despite the improvements in treatments, survival of patients remains poor. To define novel pathways that regulate susceptibility to tumor necrosis factor-related apoptosis-inducing ligand (TRAIL) in glioma, we have performed genome-wide expression profiling of microRNAs (miRs). We show that in TRAIL-resistant glioma cells, levels of different miRs are increased, and in particular, miR-30b/c and -21. We demonstrate that these miRs impair TRAIL-dependent apoptosis by inhibiting the expression of key functional proteins. T98G-sensitive cells treated with miR-21 or -30b/c become resistant to TRAIL. Furthermore, we demonstrate that miR-30b/c and miR-21 target respectively the 3' untranslated region of caspase-3 and TAP63 mRNAs, and that those proteins mediate some of the effects of miR-30 and -21 on TRAIL resistance, even in human glioblastoma primary cells and in lung cancer cells. In conclusion, we show that high expression levels of miR-21 and -30b/c are needed to maintain the TRAIL-resistant phenotype, thus making these miRs as promising therapeutic targets for TRAIL resistance in glioma.

Oncogene advance online publication, 10 September 2012; doi:10.1038/onc.2012.410

Keywords: glioblastoma; TRAIL; therapy; microRNA; treatment; apoptosis

INTRODUCTION

Glioblastomas are the most common primary tumors of the brain and are divided into four clinical grades on the basis of their histology and prognosis.¹ These tumors are highly invasive, very aggressive and are one of the most incurable forms of cancer in humans.² The treatment strategies for this disease have not changed appreciably for many years, and failure of treatment occurs in the majority of patients owing to the strong resistant phenotype. Therefore, the development of new therapeutic strategies is necessary for this type of cancer.

A novel interesting therapeutic approach is the reactivation of apoptosis using member of TNF (tumor necrosis factor)-family, of which the tumor necrosis factor-related apoptosis-inducing ligand (TRAIL) holds the greatest interest. Apoptosis is a particularly desirable treatment outcome, as it eradicates cancer cells without causing a major inflammatory response, which could provide unwanted survival signals. However, many cancers develop functional defects in the drug-induced apoptosis pathway, which may lead to constitutive or acquired resistance. To this end, alternative pathways, such as the one activated by death receptors including Fas/Apo-1, or DR4 (TRAIL-R1) and DR5 (TRAIL-R2), are being explored for cancer treatment. TRAIL is a relatively new member of the TNF family, known to induce apoptosis in a variety of cancers.³ Treatment with TRAIL induces programmed cell death in a wide range of transformed cells, both *in vivo* and *in vitro*, without producing significant effects in normal cells.^{3,4} Therefore, recombinant TRAIL or monoclonal antibodies against its receptors (TRAIL-R1 and TRAIL-R2) are in phase II/III

clinical trials for different kinds of tumors, either as a single agent or in combination with chemotherapy.^{5,6}

However, a significant proportion of human cancer cells are resistant to TRAIL-induced apoptosis, and the mechanisms of sensitization seem to differ among cell types. Different studies relate resistance to TRAIL-induced cell death to downstream factors. It has been shown that downregulation of two anti-apoptotic proteins such as PED (Phosphoprotein enriched in diabetes) or cellular-FLICE such as inhibitory protein (c-FLIP) can sensitize cells to TRAIL-induced apoptosis.^{7–9} However the mechanism of TRAIL resistance is still largely unknown.

miRs are a class of endogenous non-coding RNA of 19–24 nucleotides in length that has an important role in the negative regulation of gene expression blocking translation or directly cleaving the targeted mRNA.¹⁰ miRs are involved in the pathogenesis of most cancers.¹⁰ In the last few years, our understanding of the role of miRNA has expanded from the initially identified functions in the development of round worms to a highly expressed and ubiquitous regulators implicated in a wide array of critical processes, including proliferation, cell death and differentiation, metabolism and, importantly, tumorigenesis.¹¹ We have recently showed an important role of microRNAs in TRAIL sensitivity in non-small cell lung cancer (NSCLC).^{12–14}

In this study, to identify novel mechanisms implicated in TRAIL resistance in human glioma, we performed a genome-wide expression profiling of miRs in different cell lines. We found that miR-30b/c and -21 are markedly upregulated in TRAIL-resistant, and downregulated in TRAIL-sensitive glioma cells.

¹Department of Cellular and Molecular Biology and Pathology, 'Federico II' University of Naples, Naples, Italy; ²IEOS, CNR, Naples, Italy; ³Fondazione IRCCS SDN, Naples, Italy;

⁴Department of Molecular Virology, Immunology and Medical Genetics, Human Cancer Genetics Program, Comprehensive Cancer Center, The Ohio State University, Columbus, OH, USA; ⁵Neurosurgery Unit, Ospedale A. Cardarelli, Napoli, Italy and ⁶Facoltà di Scienze Biologiche, 'Federico II' University of Naples, Naples, Italy. Correspondence: Professor G Condorelli, Department of Cellular and Molecular Biology and Pathology, 'Federico II' University of Naples, Via Pansini, 5, Ed 19 A, II floor, Naples 80131, Italy.

E-mail: gecondor@unina.it

⁷These authors contributed equally to this work.

Received 28 February 2012; revised 13 June 2012; accepted 23 July 2012

Our experiments indicate that miR-30b/c and -21 modulate TRAIL sensitivity in glioma cells mainly by modulating caspase-3 and *Tap63* expression and TRAIL-induced caspase machinery.

RESULTS

Selection of TRAIL-sensitive vs TRAIL-resistant glioma cell lines

We analyzed TRAIL sensitivity of different human glioma cell lines. Cells were exposed to TRAIL at two different concentrations for 24 h and cell death was assessed using the MTT assay (Figure 1a) or propidium iodide staining (Figure 1b). As shown in Figure 1, we can distinguish two sets of cells: TB10, LN229, U251 and U87MG cells exhibited total or partial TRAIL resistance, whereas T98G and LN18 cells underwent TRAIL-induced cell death.

miRs expression screening in TRAIL-resistant vs TRAIL-sensitive glioma cell lines

To investigate the involvement of miRs in TRAIL resistance in glioblastoma cell lines, we analyzed the miRs expression profile in the most TRAIL-resistant glioma cells (TB10 and LN229) vs the TRAIL-sensitive cells (T98G and LN18). The analysis was performed with a microarray chip containing 1150 miR probes, including 326 human and 249 mouse miRs, spotted in duplicates. Data obtained indicated that seven miRs (miR-21, -30b, -30c, -181a, -181d, -146 and -125b) were significantly overexpressed in resistant glioma cells with at least >1.9-fold change (Table 1). Quantitative real-time-polymerase chain reaction (qRT-PCR) validated the microarray analysis (data not shown).

Role of miRs in TRAIL resistance in glioma

To test the role of these overexpressed miRs in TRAIL sensitivity in glioma, we transfected T98G TRAIL-sensitive cells with miR-21, -30b, -30c, -181a, -146 and -125b. TRAIL sensitivity was evaluated by MTT assay, propidium iodide staining and colony assay. We obtained significant results only for miR-30b/c and miR-21 that

were then extensively investigated. In fact, data obtained with MTT assay and FACS analysis showed that the overexpression of miR-30b/c and -21 was able to revert TRAIL sensitivity in T98G (Figures 2a and b). Similar results were obtained in LN18 cells (Figures 2c and d). This effect was not restricted to glioma, as miR-30 and miR-21 were able to exert an anti-apoptotic action also in non small cell lung cancer (NSCLC) (Supplementary Figure 3B). We further evaluated TRAIL sensitivity by colony assay. T98G and LN18 cells were transfected with miR-scrambled, miR-30b/c and miR-21 for 48 h and then were treated with 50 or 100 ng/ml of superKiller TRAIL for 24 h. Cells were grown for 6 days and then coloured with crystal violet-methanol solution (Supplementary Figures 1A and B). The results indicated that both miRs induced an increase of TRAIL resistance.

To further explore the role of miR-21 and -30b/c on TRAIL sensitivity, we transfected U251 (Figure 3a) or LN229 (Figure 3b) TRAIL-resistant cells with anti-miR-21, -30b, 30c, or with a scrambled sequence. As shown in Figures 3a and b, transfection of the anti-miR sequences was able to sensitize U251 and LN229 cells to TRAIL. Anti-miR-21 and -30c were also able to sensitize to TRAIL the CALU-1-resistant non-small cell lung cancer (NSCLC) TRAIL-resistant cell lines (Supplementary Figure 3C), indicating that this effect was not restricted to glioma.

Identification of cellular targets of miR-30b/c and miR-21 in glioma cells

To identify cellular targets of miR-30b/c and -21, we used as first attempt a bioinformatic search, using programs available on the web including Pictar, TargetScan, miRanda and Microcosm target.

miR-21 targets different tumor suppressor genes and proteins potentially involved in TRAIL resistance in glioblastoma cells, such as PTEN (phosphatase and tensin homologue), PDCD4 (programmed cell death 4), TPM1 (Tropomyosin 1) and p53.^{15–17} Computer-assisted analysis identified the presence of evolutionary-conserved binding sites for miR-21 in *Tap63* gene. We focused our attention on this p53 family member, as it regulates the expression of TRAIL receptors and molecules involved in TRAIL signaling.¹⁸ We also searched for miR-30 targets and among them we focused on caspase-3.

TRAIL-resistant and TRAIL-sensitive glioma or NSCLC cells exhibited different levels of miR-21 and -30c assessed by either qRT-PCR (Figure 4a and Supplementary Figure 3A) or by northern blot analysis (Supplementary Figure 4). Interestingly, we observed a reduction of protein (Figure 4b and Supplementary Figure 3D) and mRNA (Figure 4c) levels of *Tap63* and caspase-3 upon, respectively, miR-21 or miR-30c and miR-30b (data not shown) transfection in TRAIL-sensitive cell lines. We didn't observe a

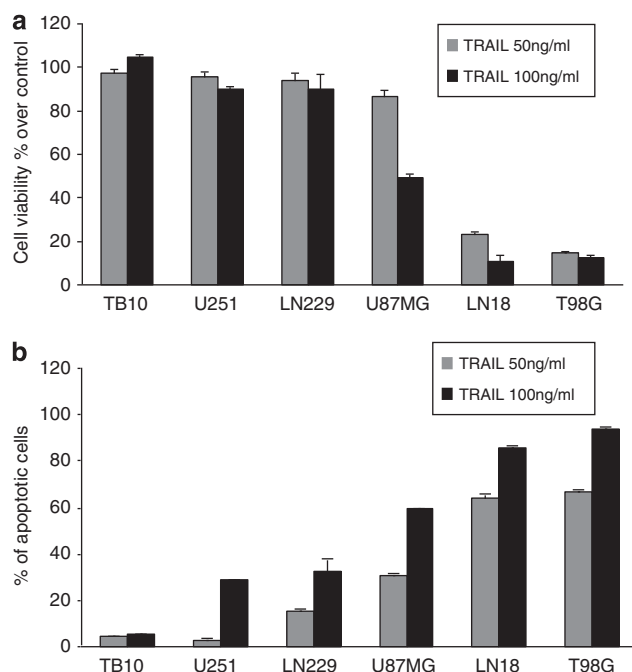


Figure 1. TRAIL sensitivity of glioblastoma cells. Glioblastoma cell lines (10^4 cell) were treated with superKiller TRAIL. After 24 h of treatment, the effect on cell death was assessed with MTT assay (a) or by propidium iodide staining and FACS analysis (b).

Table 1. microRNA identified in TRAIL-resistant glioma (LN229 and TB10) compared with TRAIL-sensitive (T98G, LN18) cells

miR	P-value	Fold difference
hsa-miR-125b1-A	6.09e – 05	3.033
hsa-miR-30b-A	9.14e – 05	2.041
hsa-miR-30c-A	0.0001199	2.337
hsa-miR-146b-A	0.0001556	5.972
hsa-miR-181a-5p-A	0.0004698	2.66
hsa-miR-181d-A	0.0004817	3.035
hsa-miR-21-A	0.0032482	1.949

miRNA expression profiles in TRAIL-sensitive vs TRAIL-resistant cells. miRNA screening was performed in triplicate for TRAIL-sensitive and TRAIL-resistant cell lines by a microarray as described in Materials and methods. A two-tailed, two-sample t-test was used ($P < 0.05$). Seven miRNAs were found to be significantly deregulated in TRAIL-resistant cells compared with the TRAIL sensitive.

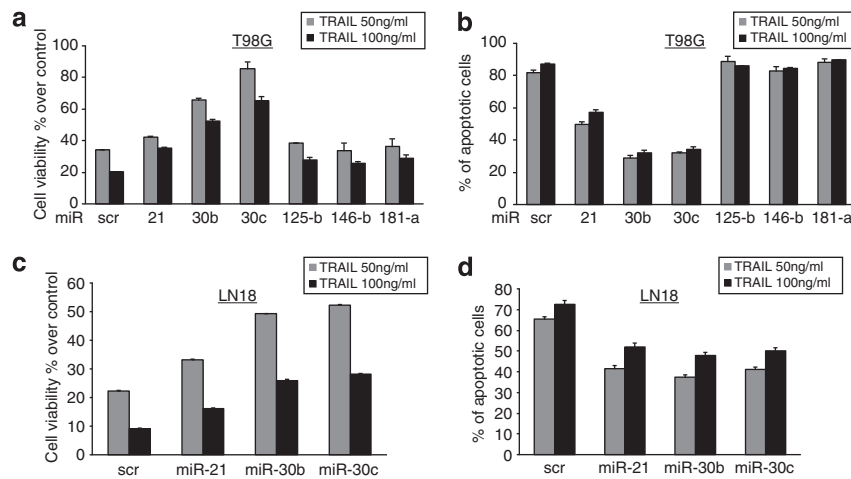


Figure 2. Effect of miR-21 and miR-30c overexpression on TRAIL-sensitive glioblastoma cells. T98G (**a, b**) cells were transfected with miR-21, miR-30b, miR-30c, miR-125b, miR-146b and miR-181a. LN18 (**c, d**) were transfected with miR-21, miR-30b and miR-30c. 10^4 cells were then treated with two different concentrations of superkiller TRAIL. After 24 h of treatment, cell viability was assessed with MTT assay (**a, c**) or with propidium iodide staining and FACS analysis (**b, d**). Both miR-21 and miR-30 induce TRAIL resistance in glioma cells.

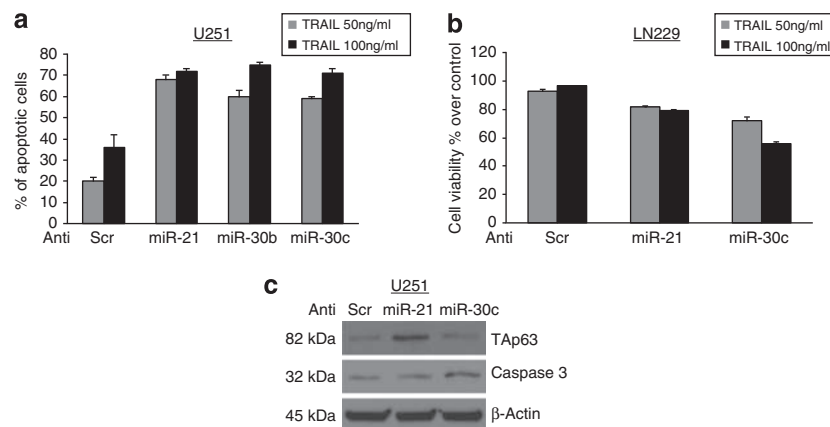


Figure 3. Effects of anti-miR-21 and anti-miR-30b/c on TRAIL sensitivity. Knock down of miR-21 and anti-miR-30b/c increases the percentage of apoptotic cells as assessed by propidium iodide staining in U251 cells (**a**) and decreases the cell viability of LN229 (**b**). (**c**) Tap63 and caspase-3 western blot analysis of U251 cells transfected with a scrambled sequence as negative control and with anti-miR-21 or anti-miR-30c, as indicated.

decrease in the levels of other caspases upon miR-30c transfection (Figure 4b). On the contrary, Tap63 and caspase-3 protein levels increased upon anti-miR-21 and anti-miR-30c transfection (Figure 3c and Supplementary Figure 3D) in TRAIL-resistant cell lines. To verify a direct link between the miR-21/Tap63 and miR-30b/c and caspase-3, we performed luciferase assay by co-transfecting pGL3-3' untranslated region (UTR) vectors along with miR-21 or miR-30c. The results obtained indicated a direct interaction of miR-21 with Tap63 and miR-30c with caspase-3 (Figure 4d). As indicated in Figure 4d, miR-30b and -30c have the same seed sequence that recognizes caspase-3, differing only at the latest four nucleotides of the 5'. Therefore, miR-30b down-regulates caspase-3 at the same extent than miR-30c (data not shown). Deletions in seed complementary sites rescued the repression of miR-21 and miR-30c on their identified targets (Figure 4d).

Validation of miR-21 and miR-30b/c mechanisms of action

To demonstrate that miR-21 and miR-30b/c, by downregulating Tap63 and caspase-3, are responsible for the TRAIL resistance observed in T98G and LN18 cells, we transfected T98G with

caspase-3 or Tap63 complementary DNAs lacking the miRNA-binding site in their 3'UTR or with a control vector and miR-30c (Figure 5a) or miR-21 (Figure 5b). Interestingly, transfection of Tap63 and caspase-3 was able to overcome the effects of miR-21 and miR-30c, decreasing cell viability and increasing apoptosis (Figures 5a and b). The data were confirmed by colony assay in T98G cells (Supplementary Figures 2A and B). Similar results were obtained when we analyzed miR-30b (data not shown). These rescue experiments proved the causative link between miR-21/Tap63 and caspase-3/miR-30b/c and TRAIL sensitivity.

Effect of miR-21 and miR-30c expression on TRAIL sensitivity in primary human glioma cell lines

MiR-21 and miR-30c expression levels were measured by qRT-PCR in nine different human primary cell lines (Figure 6a), eight derived from glioblastoma tumors (patient no. 1 to no. 8) and one from tissue surrounding the tumor (patient no. 9), and compared with TRAIL sensitivity. As shown in Figure 6b, TRAIL sensitivity correlated with miR-21 and miR-30c expression levels in all cases analyzed, with the exception of control sample that did not respond to TRAIL. Moreover, anti-miRs expression in TRAIL-

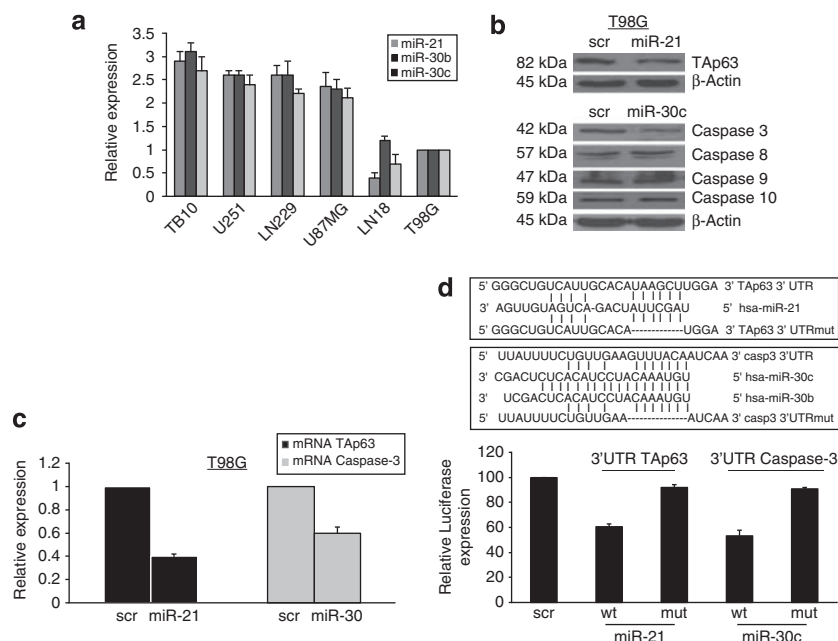


Figure 4. Tap63 and caspase-3 are targets of miR-21 and miR-30c. **(a)** qRT-PCR expression of miR-21, miR-30c and miR-30b in TB10, LN229, U251, U87MG, LN18 and T98G glioma cells. **(b)** Tap63 and caspase-3, caspase-8, caspase-9 and caspase-10 western blot analysis of T98G cells transfected with a scrambled sequence as negative control and with miR-21 and miR-30c, as indicated. **(c)** qRT-PCR of Tap63 and caspase-3 mRNA in T98G transfected with a negative control and with miR-21 and miR-30c, as indicated. **(d)** Alignment between miR-21 and 3'UTR Tap63 wild type or mutant and between miR-30c and 3'UTR caspase-3 wild type or mutant. Luciferase activity of PGL3-3'UTR Tap63 and of PGL3-3'UTR caspase-3 vector after HEK-293 transfection with scrambled miR, miR-21 and miR-30c wild type or mutated, as indicated.

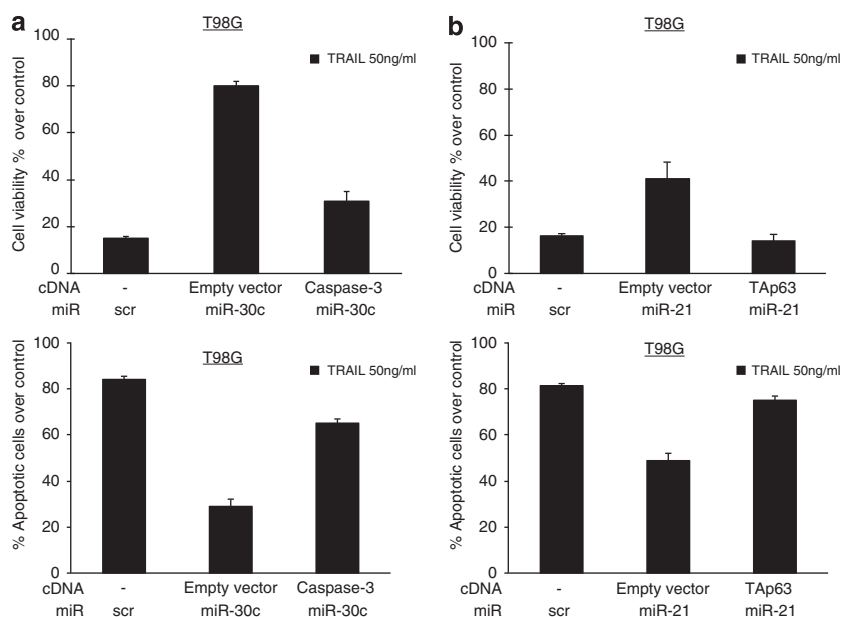


Figure 5. Validation of the involvement of caspase-3 and Tap63 in TRAIL sensitivity. Cell viability assay (upper panels) and propidium iodide staining (lower panels) of T98G cells transfected with miR-30c **(a)** and miR-21 **(b)** in the presence of cDNA for caspase-3 or Tap63.

resistant primary cultured cells (patient no. 1 and no. 2) was able to determine an increase of TRAIL sensitivity (Figure 6c) and concomitantly an increase of the levels of Tap63 and caspase-3 (Figure 6d).

DISCUSSION

Sensitization of cancer cells to apoptosis could be a valuable strategy to define new treatment options for cancer, in particular

when using agents that aim to directly activate apoptotic pathways. A promising agent is the death receptor ligand TRAIL,¹⁹ as it induces apoptosis in most cancer cells, but not in normal cells.^{20,21} Moreover, TRAIL exhibits potent tumoricidal activity *in vivo* in several xenograft models, including malignant glioma.^{22,23} Indeed, agonistic anti-TRAIL receptor monoclonal antibodies (mAbs), including mapatumumab (HGS-ETR1, anti-human DR4 mAb),²⁴ lexatumumab (HGS-ETR2, anti-human DR5 mAb)²⁵ and MD5-1 (anti-mouse DR5 mAb) are currently under

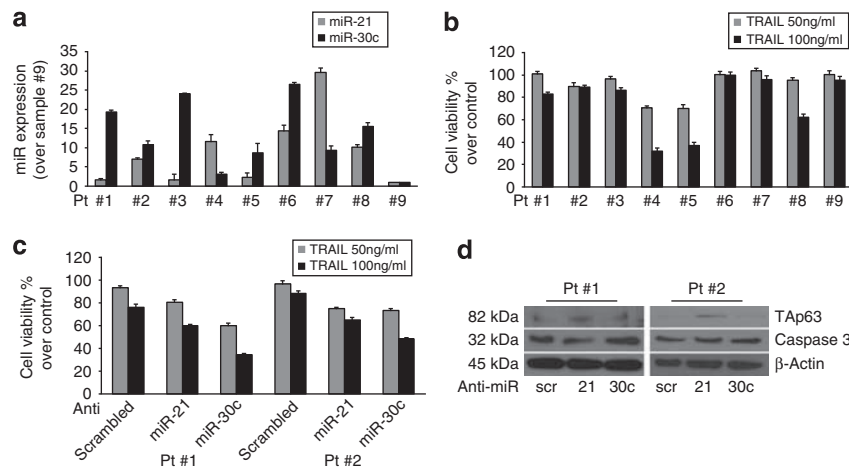


Figure 6. Effect of miR-21 and 30c on primary glioblastoma cell lines. **(a)** qRT-PCR analysis of miR-21 and miR-30c levels in eight primary glioblastoma cancer cell lines and one primary cell line derived from the surrounding tumor tissue used as control. **(b)** TRAIL sensitivity of primary cell lines (10^4 cells) treated with two different doses of SuperKiller TRAIL for 24 h, as indicated. **(c)** Cell viability assay of glioblastoma cells from two patients (#1 and #2) transfected with anti-miR-21 and anti-miR-30c and then treated with 50 ng/ml and 100 ng/ml of TRAIL for 24 h. Anti-miRs treatment sensitized glioblastoma cells to TRAIL. **(d)** Western blot analysis of Tap63 and caspase-3 after anti-miR-21 and anti-miR-30c transfection in patient #1 and #2.

intensive investigation. The former two mAbs have been tested in phase 1 clinical trials in patients with systemic malignancy, exhibiting excellent safety profiles. Anti-mouse DR5 mAb MD5-1 could also be administered safely without inducing hepatotoxicity either alone or in combination with histone deacetylase inhibitors in mice.²⁶ The induction of apoptosis by TRAIL is essentially dependent on the expression of specific TRAIL receptors and on the activation of caspases,²⁰ thus the regulation of the expression levels of those molecules is of fundamental importance.

MicroRNAs are emerging as key regulators of multiple pathways involved in cancer development and progression,^{27–29} and may become the next targeted therapy in glioma. The present study shows that microRNA expression may modulate TRAIL-induced apoptosis in glioma cells, by the regulation of caspase-3 and Tap63 levels. We analyzed the miRs profile of TRAIL-resistant compared with TRAIL-sensitive glioma cells. We then focused our attention on miR-30b/c and miR-21, as only these miRs among those identified by the array, demonstrated the ability to revert the TRAIL-sensitive phenotype. We also provided evidences that this regulation is not restricted to glioma, but it is present also in a different type of cancer such as NSCLC.

MiR-21 has been found overexpressed in high-grade glioma patients³⁰ and studies have identified different miR-21 key targets for glioma biology, such as *RECK*, *TIMP3*, *Spry2* and *Pdcd4* genes, which are suppressors of malignancy and inhibitors of matrix metalloproteinase.^{16,31–33} Moreover, levels of expression of miR-21 have been associated to patients survival.³⁴

Other studies indicate that knockdown of miR-21 in cultured glioblastoma cells triggers activation of caspases and leads to increased apoptotic cell death.³⁵ Corsten *et al.*³⁶ hypothesized that suppression of miR-21 might sensitize gliomas for cytotoxic tumor therapy. With the use of locked nucleic acid (LNA)-anti-miR-21 oligonucleotides and neural precursor cells (NPC) expressing a secretable variant of TRAIL (S-TRAIL), they showed that the combined suppression of miR-21 and NPC-S-TRAIL leads to a synergistic increase in caspase activity and a decreased cell viability in human glioma cells *in vitro* and *in vivo* in xenograft experiments. Interestingly, Papagiannakopoulos *et al.*¹⁵ described that miR-21 targets multiple important components of the p53 tumor-suppressive pathways. They showed that downregulation of miR-21 in glioblastoma cells leads to repression of growth,

increased apoptosis and cell cycle arrest, through the regulation of target proteins such as HNRPK and Tap63. Our study describes for the first time the direct link between miR-21, Tap63 and TRAIL sensitivity. We demonstrated that miR-21 targets the 3'UTR sequence of Tap63, and that transfection of miR-21 is able to downregulate Tap63 at both mRNA and protein levels. More importantly, we demonstrated that miR-21, through Tap63, is able to modulate TRAIL sensitivity, as the co-transfection of miR-21 and Tap63 cDNA renders the cells again responsive to TRAIL. Tap63 is a transcription factor that regulates the expression levels of different apoptosis-regulating genes, such as TRAIL receptors, bcl2l1 and Apaf1.¹⁸ Thus, it is possible that those apoptosis-regulating molecules are regulated by miR-21 through Tap63.

Several studies link miR-30 to apoptosis and human cancer. Li *et al.*³⁷ demonstrated that miR-30 family members inhibited mitochondrial fission through the suppression of the expression of p53 and its downstream target Drp1, whereas, Joglekar *et al.*³⁸ demonstrated that miR-30 may have a role in epithelial-to-mesenchymal transition. Our recent data demonstrate that miR-30 targets the anti-apoptotic protein BIM, participating to gefitinib resistance in lung cancer.³⁹ MiR-30 has been also associated with stem cell properties. Yu *et al.*⁴⁰ described that miR-30 is reduced in breast tumor stem cells (BT-ICs), and demonstrated that enforced expression of miR-30 in BT-ICs inhibits their self-renewal capacity by reducing Ubc9, and induces apoptosis through silencing ITGB3. In our hands, miR-30 overexpression inhibits TRAIL-induced apoptosis in glioma cells by targeting caspase-3. In fact, modulating the expression of either miR-30 or caspase-3, we observed a modification of TRAIL sensitivity of glioma cells. The opposing results on the role of miR-30 on cell death may be ascribed either to different cell system (breast vs glioma), or to different type of cancer cell (stem vs differentiated cells). In favour of this hypothesis, many reports describe opposing role of miRs in a different cell context.²⁸ Recently, miR-30d has been described to target caspase-3 in breast cancer cells, and thus to regulate apoptosis.⁴¹ The seed sequence recognizing the 3'UTR of caspase-3 is highly homologous within the members of the miR-30 family (miR-30b/c/d) suggesting a more generalized role of miR-30 family members in the regulation of cell death and cancer progression.

In many experiments, we observed that there is a redundancy within miR-21 and miR-30 in the regulation of TRAIL sensitivity. Our data, either in primary or in established cell lines, demonstrates that it is sufficient that one of the two miRs is highly expressed in the cells, that apoptosis resistance will manifest. We have also observed that miR-30 has a predominant effect in contrasting TRAIL-induced apoptosis. This may be related to the effect of this miR in targeting one important component of the cell death machinery, that is, caspase-3.

In conclusion, our study analyzed microRNA expression pattern in TRAIL-resistant and TRAIL-sensitive glioma cells, and identified specific miRs and their targets involved in the regulation of the apoptotic programme. This may be of relevance for future cancer therapy improvement in glioma.

MATERIALS AND METHODS

Cell culture and transfection

U87MG, T98G, U251, TB10, CALU-1 and 293 cells were grown in Dulbecco's modified Eagle's medium (DMEM). H460 were grown in RPMI. Media were supplemented with 10% heat-inactivated fetal bovine serum, 2 mM L-glutamine and 100 U/ml penicillin/streptomycin. LN229 and LN18 were grown in Advanced DMEM (Invitrogen, Milan Italy) + 2 mM Glutamine + 5% fetal bovine serum. For miRs transient transfection, cells at 50% confluency were transfected using Oligofectamine (Invitrogen) with 100 nM of pre-miR-30c, -30b, -125b, -146b, -181a, -21, miR-scrambled or anti-miR- (Applied Biosystems, Milan, Italy). For caspase-3 and TAp63 transient transfection, cells were transfected using Lipofectamine and Plus Reagent with 4 µg of caspase-3 cDNA (Origene, Rockville, MD, USA) or TAp63 cDNA for 24 h. TAp63 cDNA was obtained from Professor Viola Calabrò (Naples). SuperKiller TRAIL for cell treatment was purchased from Enzo Biochem (New York, NY, USA).

Primary cell cultures

Glioblastoma specimens were collected at neurosurgical Unit of Cardarelli hospital (Naples). All the samples were collected according to a prior consent of the donor before the collection, acquisition or use of human tissue. To obtain the cells, samples were mechanically disaggregated, then the lysates were grown in DMEM-F12 medium supplemented with 10% fetal bovine serum 1% penicillin streptomycin and 20 ng/ml EGF (Sigma-Aldrich, Milan, Italy). To exclude a fibroblast contamination, cells were stained for GFAP, a protein found in glial cells.

Protein isolation and western blotting

Cells were washed twice in ice-cold phosphate-buffered saline, and lysed in JS buffer (50 mM HEPES pH 7.5 containing 150 mM NaCl, 1% Glycerol, 1% Triton X-100, 1.5 mM MgCl₂, 5 mM EGTA, 1 mM Na₃VO₄ and 1 × protease inhibitor cocktail). Protein concentration was determined by the Bradford assay (Bio-Rad, Milan, Italy) using bovine serum albumin as the standard, and equal amounts of proteins were analyzed by SDS-PAGE (12.5% acrylamide). Gels were electroblotted onto nitrocellulose membranes (Millipore, Bedford, MA, USA). For immunoblot experiments, membranes were blocked for 1 h with 5% non-fat dry milk in Tris-buffered saline containing 0.1% Tween-20, and incubated at 4 °C over night with primary antibody. Detection was performed by peroxidase-conjugated secondary antibodies using the enhanced chemiluminescence system (GE Healthcare, Milan, Italy). Primary antibodies used were: anti-βActin from Sigma-Aldrich; anti-caspase-8, 9 and 10 were from Cell Signalling Technology (Boston, MA, USA); anti-Caspase 3 and anti-TAp63 from Santa Cruz Biotechnologies (Santa Cruz, CA, USA).

miRNA microarray experiments

From each sample, 5 µg of total RNA (from T98G, LN18, TB10, LN229 cells) was reverse transcribed using biotin-end-labelled random-octamer oligonucleotide primer. Hybridization of biotin-labelled cDNA was performed on an Ohio State University custom miRNA microarray chip (OSU_CCC version 3.0), which contains 1150 miRNA probes, including 326 human and 249 mouse miRNA genes, spotted in duplicates. The hybridized chips were washed and processed to detect biotin-containing transcripts by streptavidin-Alexa647 conjugate and scanned on an Axon 4000B microarray scanner (Axon Instruments, Sunnyvale, CA, USA).

Raw data were normalized and analyzed with GENESPRING 7.2 software (zcomSilicon Genetics, Redwood City, CA, USA). Expression data were median-centered by using both the GENESPRING normalization option and the global median normalization of the BIOCONDUCTOR package (www.bioconductor.org) with similar results. Statistical comparisons were done by using the GENESPRING ANOVA tool, predictive analysis of microarray and the significance analysis of microarray software (<http://www-stat.stanford.edu/~tibs/SAM/index.html>).

RNA extraction and real-time PCR

Total RNAs (miRNA and mRNA) were extracted using Trizol (Invitrogen) according to the manufacturer's protocol. Reverse transcription of total miRNA was performed starting from equal amounts of total RNA per sample (1 µg) using miScript reverse Transcription Kit (Qiagen, Milan, Italy), for mRNAs SuperScript III Reverse Transcriptase (Invitrogen) was used. For cultured cells, quantitative analysis of Caspase-3, TAp63, β-Actin (as an internal reference), miR-30b/c, miR-21 and RNU5A (as an internal reference) were performed by real-time PCR using specific primers (Qiagen), miScript SYBR Green PCR Kit (Qiagen) and iQ SYBR Green Supermix (Bio-Rad), respectively. The reaction for detection of mRNAs was performed as follow: 95 °C for 15', 40 cycles of 94 °C for 15', 60 °C for 30' and 72 °C for 30'. The reaction for detection of miRNAs was performed as follow: 95 °C for 15', 40 cycles of 94 °C for 15', 55 °C for 30' and 70 °C for 30'. All reactions were run in triplicate. The threshold cycle (CT) is defined as the fractional cycle number at which the fluorescence passes the fixed threshold. For relative quantization, the 2^(-ΔCT) method was used as previously described.⁴² Experiments were carried out in triplicate for each data point, and data analysis was performed by using software (Bio-Rad).

Northern blot analysis

RNA samples (30 µg) were separated by electrophoresis on 15% acrylamide, 7 mol/l urea gels (Bio-Rad, Hercules, CA, USA) and transferred onto Hybond-N+ membrane (Amersham Biosciences, Piscataway, NJ, USA). Hybridization was performed at 37 °C in 7% SDS/0.2 mol/l Na₂PO₄ (pH 7.0) for 16 h. Membranes were washed at 42 °C, twice with 2 × standard saline phosphate (0.18 mol/l NaCl/10 mmol/l phosphate (pH 7.4)), 1 mmol/l EDTA (saline-sodium phosphate-EDTA; SSPE) and 0.1% SDS and twice with 0.5 × SSPE/0.1% SDS. The oligonucleotides (PRIMM, Milan, Italy) used, complementary to the sequences of the mature miRNAs, were: miR-21-probe 5'-TCAACATCAGTCTGATAAGCTA-3'; miR-30c-probe 5'-GCTGAG AGTGTAGGATGTTTACA-3'. An oligonucleotide complementary to the U6 RNA (5'-GCAGGGGCCATGCTAATCTTCTGTATCG-3') was used to normalize the expression levels. Totally, 100 pmol of each probe were end labelled with 50 mCi [γ-32P]ATP using the poly-nucleotide kinase (Roche, Basel, Switzerland). Blots were stripped by boiling in 0.1% SDS for 10 min before re-hybridization.

Luciferase assay

The 3' UTR of the human Caspase-3 genes was PCR amplified using the following primers: Caspase-3 forward: 5'-TCTAGAGGGCGCCATCGCCAAG TAAGAAA-3', Caspase-3 reverse: 5'-TCTAGACCCGTGAAATGTCATACGA CAG-3' and cloned downstream of the Renilla luciferase stop codon in pGL3 control vector (Promega, Milan, Italy). A deletion was introduced into the miRNA-binding sites by using the QuikChange Mutagenesis Kit (Stratagene, La Jolla, CA, USA) using the following primers: Caspase-3 mut forward 5'-GCAAAATCTTAAGTATGTTATTTCTGTTGAAATCAAAGGA AAATAGTAATGTTTATACT-3'. Caspase-3mut reverse 5'-AGTATAAAACAT TACTATTTTCCTTTGATTTCAACAGAAAATAACATACTTAAGAATTTTGC-3'.

The 3' UTR of the human TAp63 gene was PCR amplified using the following primers: TAp63 forward: 5'-TCTAGAGCAAGAGATAAGTCTTT CATGGCTGCTG-3', TAp63 reverse: 5'-TCTAGATGGAATCCCACTATCCCA AG-3', and cloned downstream of the Renilla luciferase stop codon in pGL3 control vector (Promega). A deletion was introduced into the miRNA-binding sites by using the QuikChange Mutagenesis Kit (Stratagene) using the following primers: TAp63 mut forward 5'-CTGGTCAAGGGCTGTCATTG CACTCCATTTAATTT-3' TAp63 mut reverse 5'-AAATTAAATGGAGTGCAAT GACAGCCCTTGACCAAG-3'.

Hek-293 cells were cotransfected with 1.2 µg of generated plasmid and 400 µg of a Renilla luciferase expression construct pRL-TK (Promega) with Lipofectamine 2000 (Invitrogen). Cells were harvested 24 h post transfection and assayed with Dual Luciferase Assay (Promega) according to the

manufacturer's instructions. Three independent experiments were performed in triplicate.

Cell death quantification

Cells were plated in 96-well plates in triplicate, stimulated and incubated at 37 °C in a 5% CO₂ incubator. SuperKiller TRAIL was used at final concentration of 50 or 100 ng/ml for 24 h. Apoptosis was analyzed via propidium iodide incorporation in permeabilized cells by flow cytometry. The cells (2×10^5) were washed in phosphate-buffered saline and resuspended in 200 µl of a solution containing 0.1% sodium citrate, 0.1% Triton X-100 and 50 µg/ml propidium iodide (Sigma). Following incubation at 4 °C for 30 min in the dark, nuclei were analyzed with a Becton Dickinson FACScan flow cytometer (Becton Dickinson, Milan, Italy). Cellular debris was excluded from analyses by raising the forward scatter threshold, and the DNA content of the nuclei was registered on a logarithmic scale. The percentage of elements in the hypodiploid region was calculated. Cell viability was evaluated with the CellTiter 96 AQueous One Solution Cell Proliferation Assay (Promega) according to the manufacturer's protocol. Metabolically active cells were detected by adding 20 µl of MTS to each well. After 2 h of incubation, the plates were analyzed in a Multilabel Counter (BioTek, Milan, Italy).

Colony assay

Cells were transfected with miR-scrambled, miR-30b/c or miR-21 for 24 h, then were harvested and 2.4×10^4 cells were plated in six-well plates. After 24 h, cells were treated with 50 or 100 ng/ml of superKiller TRAIL for 24 h, as indicated. Cells were transferred to 100 mm dishes and let grown for 6 days. Finally, the cells were coloured with 0.1% crystal violet dissolved in 25% methanol for 20 min at 4 °C. Dishes were washed with water and then let dry on the bench, and then photographs were taken.

ACKNOWLEDGEMENTS

This work was partially supported by funds from Associazione Italiana Ricerca sul Cancro, AIRC to GC (grant n.ro 10620), and MERIT (RBNE08E8CZ_002) to GC. CQ and MI are supported by the 'Federazione Italiana Ricerca sul Cancro' (FIRC) Post-Doctoral Research Fellowship. GR is supported by a MERIT project Fellowship.

REFERENCES

- 1 Tran B, Rosenthal MA. Survival comparison between glioblastoma multiforme and other incurable cancers. *J Clin Neurosci* 2010; **17**: 417–421.
- 2 Purow B, Schiff D. Advances in the genetics of glioblastoma: are we reaching critical mass? *Nat Rev Neurol* 2009; **5**: 419–426.
- 3 Schaefer U, Voloshanenko O, Willen D, Walczak H. TRAIL: a multifunctional cytokine. *Front Biosci* 2007; **12**: 3813–3824.
- 4 Falschlehner C, Emmerich CH, Gerlach B, Walczak H. TRAIL signalling: Decisions between life and death. *Int J Biochem Cell Biol* 2007; **39**: 1462–1475.
- 5 Younes A, Vose JM, Zelenetz AD, Smith MR, Burris HA, Ansell SM et al. A Phase 1b/2 trial of mapatumumab in patients with relapsed/refractory non-Hodgkin's lymphoma. *Br J Cancer* 2010; **103**: 1783–1787.
- 6 Trarbach T, Moehler M, Heinemann V, Kohne CH, Przyborek M, Schulz C et al. Phase II trial of mapatumumab, a fully human agonistic monoclonal antibody that targets and activates the tumour necrosis factor apoptosis-inducing ligand receptor-1 (TRAIL-R1), in patients with refractory colorectal cancer. *Br J Cancer* 2010; **102**: 506–512.
- 7 Garofalo M, Romano G, Quintavalle C, Romano MF, Chiurazzi F, Zanca C et al. Selective inhibition of PED protein expression sensitizes B-cell chronic lymphocytic leukaemia cells to TRAIL-induced apoptosis. *Int J Cancer* 2007; **120**: 1215–1222.
- 8 Zanca C, Garofalo M, Quintavalle C, Romano G, Acunzo M, Ragno P et al. PED is overexpressed and mediates TRAIL resistance in human non-small cell lung cancer. *J Cell Mol Med* 2008; **12**: 2416–2426.
- 9 Quintavalle C, Incoronato M, Puca L, Acunzo M, Zanca C, Romano G et al. c-FLIPL enhances anti-apoptotic Akt functions by modulation of Gsk3β activity. *Cell Death Differ* 2010; **17**: 1908–1916.
- 10 Calin GA, Croce CM. MicroRNA signatures in human cancers. *Nat Rev Cancer* 2006; **6**: 857–866.
- 11 Croce CM. Causes and consequences of microRNA dysregulation in cancer. *Nat Rev Genet* 2009; **10**: 704–714.
- 12 Garofalo M, Di Leva G, Romano G, Nuovo G, Suh SS, Ngankou A et al. miR-221 & 222 regulate TRAIL resistance and enhance tumorigenicity through PTEN and TIMP3 downregulation. *Cancer Cell* 2009; **16**: 498–509.

- 13 Garofalo M, Quintavalle C, Di Leva G, Zanca C, Romano G, Taccioli C et al. MicroRNA signatures of TRAIL resistance in human non-small cell lung cancer. *Oncogene* 2008; **27**: 3845–3855.
- 14 Incoronato M, Garofalo M, Urso L, Romano G, Quintavalle C, Zanca C et al. miR-212 increases tumor necrosis factor-related apoptosis-inducing ligand sensitivity in non-small cell lung cancer by targeting the antiapoptotic protein PED. *Cancer Res* 2010; **70**: 3638–3646.
- 15 Papagiannakopoulos T, Shapiro A, Kosik KS. MicroRNA-21 targets a network of key tumor-suppressive pathways in glioblastoma cells. *Cancer Res* 2008; **68**: 8164–8172.
- 16 Gaur AB, Holbeck SL, Colburn NH, Israel MA. Downregulation of Pdc4 by mir-21 facilitates glioblastoma proliferation *in vivo*. *Neuro-Oncology* 2011; **13**: 580–590.
- 17 Zhu S, Si M-L, Wu H, Mo Y-Y. MicroRNA-21 Targets the Tumor Suppressor Gene Tropomyosin 1 (TPM1). *J Biol Chem* 2007; **282**: 14328–14336.
- 18 Gressner O, Schilling T, Lorenz K, Schulze Schleithoff E, Koch A, Schulze-Bergkamen H et al. TAp63[α] induces apoptosis by activating signaling via death receptors and mitochondria. *EMBO J* 2005; **24**: 2458–2471.
- 19 Nagane M, Huang HJS, Cavenee WK. The potential of TRAIL for cancer chemotherapy. *Apoptosis* 2001; **6**: 191–197.
- 20 Gonzalez F, Ashkenazi A. New insights into apoptosis signaling by Apo2L/TRAIL. *Oncogene* 2010; **29**: 4752–4765.
- 21 Walczak H, Bouchon A, Stahl H, Krammer PH. Tumor necrosis factor-related apoptosis-inducing ligand retains its apoptosis-inducing capacity on Bcl-2- or Bcl-xL-overexpressing chemotherapy-resistant tumor cells. *Cancer Res* 2000; **60**: 3051–3057.
- 22 Balyasnikova IV, Ferguson SD, Han Y, Liu F, Lesniak MS. Therapeutic effect of neural stem cells expressing TRAIL and bortezomib in mice with glioma xenografts. *Cancer Lett* 2011; **310**: 148–159.
- 23 Unterkircher T, Cristofanon S, Vellanki SHK, Nonnenmacher L, Karpel-Massler G, Wirtz CR et al. Bortezomib primes glioblastoma, including glioblastoma stem cells, for TRAIL by increasing tBid stability and mitochondrial apoptosis. *Clin Cancer Res* 2011; **17**: 4019–4030.
- 24 Chuntharapai A, Dodge K, Grimmer K, Schroeder K, Masters SA, Koeppe H et al. Isotype-dependent inhibition of tumor growth *in vivo* by monoclonal antibodies to death receptor 4. *J Immunol* 2001; **166**: 4891–4898.
- 25 Plummer R, Attard G, Pacey S, Li L, Razak A, Perrett R et al. Phase 1 and pharmacokinetic study of lexatumumab in patients with advanced cancers. *Clin Cancer Res* 2007; **13**: 6187–6194.
- 26 Ichikawa K, Liu W, Zhao L, Wang Z, Liu D, Ohtsuka T et al. Tumoricidal activity of a novel anti-human DR5 monoclonal antibody without hepatocyte cytotoxicity. *Nat Med* 2001; **7**: 954–960.
- 27 Garofalo M, Condorelli G, Croce CM. MicroRNAs in diseases and drug response. *Curr Opin Pharmacol* 2008; **8**: 661–667.
- 28 Garofalo M, Quintavalle C, Romano G, Croce CM, Condorelli G. miR221/222 in cancer: their role in tumor progression and response to therapy. *Curr Mol Med* 2012; **12**: 27–33.
- 29 Garofalo M, Condorelli GL, Croce CM, Condorelli G. MicroRNAs as regulators of death receptors signaling. *Cell Death Differ* 2010; **17**: 200–208.
- 30 Malzkorn B, Wolter M, Liesenberg F, Grzendowski M, Stühler K, Meyer HE et al. Identification and functional characterization of microRNAs involved in the malignant progression of gliomas. *Brain Pathol* 2009; **20**: 539–550.
- 31 Gabriely G, Wurdinger T, Kesari S, Esau CC, Burchard J, Linsley PS et al. MicroRNA 21 promotes glioma invasion by targeting matrix metalloproteinase regulators. *Mol Cell Biol* 2008; **28**: 5369–5380.
- 32 Kwak HJ, Kim YJ, Chun KR, Woo YM, Park SJ, Jeong JA et al. Downregulation of Spry2 by miR-21 triggers malignancy in human gliomas. *Oncogene* 2011; **30**: 2433–2442.
- 33 Moore LM, Zhang W. Targeting miR-21 in glioma: a small RNA with big potential. *Expert Opin Ther Targets* 2010; **14**: 1247–1257.
- 34 Lakomy R, Sana J, Hankeova S, Fadrus P, Kren L, Lzicarova E et al. MiR-195, miR-196b, miR-181c, miR-21 expression levels and O-6-methylguanine-DNA methyltransferase methylation status are associated with clinical outcome in glioblastoma patients. *Cancer Sci* 2011; **102**: 2186–2190.
- 35 Chan JA, Krichevsky AM, Kosik KS. MicroRNA-21 is an antiapoptotic factor in human glioblastoma cells. *Cancer Res* 2005; **65**: 6029–6033.
- 36 Corsten MF, Miranda R, Kasmieh R, Krichevsky AM, Weissleder R, Shah K. MicroRNA-21 knockdown disrupts glioma growth *in vivo* and displays synergistic cytotoxicity with neural precursor cell delivered S-TRAIL in human gliomas. *Cancer Res* 2007; **67**: 8994–9000.
- 37 Li J, Donath S, Li Y, Qin D, Prabhakar BS, Li P. miR-30 regulates mitochondrial fission through targeting p53 and the dynamin-related protein-1 pathway. *PLoS Genet* 2010; **6**: e1000795.
- 38 Joglekar MV, Patil D, Joglekar VM, Rao GV, Reddy ND, Mitnala S et al. The miR-30 family microRNAs confer epithelial phenotype to human pancreatic cells. *Islets* 2009; **1**: 137–147.

- 39 Garofalo M, Romano G, Di Leva G, Nuovo G, Jeon Y-J, Nganheu A *et al*. EGFR and MET receptor tyrosine kinase-altered microRNA expression induces tumorigenesis and gefitinib resistance in lung cancers. *Nat Med* 2011; **18**: 74–82.
- 40 Yu F, Deng H, Yao H, Liu Q, Su F, Song E. Mir-30 reduction maintains self-renewal and inhibits apoptosis in breast tumor-initiating cells. *Oncogene* 2010; **29**: 4194–4204.
- 41 Li N, Kaur S, Greshock J, Lassus H, Zhong X, Wang Y *et al*. A combined array-based comparative genomic hybridization and functional library screening approach identifies mir-30d as an oncomir in cancer. *Cancer Res* 2011; **72**: 154–164.
- 42 Livak KJ, Schmittgen TD. Analysis of relative gene expression data using real-time quantitative PCR and the $2^{-\Delta\Delta C(T)}$ Method. *Methods* 2001; **25**: 402–408.

Supplementary Information accompanies the paper on the Oncogene website (<http://www.nature.com/onc>)